Robotics 2

Human-Robot
Coexistence and Collaboration

Prof. Alessandro De Luca

Dipartimento di Ingegneria Informatica
Automatica e Gestionale Antonio Ruberti

Sapienza
Università di Roma

Human-friendly robotics

The goal

traditional robotics

replacing humans

co-workers on factory floor

human-friendly robotics

collaborating with humans

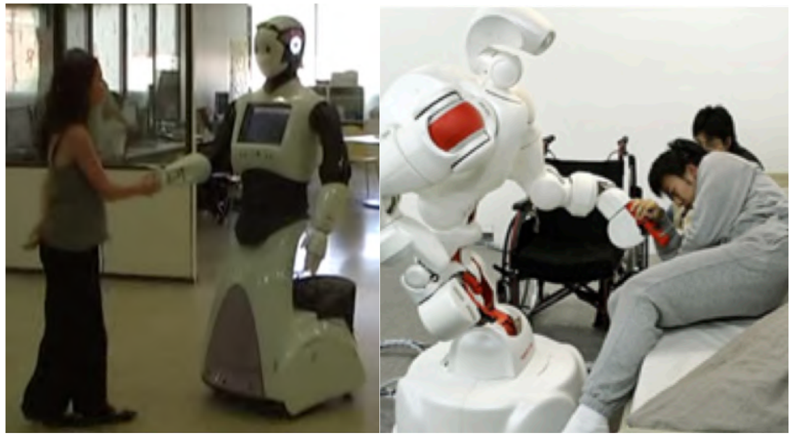

personal robots in service

SAPHARI concept

Place the human at the center of the entire robot development

FP7 ICT
EU project
(2011-15)

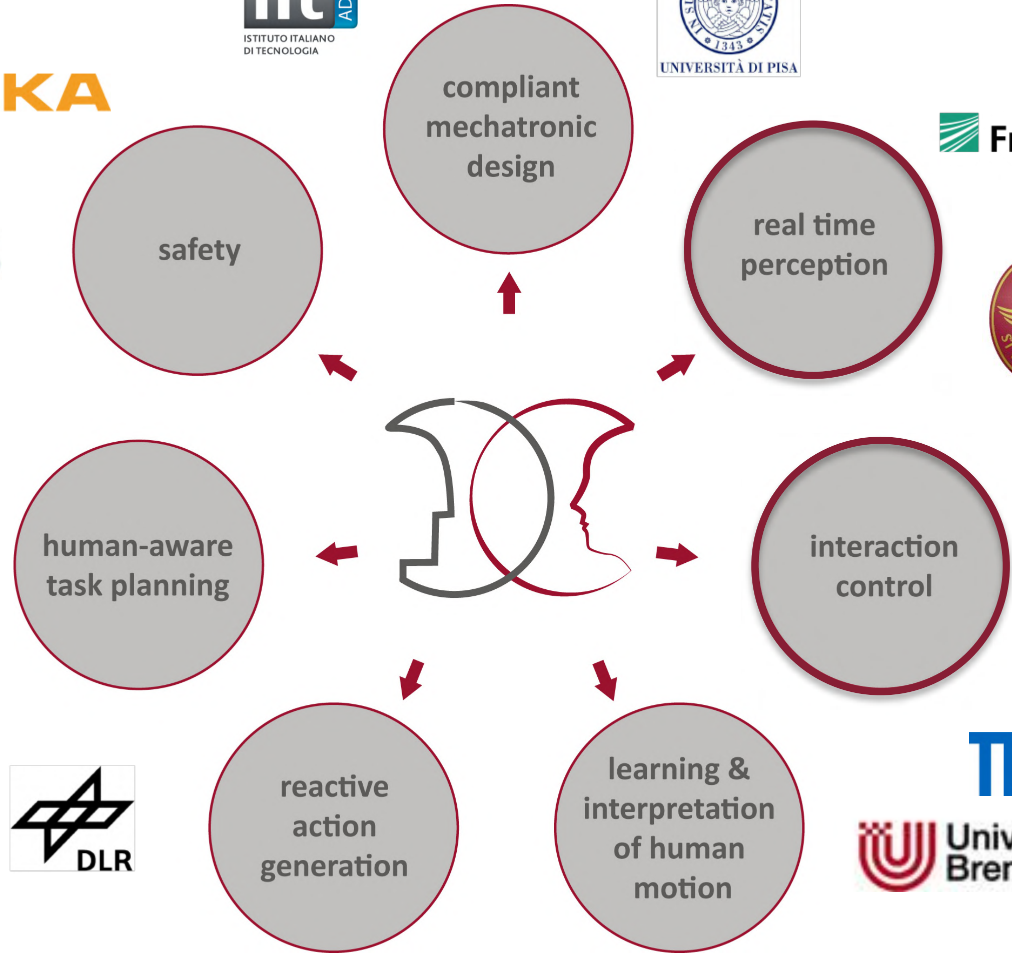

SAPIENZA UNIVERSITÀ DI ROMA (coordinator)

address all essential aspects of safe and intuitive physical interaction
between humans and complex human-like robots in a strongly integrated way

Handling of collisions and intentional contacts

Basic **safety-related control** problems in physical Human-Robot Interaction (**pHRI**)

collision detection/isolation and reaction
(**without** the use of external sensing)

workspace monitoring
for **continuous**
collision avoidance
(while the task is running)

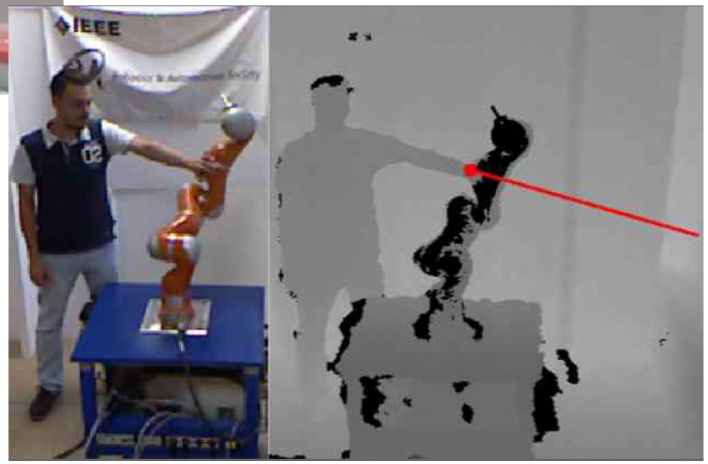

estimation and control
of intentional forces
exchanged at the contact
(**with** or **without a F/T** sensor)
for human-robot collaboration

Safe physical Human-Robot Interaction (pHRI)

Control architecture of consistent robot behaviors (De Luca, Flacco: IEEE BioRob 2012)

- **integrated design & use** of soft mechanics, actuation, (proprio- and exteroceptive) sensing, communication, and **control** algorithms

Safety

lightweight mechanical design
compliance at robot joints

Safety is the most important feature of a robot that has to work close to human beings

Classical solutions for preserving safety in industrial environments, i.e., using cages or stopping the robot in the presence of humans [**ISO 10218**], are inappropriate for pHRI

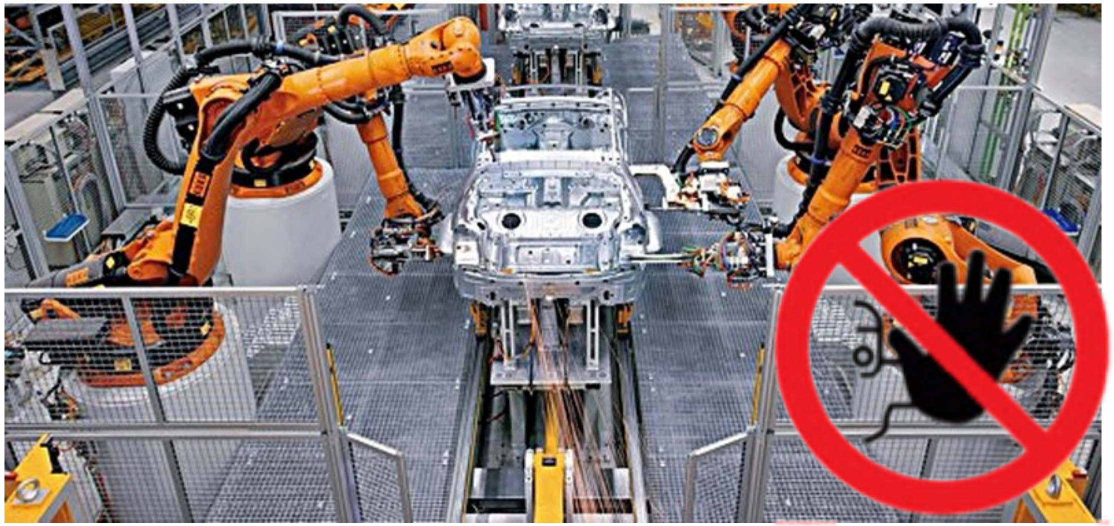

Physical HRI

Hierarchy of consistent behaviors

Safety

Coexistence

Coexistence is the robot capability of sharing the workspace with other entities, most relevant with humans

Human (and robot!) safety requirements must be always guaranteed (i.e., **safe coexistence**)

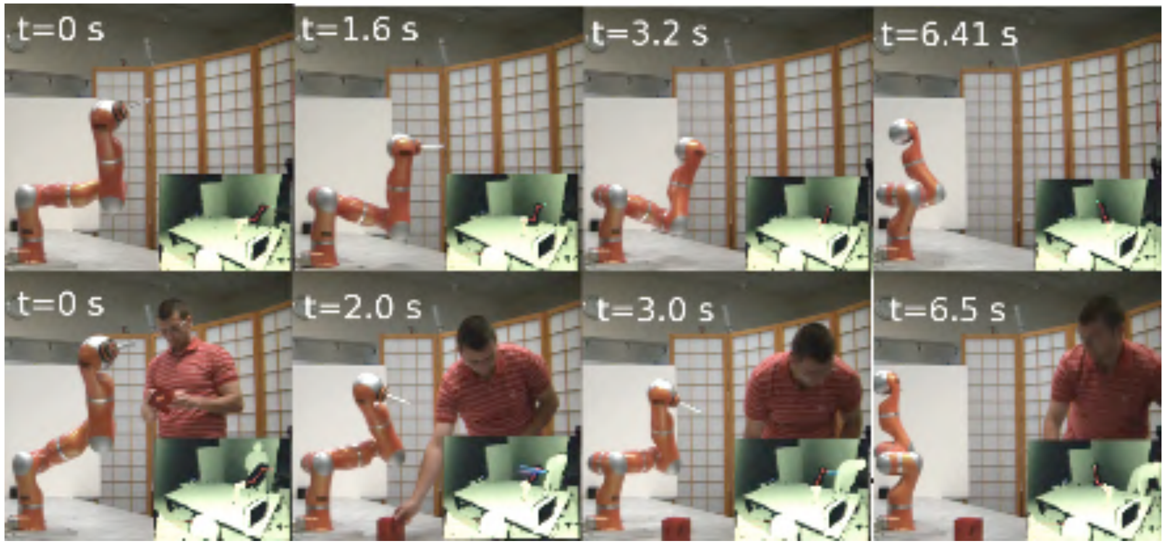

original robot task

sharing the workspace
without the need of physical contacts

safe HR coexistence

Physical HRI

Hierarchy of consistent behaviors

Collaboration occurs when the robot performs complex tasks with direct human interaction and coordination

Two modalities which are not mutually exclusive: **contactless** and **physical**

gestures or voice commands visual coordination

with intentional contact and exchange of forces

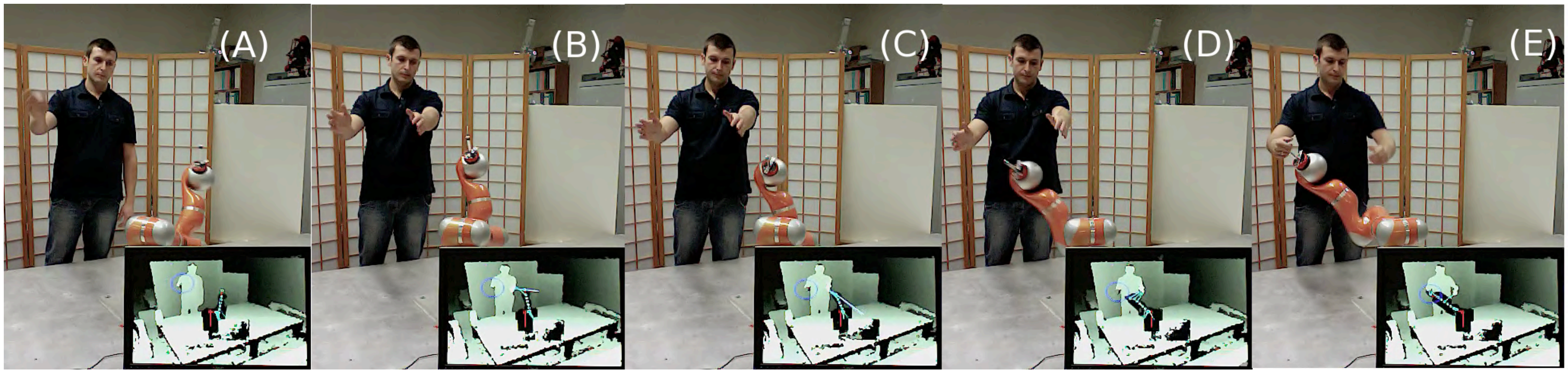

Types of collaborative operations

From ISO 10218-1:2011 & 10218-2:2011 standards (refined in ISO-TS 15066:2016)

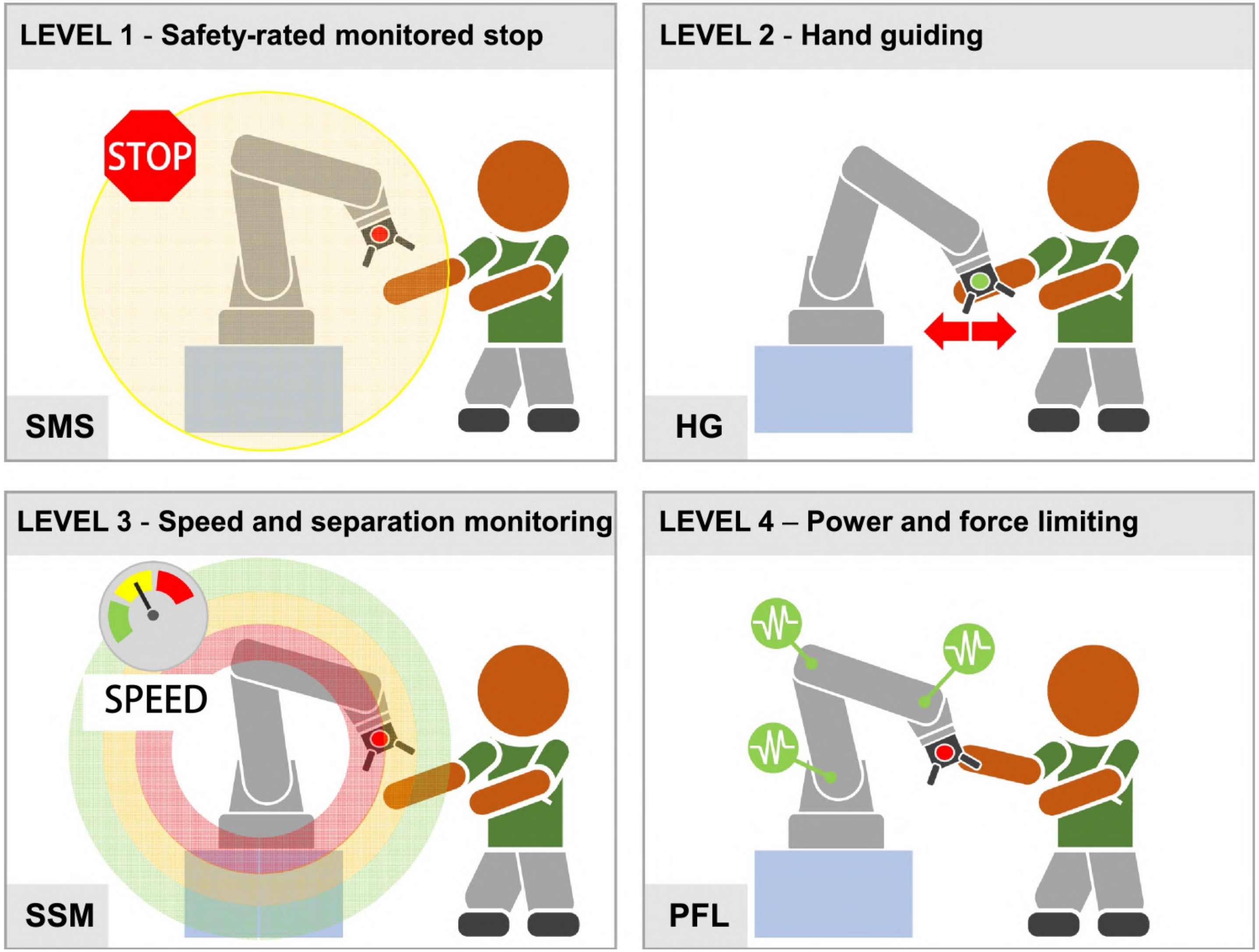

Qualification of our control architecture for pHRI

Relation with ISO Standard 10218 and Technical Specification 15066

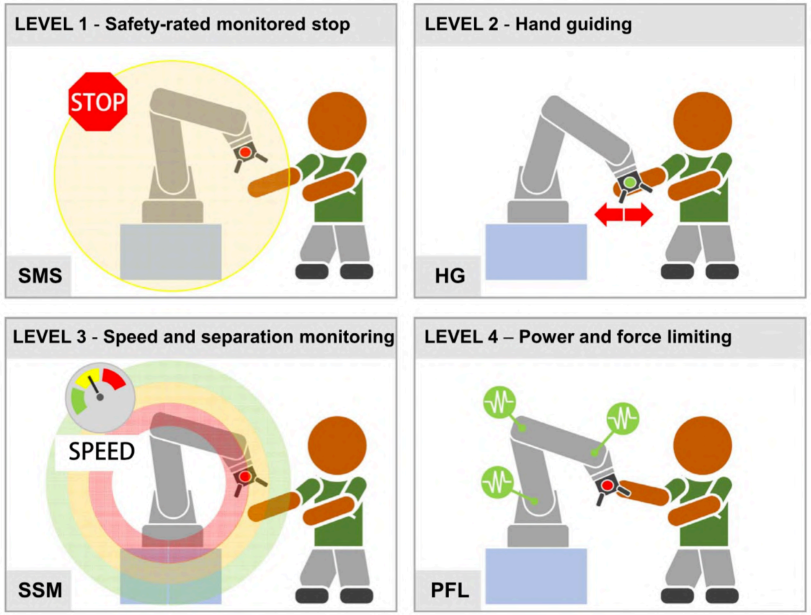

SAFETY	Speed	Separation distance	Torques	Operator controls	Main risk reduction
Safety-rated monitored stop COEXISTENCE	Zero while operator in CWS	Small or zero	Gravity + load compensation only	None while operator in CWS	No motion in presence of operator
Hand guiding COLLABORATION	Safety-rated monitored speed	Small or zero	As by direct operator input	E-stop; Enabling device; Motion input	Motion only by direct operator input
Speed and separation monitoring COEXISTENCE	Safety-rated monitored speed	Safety-rated monitored distance	As required to execute application and maintain min separation distance	None while operator in CWS	Contact between robot and operator prevented
Power and force limiting COLLABORATION	Max determined by RA to limit impact forces	Small or zero	Max determined by RA to limit static forces	As required by application	By design or control, robot cannot impart excessive force

ISO 10218-1/2:2011
ISO/TS 15066:2016

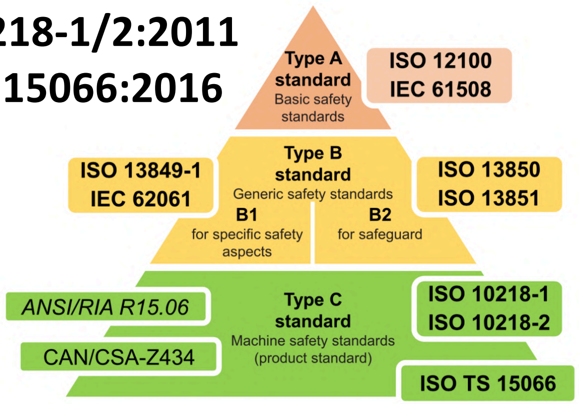

- collision detection and reaction
- workspace sharing
  - with collision avoidance
- coordinated motions & actions
  - with/without contact

Control levels in the collision event pipeline

Haddadin, De Luca, Albu-Schäffer: IEEE T-RO 2017

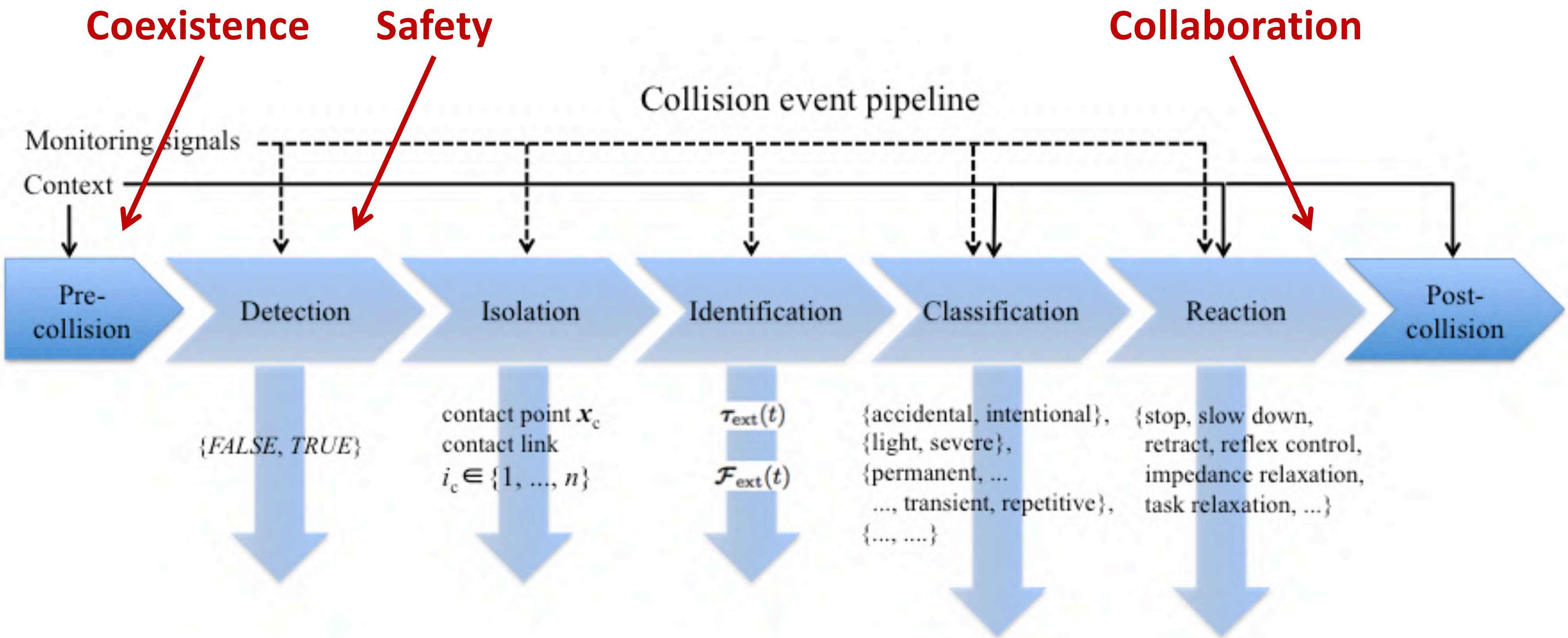

Monitoring signals can be generated from sensors or models (signal- or model-based methods)

Context information is needed (or useful) to take the right or most suitable decisions

Collision detection and reaction

Residual-based experiments on DLR LWR-III (IROS 2006, IROS 2008)

- collision detection followed by different reaction strategies
- zero-gravity behavior: gravity is always compensated first (by control)
- detection time: 2-3 ms, reaction time: + 1 ms

3 videos

admittance mode	reflex torque	reflex torque
first impact at 60°/s		first impact at 90°/s
$\dot{\boldsymbol{q}}_r = \boldsymbol{K}_Q \boldsymbol{r}$	$\boldsymbol{\tau} = \boldsymbol{K}_R \boldsymbol{r}$	

Coexistence

Early days and yesterday …

1989

video

informational video by National Institute for Occupational Safety and Health (USA)

2012

commercial video by ABB Robotics on EPS (Electronic Position Switch) and early SafeMove software

video

Coexistence

Today and tomorrow? …

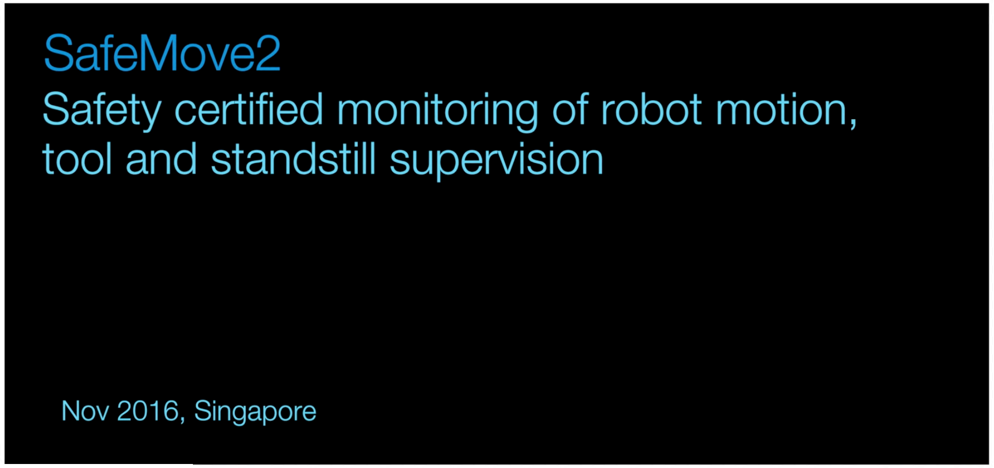

video

commercial video by ABB Robotics
of SafeMove2 software
(using 2 laser scanners)

https://youtu.be/pIlhY8E3HFg

2016

IROS 2013
Best Video Award Finalist

SAPHARI
Safe and Autonomous Physical Human-Aware Robot Interaction

(using 1 Kinect
depth sensor)

video

Collision avoidance

Using exteroceptive sensors to monitor robot workspace (ICRA 2010)

- **external sensing:** stereo-camera, TOF, structured light, depth, laser, presence, ... placed optimally to minimize occlusions (robot can be removed from images)

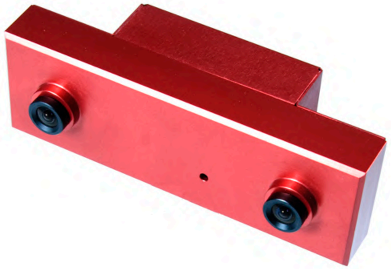

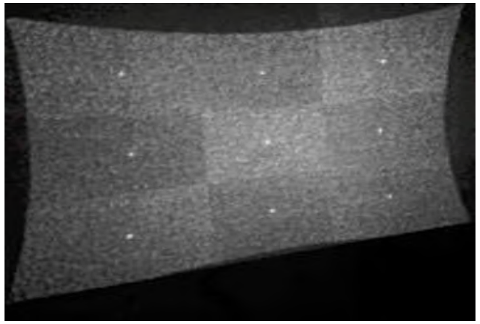

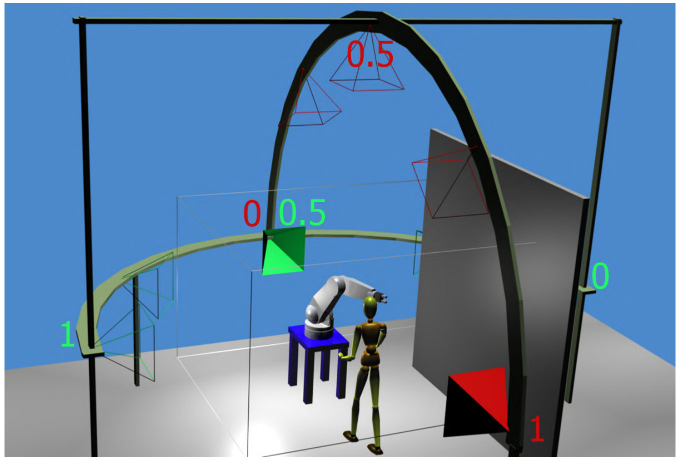

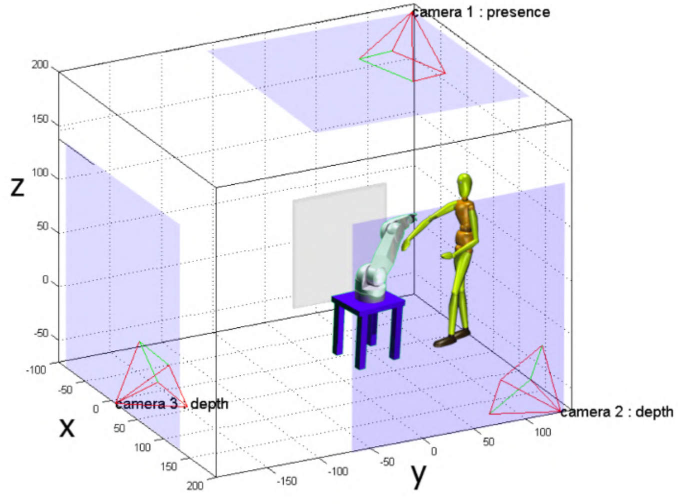

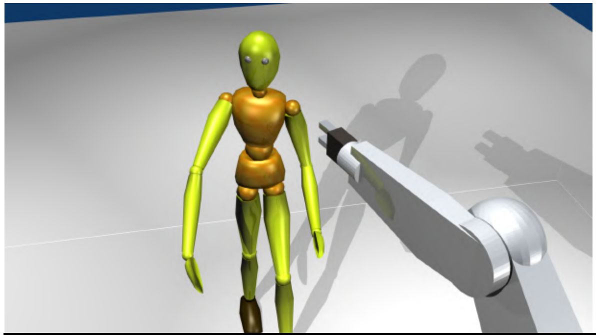

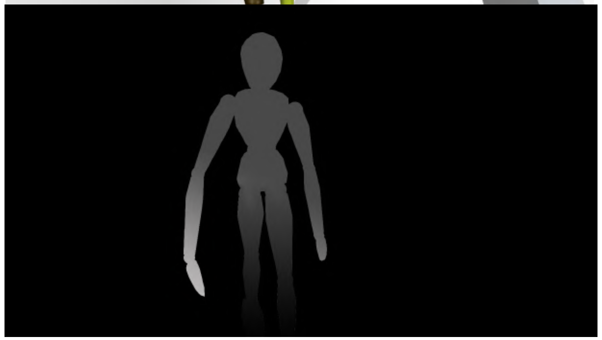

Depth image

How to use it?

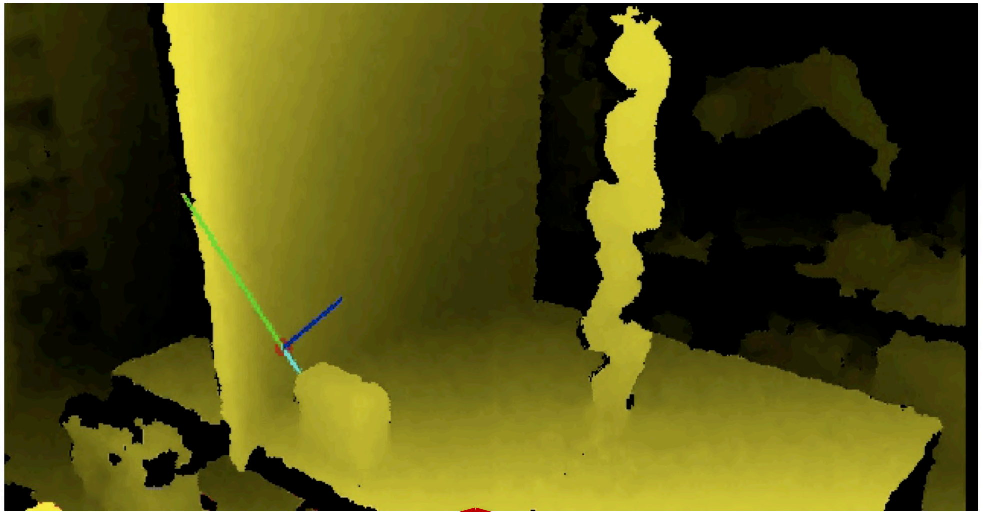

Configuration Space

Depth Space

Cartesian Space

Cartesian space

A long process

video

TU Munich

Configuration space

Possible, but tipically only for few dofs

video

Univ Pisa

Depth space

A 2.5-dimensional space

- non-homogeneous 2.5 dimensional space
  - x, y position of the point in the image plane [pixel]
  - d depth of the point with respect to the image plane [m]
- depth space is modeled as a pin-hole sensor
- point in Cartesian reference frame $\boldsymbol{P}_R = (x_R, y_R, z_R)$
- point in sensor frame $\boldsymbol{P}_C = \boldsymbol{R}\boldsymbol{P}_R + \boldsymbol{t} = (x_C, y_C, z_C)$
- point in depth space

$$
\begin{aligned}
p_x &= \frac{x_C f s_x}{z_C} + c_x \\
p_y &= \frac{y_C f s_y}{z_C} + c_y \\
d_p &= z_C
\end{aligned}
$$

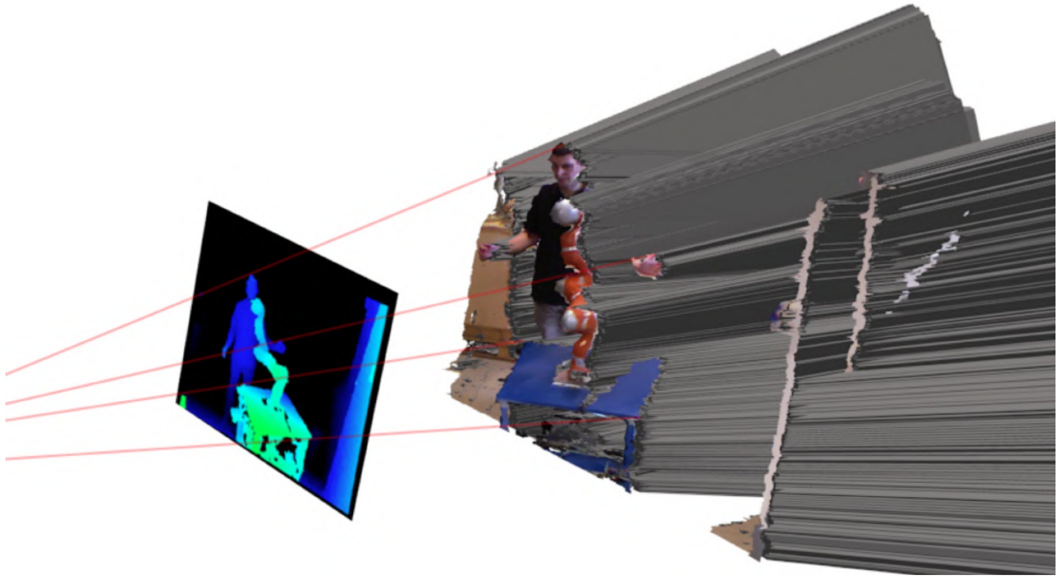

gray areas
behind the obstacles

Depth space

Distance evaluation

- distance between a point of interest $\boldsymbol{P}_D = (p_x, p_y, d_p)$

  and an obstacle point $\mathbf{O}_D = (o_x, o_y, d_o)$

$$\boxed{\mathrm{dist}(\boldsymbol{P}, \mathbf{O}) \ = \ \sqrt{v_x^2 + v_y^2 + v_z^2}}$$

$$v_x \ = \ \frac{(o_x - c_x)d_o - (p_x - c_x)d_p}{f s_x} \qquad v_y \ = \ \frac{(o_y - c_y)d_o - (p_y - c_y)d_p}{f s_y} \qquad v_z \ = \ d_o - d_p$$

(if **obstacle** point is **closer** than point of interest, **set** $d_o = d_p$)

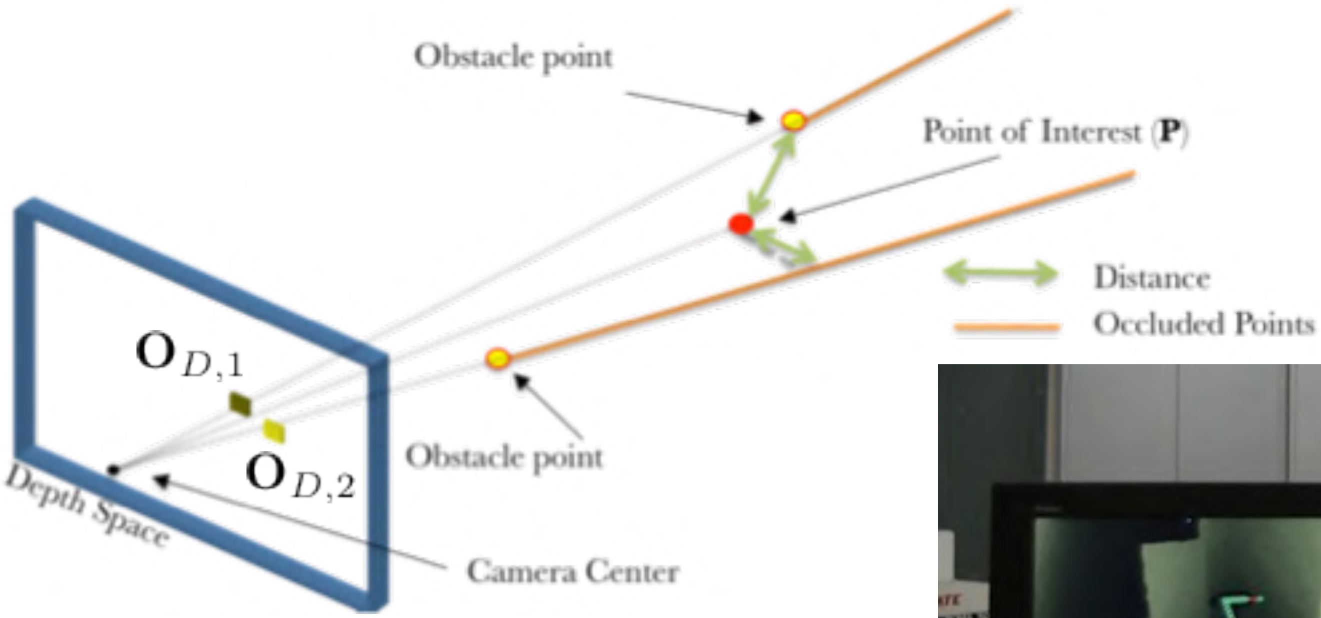

8 points of interest
on the robot

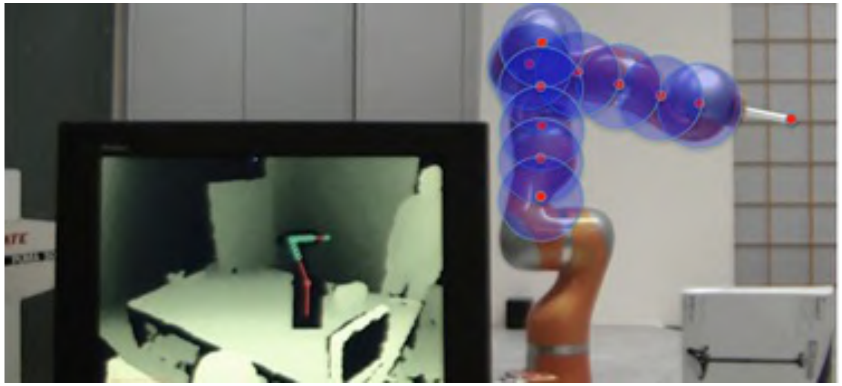

Repulsive vector

A version of artificial potentials

- repulsive vector generated from the distance vector $\boldsymbol{D}(\boldsymbol{P},\mathbf{O}) = (v_x, v_y, v_z)$

$$\boldsymbol{V}_C(\boldsymbol{P},\mathbf{O}) = v(\boldsymbol{P},\mathbf{O})\,\frac{\boldsymbol{D}(\boldsymbol{P},\mathbf{O})}{\|\boldsymbol{D}(\boldsymbol{P},\mathbf{O})\|}$$

$$v(\boldsymbol{P},\mathbf{O}) = \frac{V_{max}}{1 + e^{\|\boldsymbol{D}(\boldsymbol{P},\mathbf{O})\|(2/\rho)\alpha - \alpha}}$$

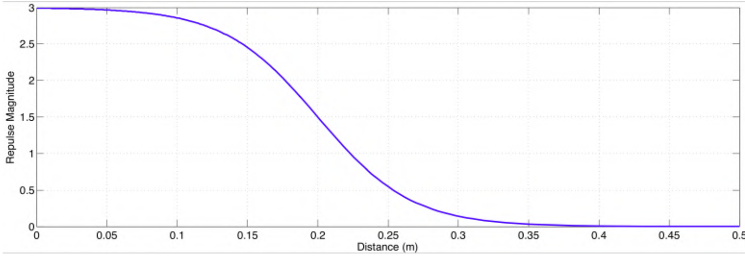

- repulsive vectors **due to all obstacles** near to point of interest are considered
  - orientation ⇒ sum of all repulsive vectors, magnitude ⇒ nearest obstacle only
  - inclusion of a pivoting strategy to avoid local minima or “too fast” obstacles

video 

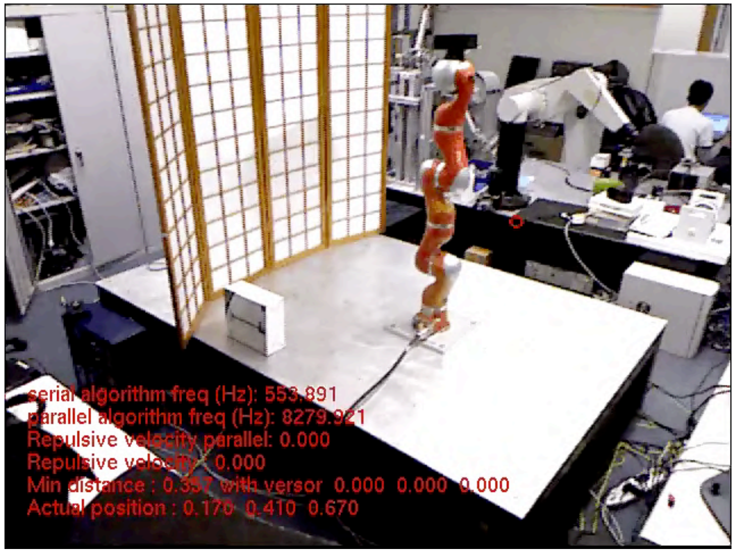 video

Obstacle velocity

The pivot method (similar to a vortex field)

- for moving obstacles that are faster than the control point (on the robot)

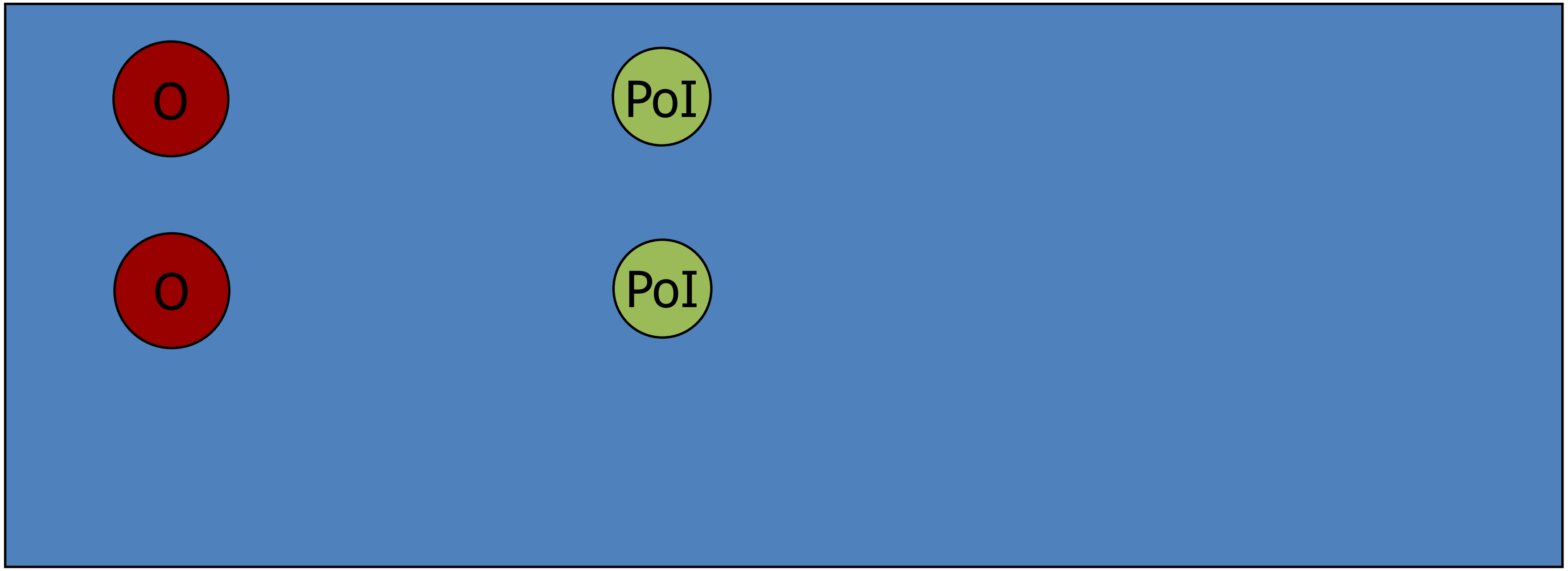

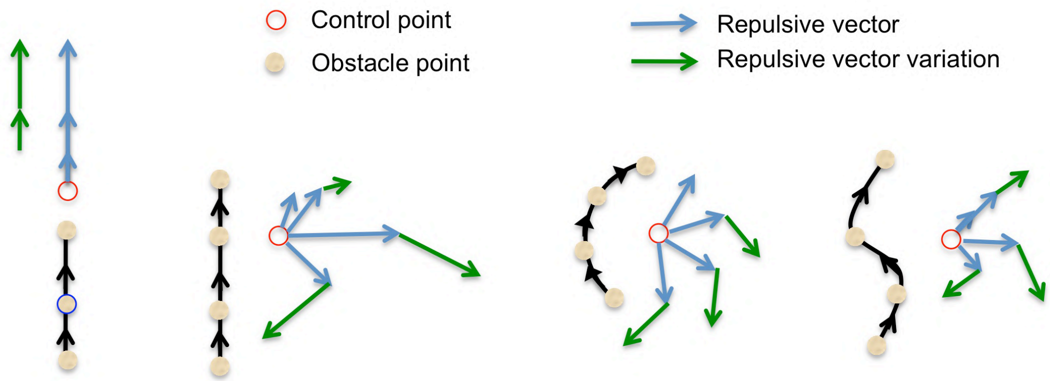

$$\boldsymbol{a} = \frac{\dot{\boldsymbol{V}}_R(\boldsymbol{P})}{\|\dot{\boldsymbol{V}}_R(\boldsymbol{P})\|}, \quad \boldsymbol{r} = \frac{\boldsymbol{V}_R(\boldsymbol{P})}{\|\boldsymbol{V}_R(\boldsymbol{P})\|}, \quad \beta = \arccos\left(\boldsymbol{a}^T \boldsymbol{r}\right)$$

if $\beta < \frac{\pi}{2}$ **then**

$$\boldsymbol{n} = \boldsymbol{a} \times \boldsymbol{r}, \qquad \boldsymbol{v} = \frac{\boldsymbol{n} \times \boldsymbol{a}}{\|\boldsymbol{n} \times \boldsymbol{a}\|},$$

$$\gamma = \beta + \frac{\beta - \frac{\pi}{2}}{1 + e^{-(\|\dot{\boldsymbol{V}}_R(\boldsymbol{P})\|(2/\dot{V}_{R_{\max}}) - 1)c}},$$

$$\boldsymbol{V}_{R_{\text{pivot}}}(\boldsymbol{P}) = \|\boldsymbol{V}_R(\boldsymbol{P})\| \left(\cos\gamma\, \boldsymbol{a} + \sin\gamma\, \boldsymbol{v}\right)$$

else

$$\boldsymbol{V}_{R_{\text{pivot}}}(\boldsymbol{P}) = \boldsymbol{V}_R(\boldsymbol{P})$$

end if

Motion control

Different handling of end-effector and other control points on the robot

- end-effector repulsive vector ➡ repulsive velocity added to the original task velocity
- collision avoidance for the whole robot body (e.g., 8 control points)
  - repulsive vector
  - Cartesian constraints
  - joint velocity limits modification (using SNS)

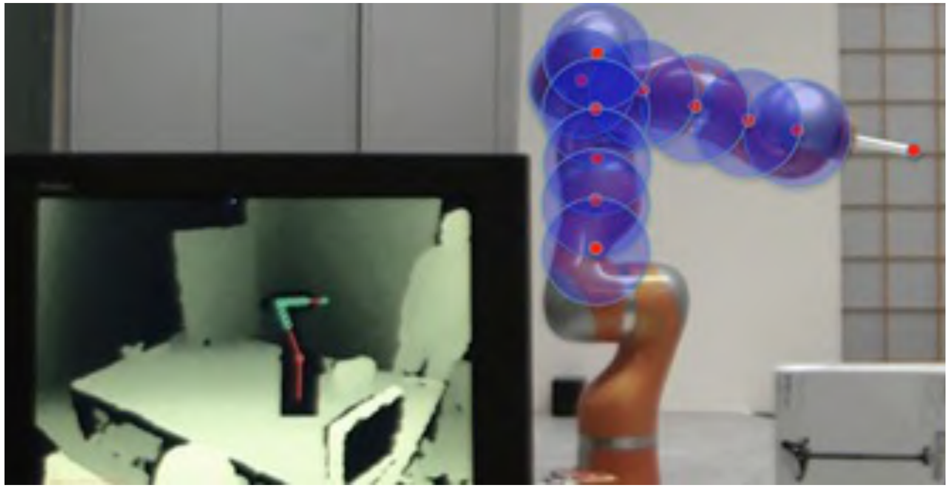

- fluid, jerk-limited motion ➡ human feeling of safety

Reflexxes GmbH

www.reflexxes.com

Safe coexistence

Collision avoidance in depth space (BioRob 2012)

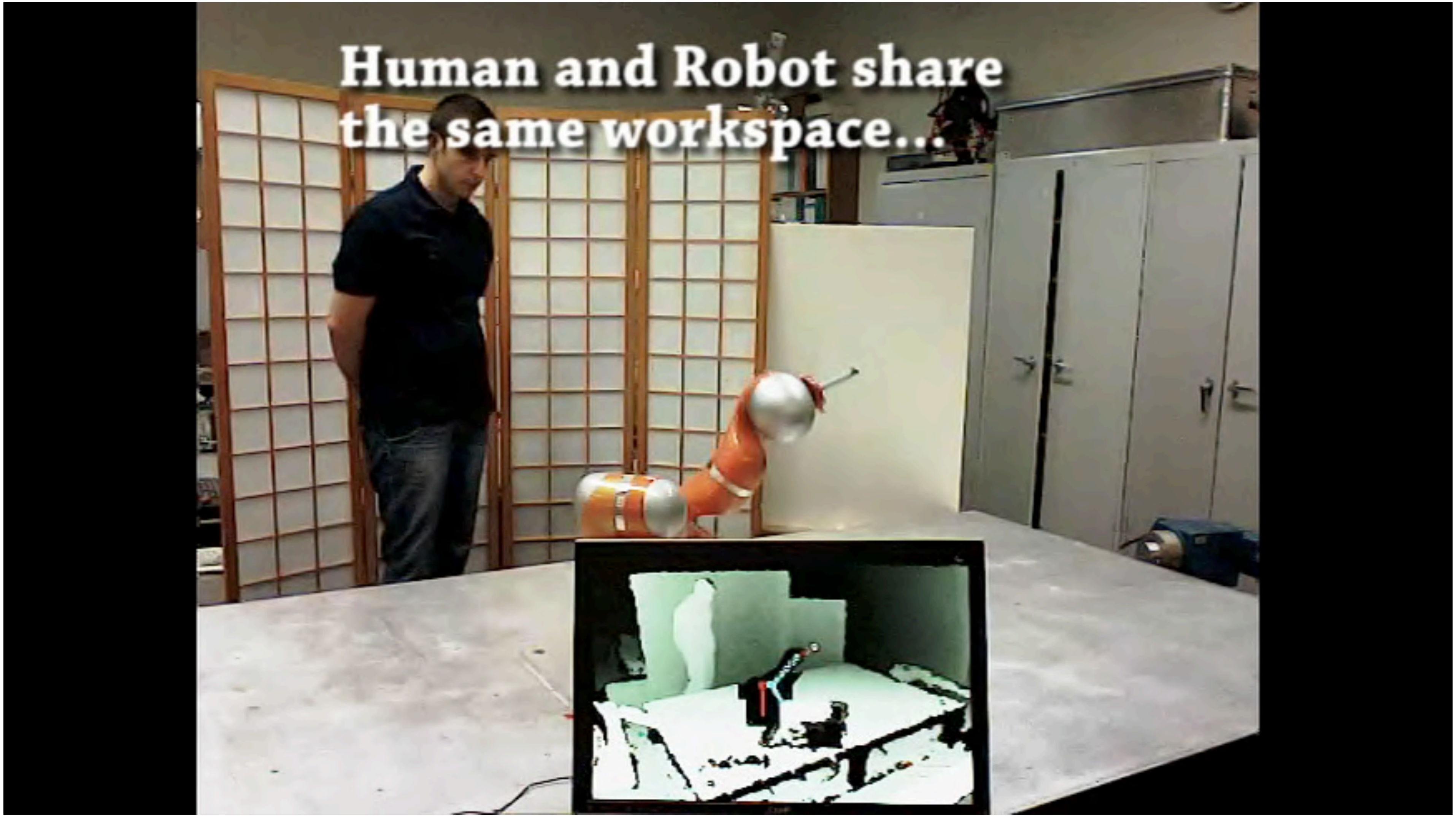

video

Safe coexistence

Collision avoidance in depth space (ICRA 2012, J. Intell. & Rob. Syst. 2015)

video

resuming a cyclic Cartesian task as soon as possible …

Monitoring the workspace with two Kinects

… without giving away the depth space computational approach (RA-L 2016)

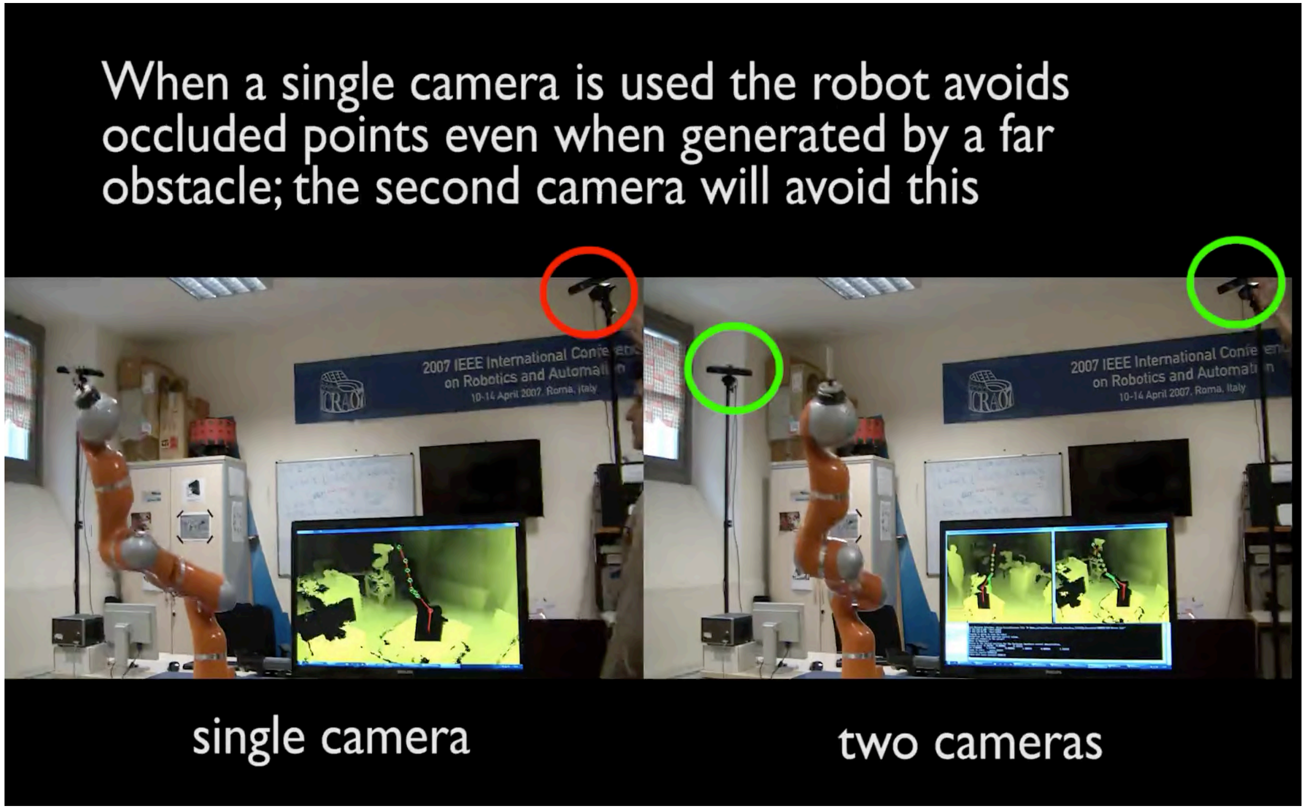

video

https://youtu.be/WIw_Uj_ooYI

real-time efficiency
algorithm extremely fast also with 2 devices: 300 Hz rate (RGB-D camera has 30 fps)

problems solved by the second camera

+ eliminates collision with false, far away “shadow” obstacles
+ reduces to a minimum gray areas, thus detects what is “behind” the robot
+ relative calibration of the two Kinects is done off-line

SYMPLEXITY cell for robotized work on metallic surfaces

For abrasive finishing/fluid jet polishing tasks & for **human-robot** quality assessment

SYMPLEXITY **H2020 FoF EU project (2015-18)**

- ABB IRB 4600-60 robot, with integrated SafeMove option
- certified communication with cell PLC, using ProfiSAFE protocol
- due to the intrinsic risks in the technological process, only for **HR coexistence** during visual check and measuring phase or for **contactless collaboration**
- **2 external** Kinects to recognize human gestures (e.g., automatic door opening, …)
- **initially** … **2 internal** Kinects (placed at the top corners of the cabin) for monitoring human-robot distances

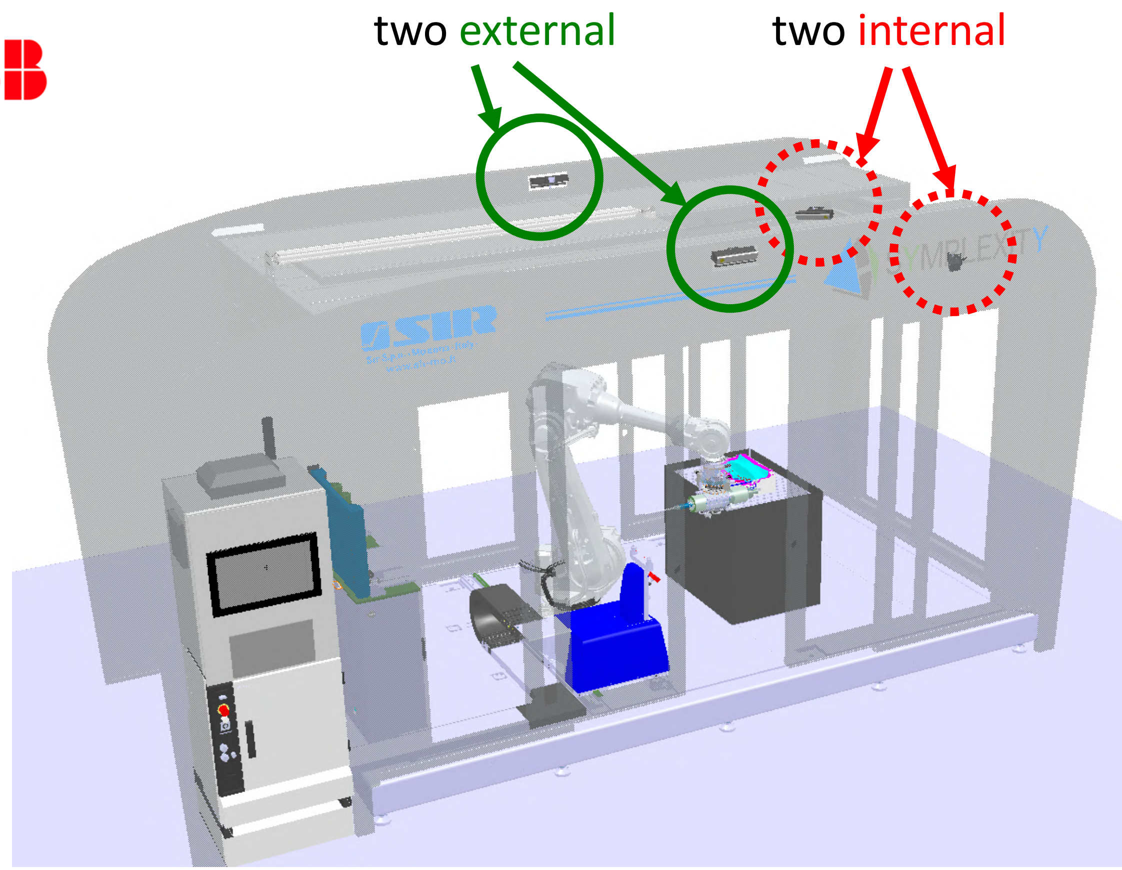

Additional safety hardware

Certified laser scanners to be used in parallel with the Kinects

SYMPLEXITY **H2020 FoF EU project (2015-18)**

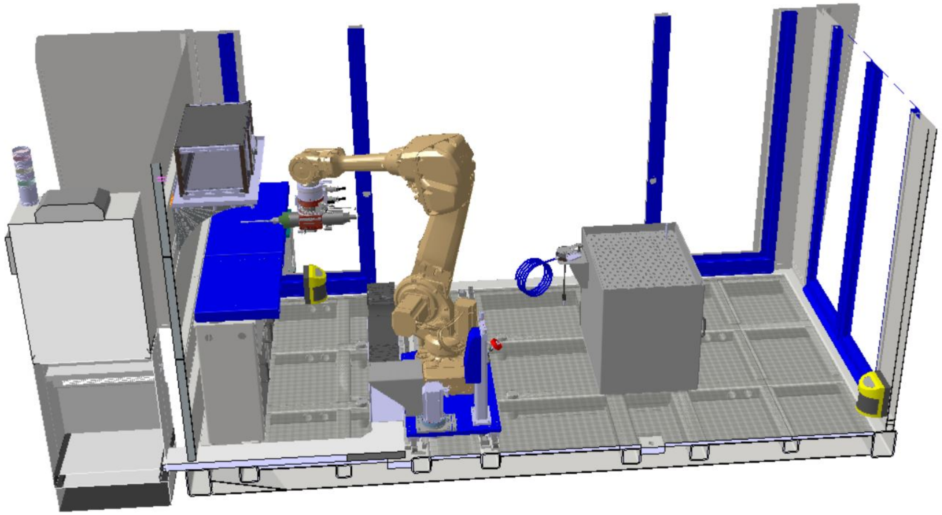

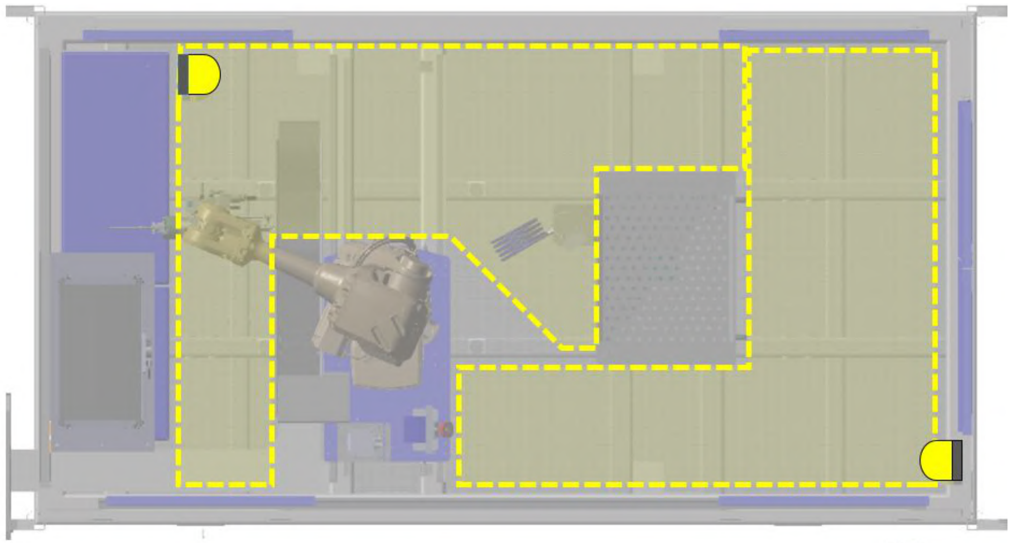

- **two laser scanners** KEYENCE SZ-V 32n placed at calf height (∼50 cm)
- maximize **coverage** of the free area inside the cell
- each sensor localizes the (radial) position of the operator in the cell, estimating an **approximate/conservative distance** to the robot
- **no missed situations**: robot slows down or stops according to sensed distance/area
- a **cascaded solution** of Kinects/laser scanners is a viable compromise between certified safety and more flexible sharing of the 3D workspace by human and robot

CAD robot model and equipment in depth images

Considering **CWS laser measuring device, cables** or other equipment in distance computation

CWS =
Coherent Wave Scattering

SYMPLEXITY **H2020 FoF EU project (2015-18)**

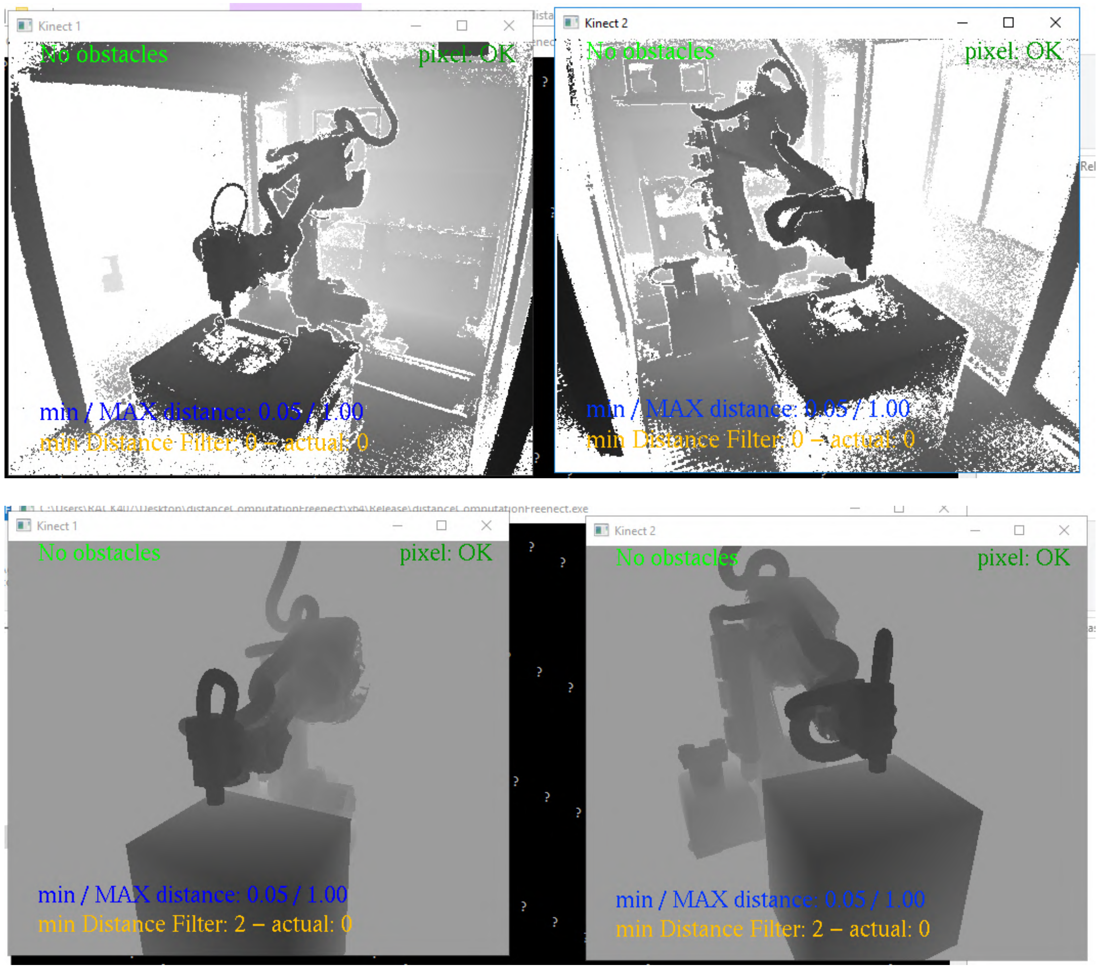

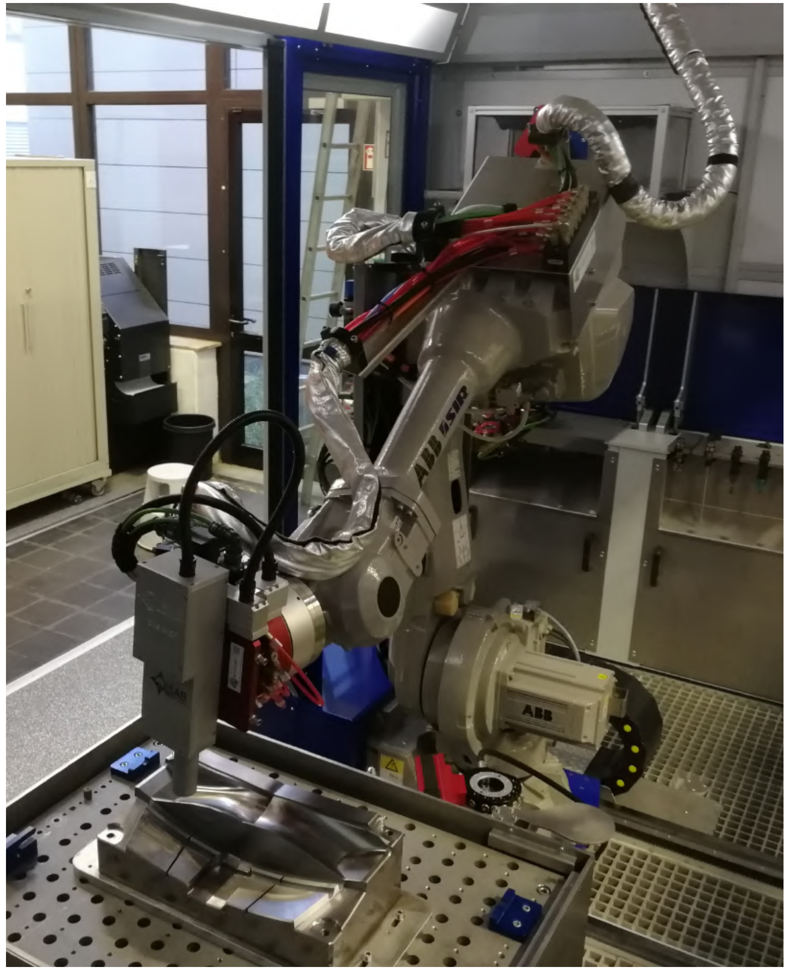

for each robotic set up, the suitable CAD model for depth space subtraction is loaded at start

Implemented control and communication architecture

Two **Kinects** for accurate HR distance monitoring, two **laser scanners** for backup safety

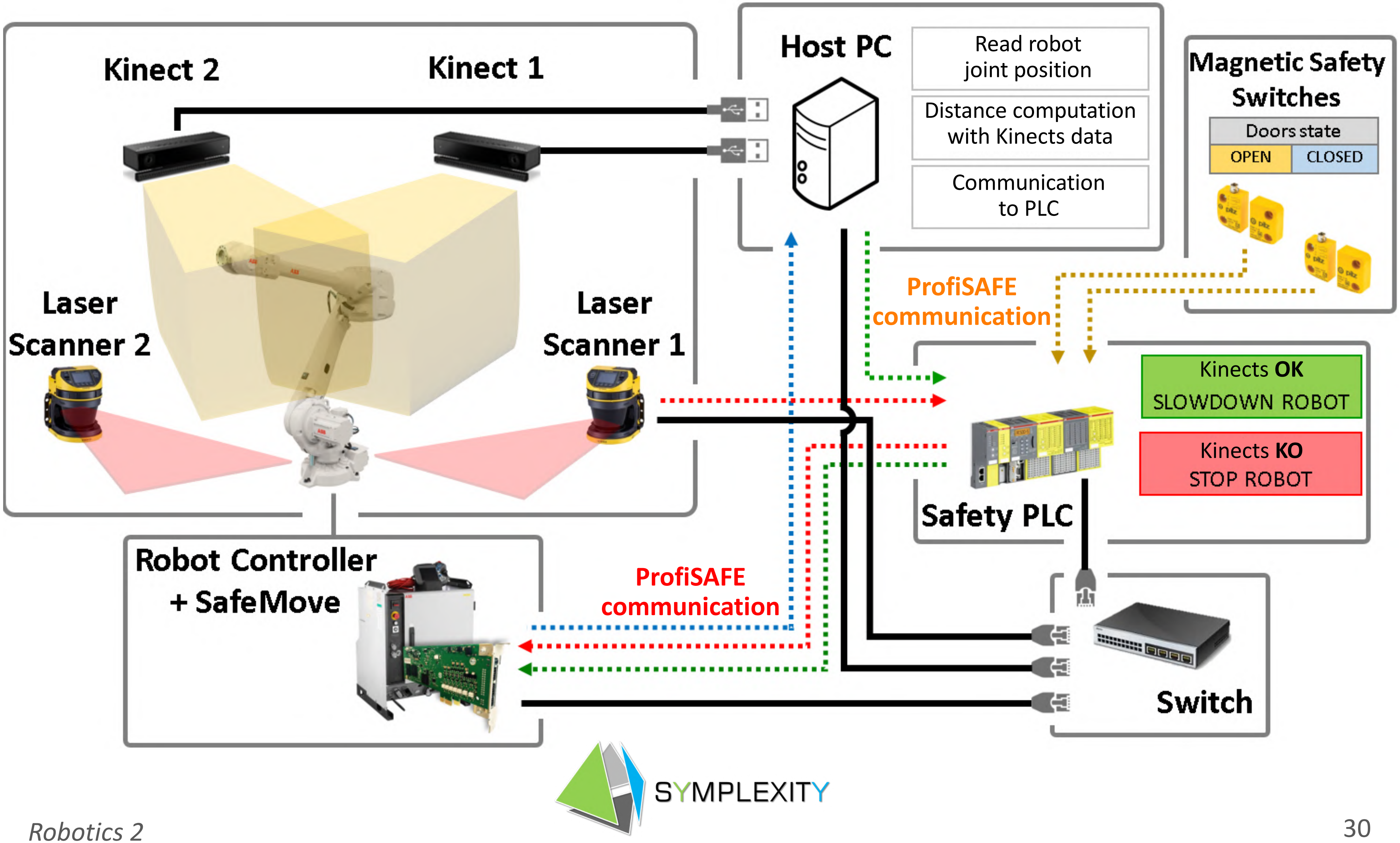

Safe coexistence in an industrial robotic cell

ABB IRB 4600 operation in an abrasive finishing cell with human access

video

video

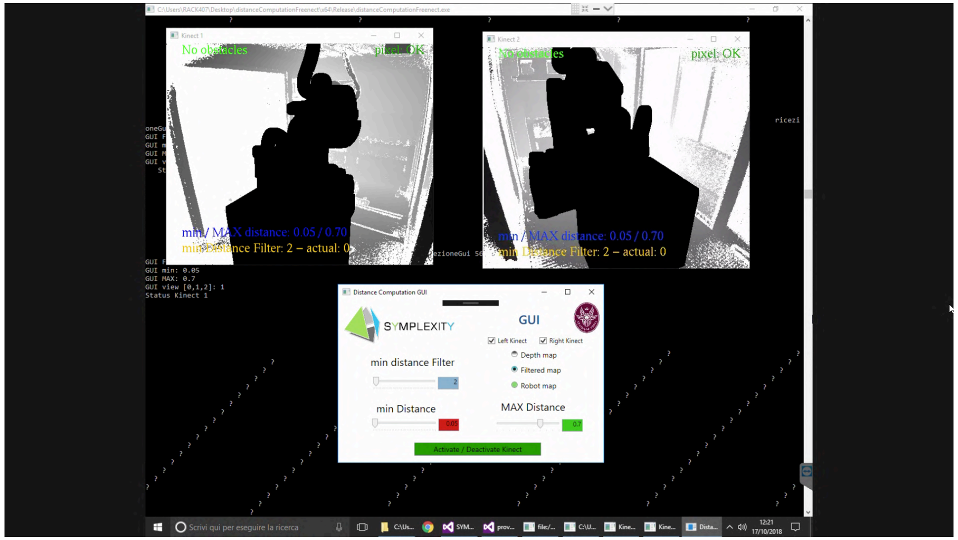

depth images and GUI

- robot is moving at max 100 mm/s
- no safety zones were defined in ABB SafeMove
- Kinects **OK** (except when the view of one of the cameras is obstructed on purpose)

SYMPLEXITY

Collaboration

Contactless or physical

- in **contactless** collaboration, robot (or human!) actions are guided or follow from an exchange of information without physical interaction
  - this can be achieved via **direct communication**, e.g., with gestures and/or voice commands
  - or via **indirect communication**, by recognizing human intention or attention, e.g., through eye gaze
  - another form is **visual coordination** in which vision is used to coordinate human-robot relative motion
- in **physical** collaboration, there is an explicit and intentional contact with exchange of forces between human and robot
  - by measuring or **estimating contact forces**, the robot can predict human motion intention and react accordingly to it
  - collaborative tasks (e.g., human and robot carrying a heavy object) require **control of exchanged forces (and motion)** at the contact

Contactless collaboration

Using gesture and voice commands

- human body parts and gesture recognition

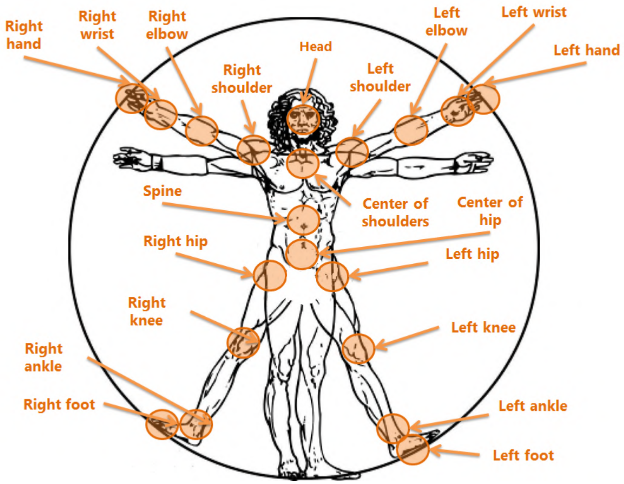

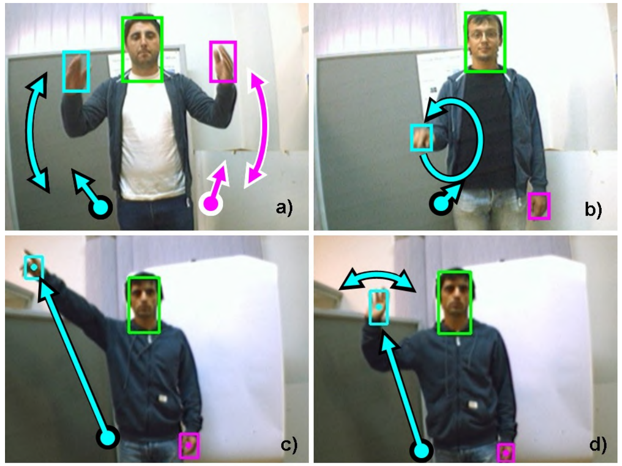

- speech recognition

voice command

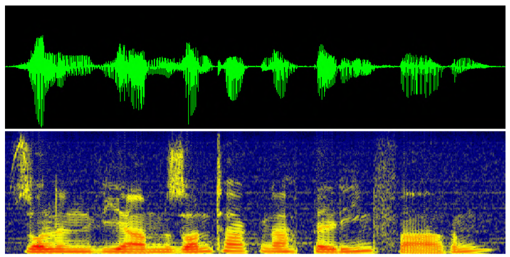

collaboration starts

Human-robot communication

Using Kinect and SDK library

- the robot end-effector **position** is commanded by voice/gestures to **follow** (or **go to**) the human **left**, **right**, or **nearest** hand

video

Gesture communication in SYMPLEXITY cell

Using Kinect 2.0 RGB-D sensor, with built-in skeleton tracking

- initial 5 sec gesture to activate
- both hands open = start motion
- both hands closed = stop robot
- left closed + right open = limit speed
- left open + right closed = recover speed
- final gesture to deactivate

video

Visual coordination task

Dual formulations of human-robot relative tracking (IROS 2017)

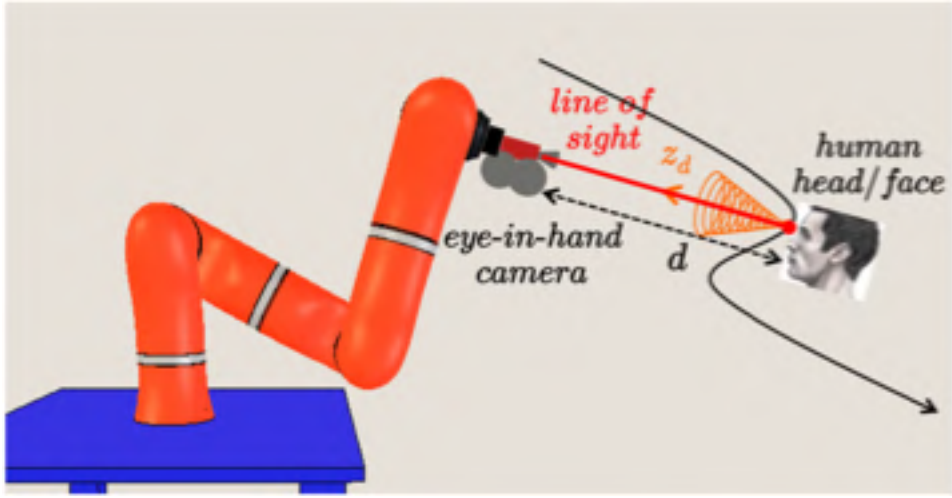

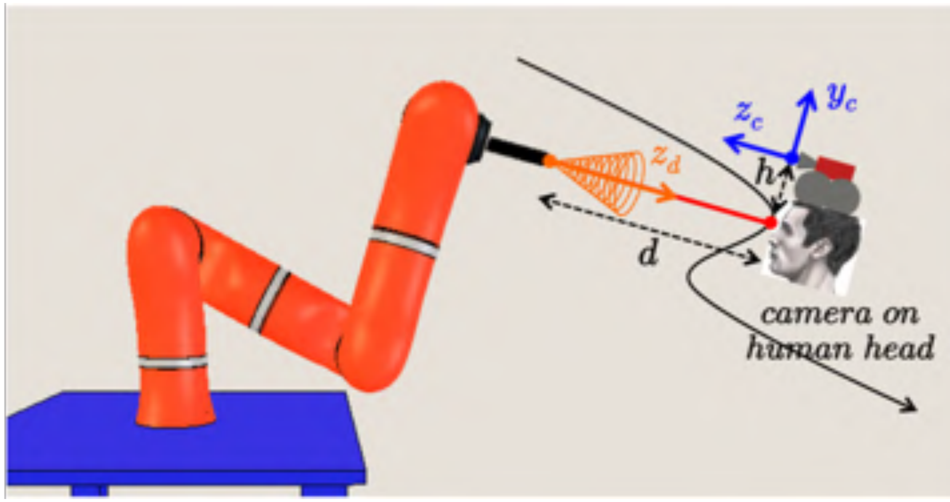

- camera on robot, pointing to moving human head/face kept at a certain relative position
- camera on human head, with robot pointing to it and kept at a certain relative position

different Cartesian motion tasks of varying dimension $m \leq n$

cone represents a relaxation of the pointing task by some relative angle α_d

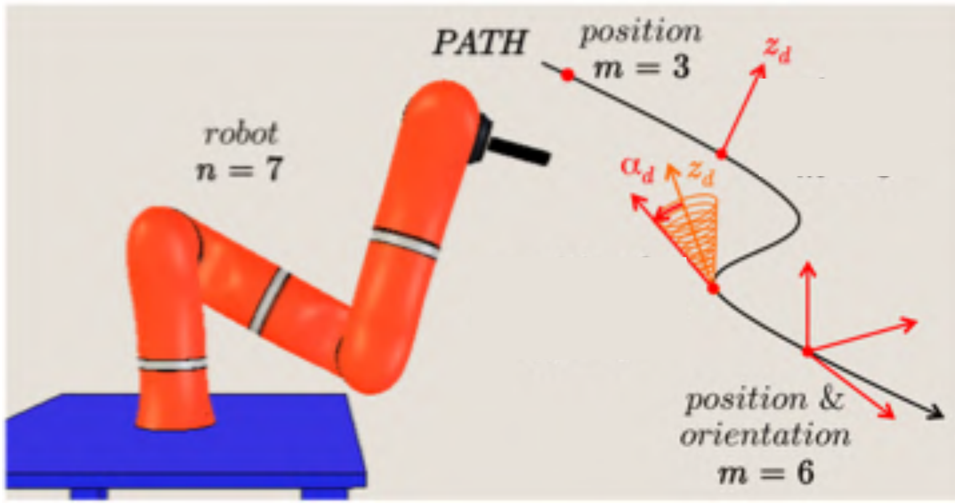

Simulation

Motion control using Task Augmentation method

- camera tracing a circle in a vertical plane, while pointing direction is kept constant

ROS environment, integrated with robot simulator V-REP

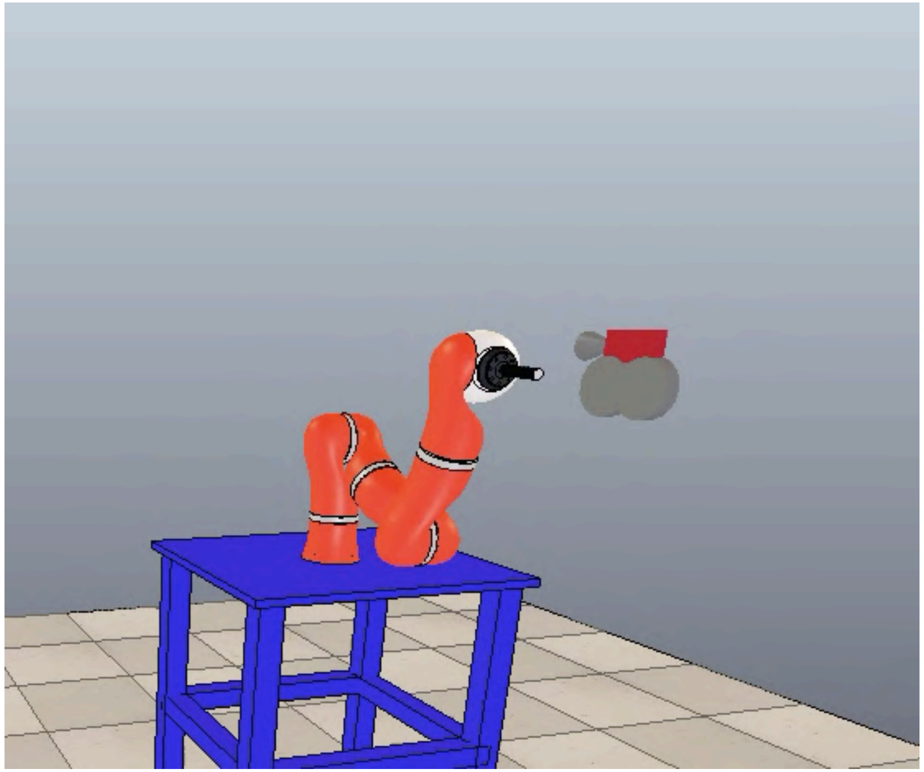

video

position errors **< 1.5 mm**

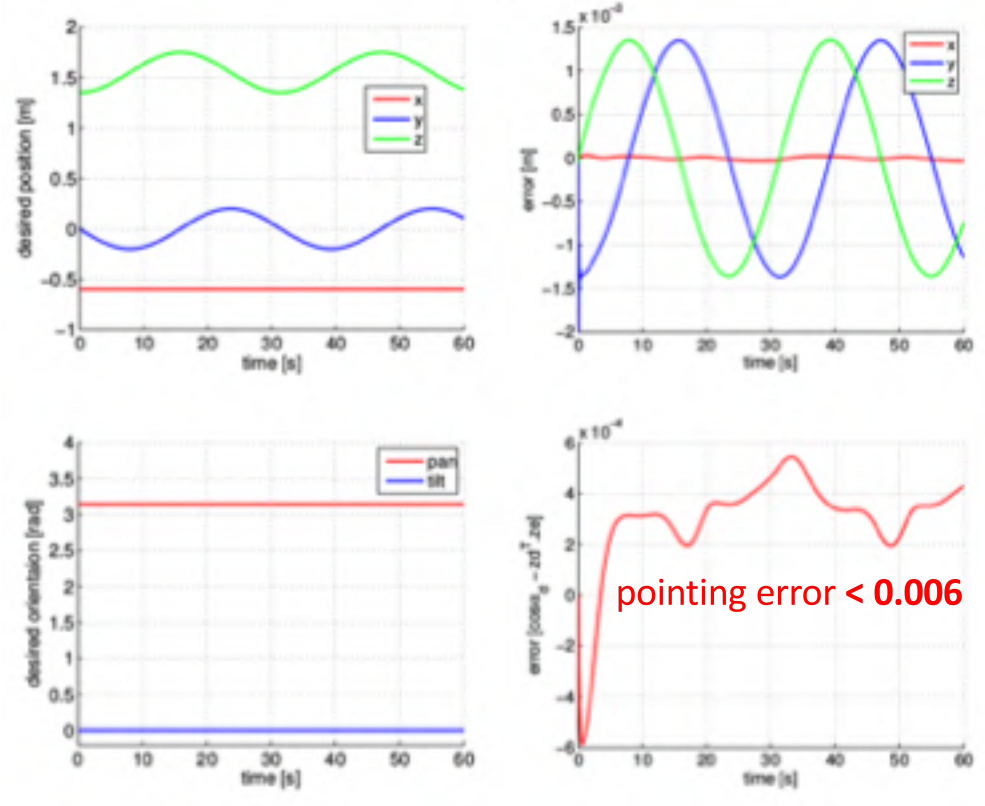

Experiment of visual coordination

KUKA LWR robot in ROS environment with FRI

https://youtu.be/SRfpNrZD7k0

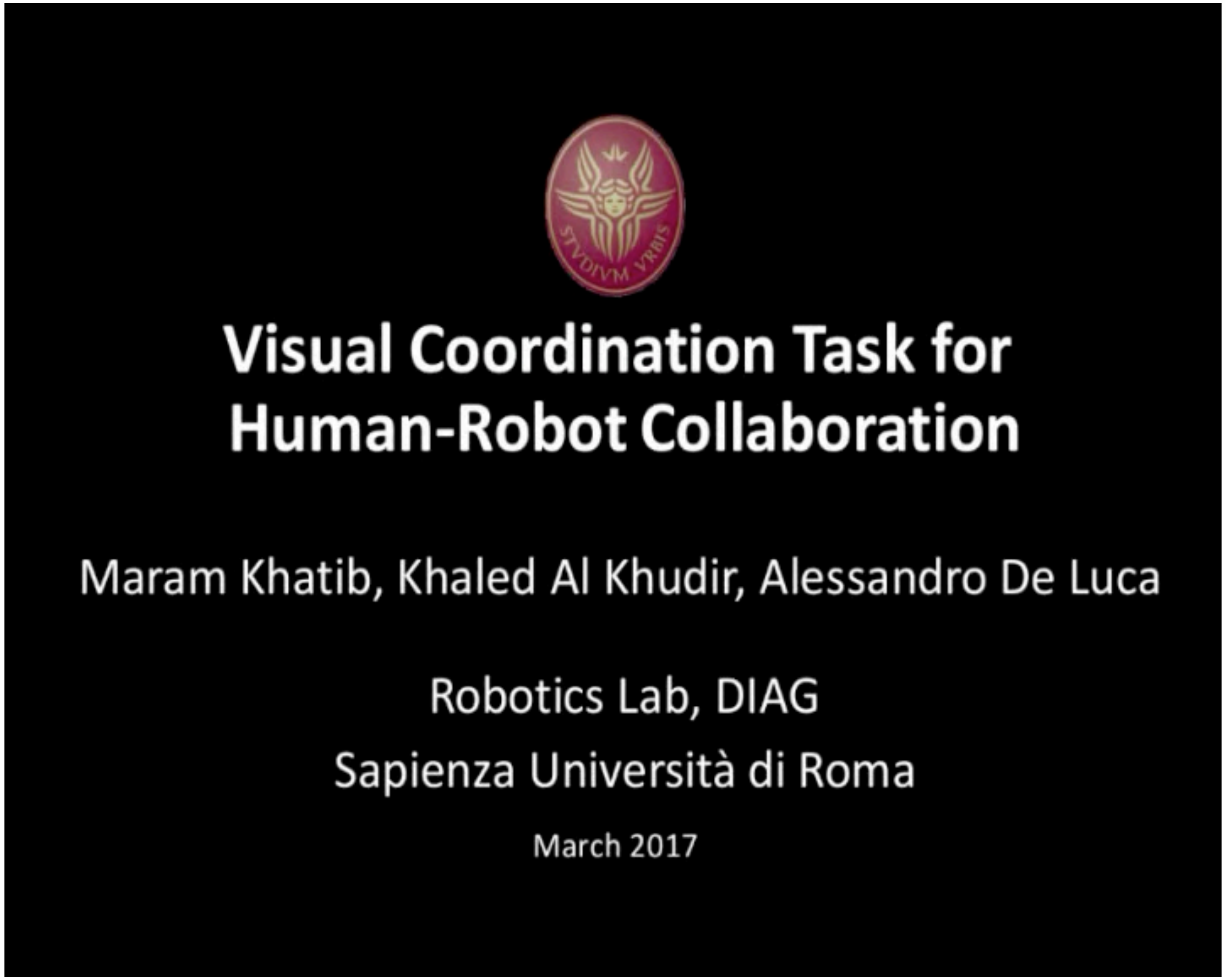

video

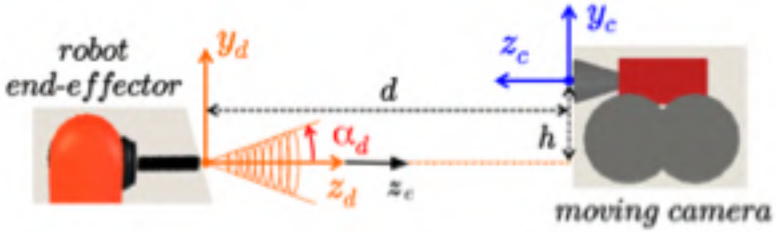

position error ≤ **5 cm** pointing error **< 0.03 rad**

also in multi-sensory operation

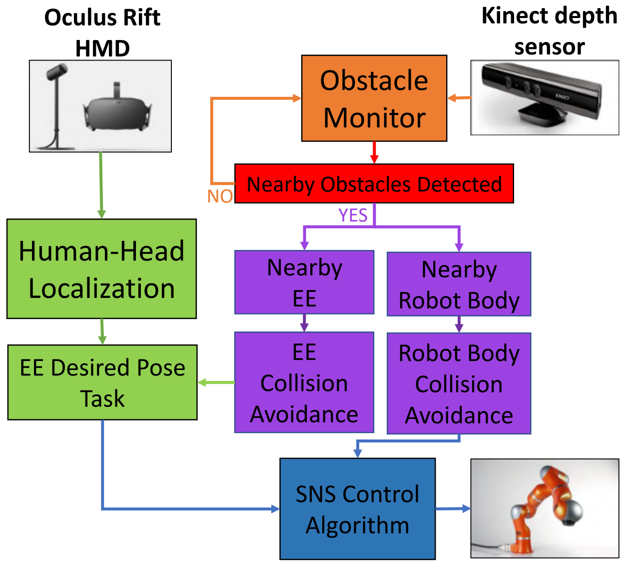

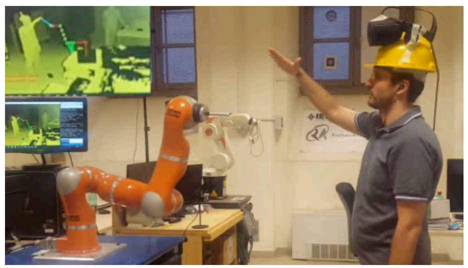

Safe human-robot interaction

From coexistence to physical collaboration

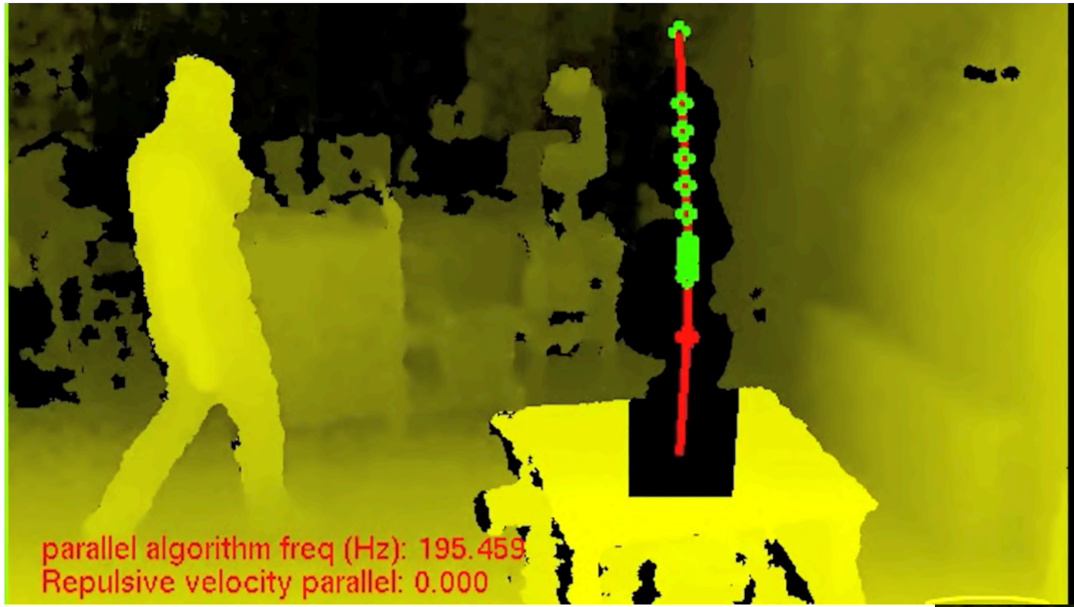

video

coexistence through
collision avoidance

https://youtu.be/pIlhY8E3HFg

video

physical collaboration through
contact identification
(here, end-effector only)

Distance and contact point localization

Using Kinect, CAD model, and distance computation to localize contact (early 2014)

- **depth image** is acquired by a Kinect
- robot is removed from image (URDF filter by TUM), starting from its 3D CAD model
- human hand tracking on filtered image
- **3D CAD model of robot** and hand position are used to localize contact point on robot surface
- surfaces of robot links are modeled using polygonal patches
- 3D robot model is projected in workspace with a calibration matrix
- **distances are computed** between vertices of patches and the human hand
- ranges vary from about 20 cm (area of interest) down to 0 (contact)
- **residuals** are always zero when robot moves in free space

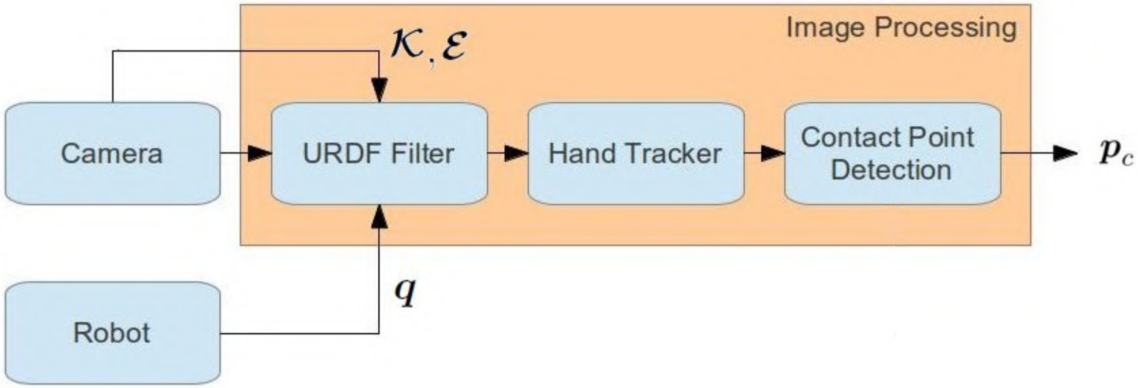

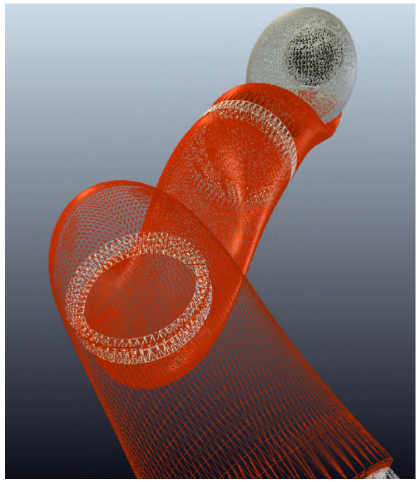

Distance and contact point localization

Use **residuals** to detect the contact event, also for multiple locations

- when the **residual** indicates a **contact/collision** (and colliding link), the **vertex** in the robot CAD surface model **with minimum distance** is taken as the **contact point**
- algorithm applied here in parallel to both **left** and **right** hand (no other body parts)

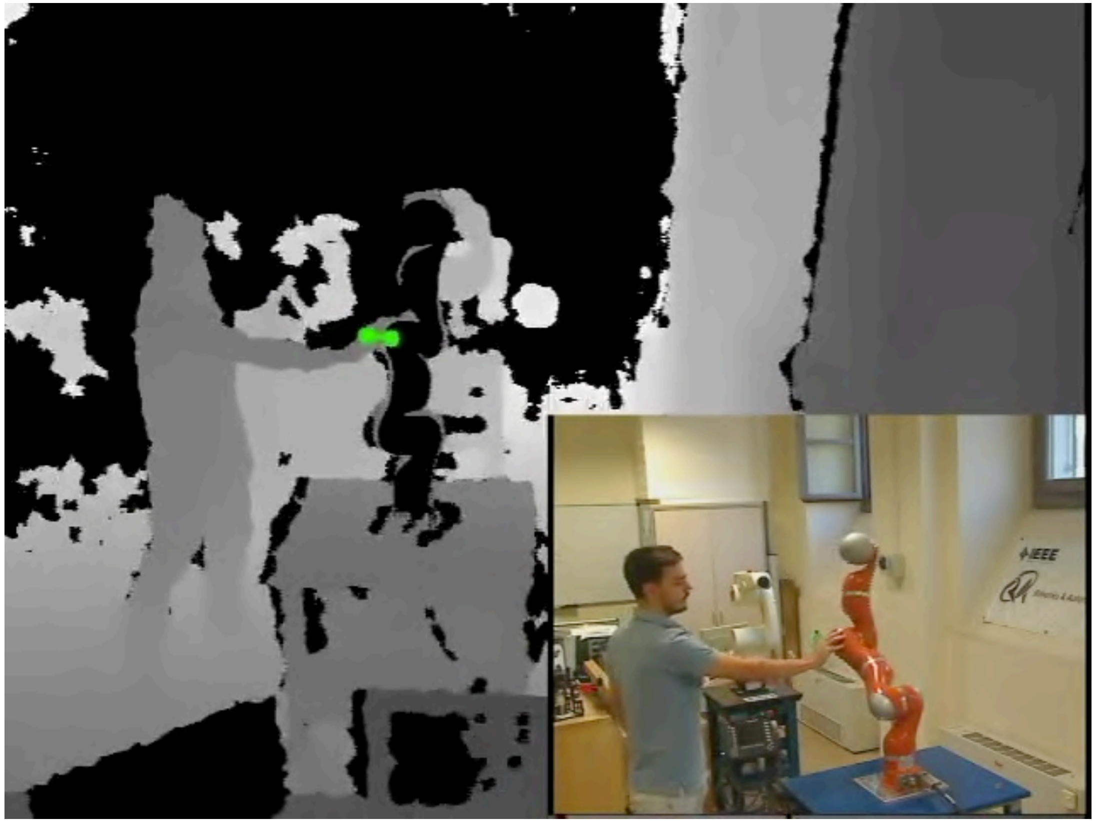

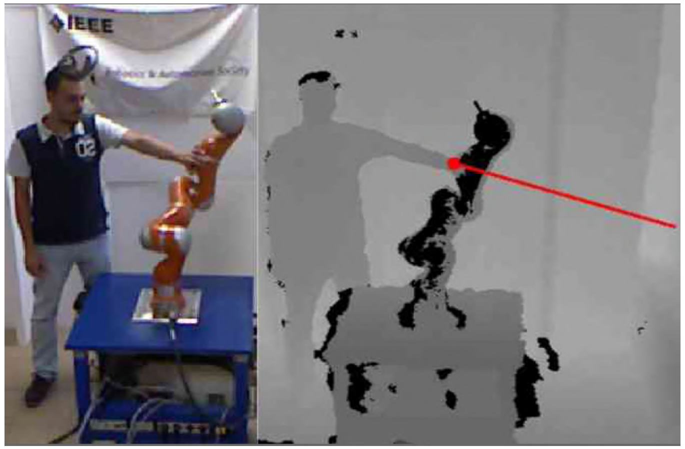

video

Improved contact point localization

Real-time localization using the CUDA framework (IROS 2017)

- the algorithm, based on distance computation in depth space, takes advantage of a **CUDA framework** for massively parallel **GPU** programming; **three 2.5D images** are processed:
  - real depth image I_r, captured by a RGB-D sensor (a Kinect)
  - virtual depth image I_v , containing only a projection of the robot CAD model
  - filtered depth image $I_f = f(I_r, I_v)$, containing only the obstacles

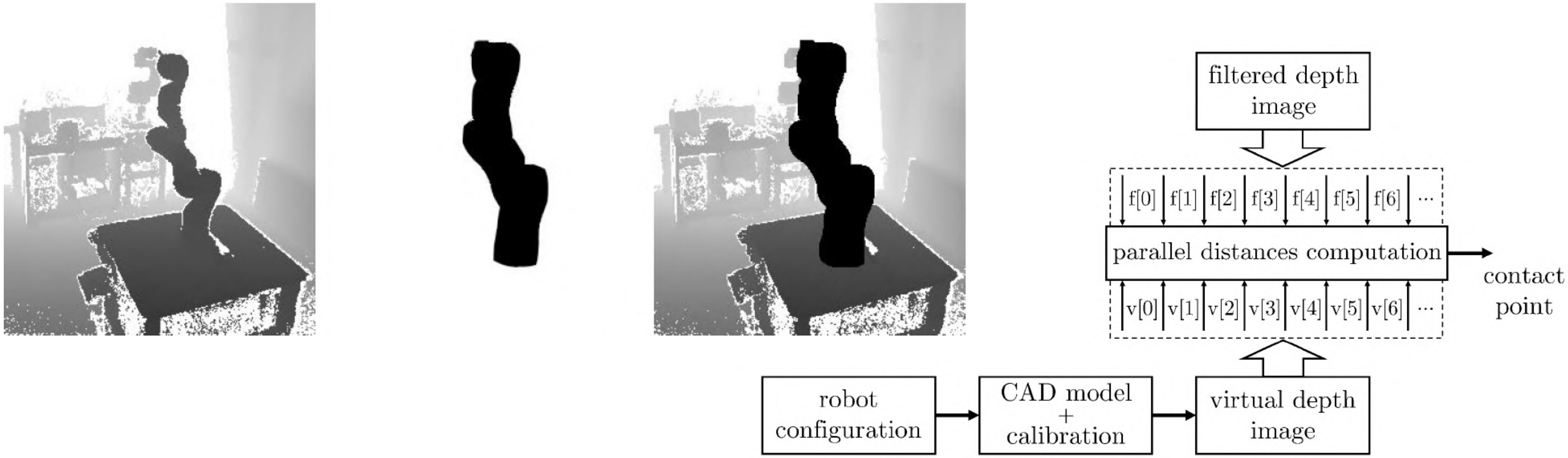

- parallel **distance computations** between **all robot points** in virtual image and **all obstacle points** in filtered image (same time needed to localize one or multiple contact points!)

Contact force estimation

Combining internal and external sensing

- task
  - localize (in the least invasive way) points on robot surface where contacts occur
  - estimate exchanged **Cartesian** forces
  - control the robot to react to these forces according to a desired behavior
- solution idea
  - use residual method to **detect** physical contact, **isolate** the colliding link, and **identify** the joint torques associated to the external contact force
  - use a depth sensor to **classify** the human parts in contact with the robot and **localize** the contact points on the robot structure (and the **contact Jacobian**)
  - **solve** a linear set of equations with the residuals, i.e., estimates of joint torques resulting from **contact wrenches** (forces/moments) applied anywhere to the robot

$$\boldsymbol{r} \simeq \boldsymbol{\tau}_{ext} = \boldsymbol{J}_c^T(\boldsymbol{q})\boldsymbol{\Gamma}_c = \begin{pmatrix} \boldsymbol{J}_{L,c}^T(\boldsymbol{q}) & \boldsymbol{J}_{A,c}^T(\boldsymbol{q}) \end{pmatrix} \begin{pmatrix} \boldsymbol{F}_c \\ \boldsymbol{M}_c \end{pmatrix}$$

Contact force estimation

Some simplifying assumptions

- dealing with contact forces
  - most **intentional** contacts with a single human part (hand, arm, fingers) are **not** able to transfer relevant **torques**
  - to estimate reliably $\boldsymbol{\Gamma}_c$ we should have rank $\boldsymbol{J}_c = 6$, which is true only if the robot has $n \geq 6$ joints and the contact occurs at a link with index ≥ 6

assume $\boldsymbol{M}_c = \mathbf{0}$

only a **pure Cartesian force** is considered

  - dimension of the task related to the contact force is now $m = 3$ and its **estimation** is

$$\boldsymbol{r} \simeq \boldsymbol{\tau}_{ext} = \boldsymbol{J}_{Lc}^T(\boldsymbol{q})\boldsymbol{F}_c \quad \Rightarrow \quad \widehat{\boldsymbol{F}}_c = \left(\boldsymbol{J}_{Lc}^T(\boldsymbol{q})\right)^{\#} \boldsymbol{r}$$

  - the contact Jacobian can be evaluated once the contact point is detected by the external depth sensor that closely monitors the robot workspace
  - this procedure represents a so-called **virtual force sensor**

Validation of virtual force sensor

Experiments in static conditions with the KUKA LWR 4 (IROS 2014)

- evaluation of estimated contact force

$$\widehat{\boldsymbol{F}}_c = \left(\boldsymbol{J}_c^T(\boldsymbol{q})\right)^{\#} \boldsymbol{r}$$

  - estimation accuracy was initially tested using known masses in known positions
  - a single mass hung either on link 4 or on link 7, to emulate a **single** (point-wise) contact

			using $\boldsymbol{J}_{Lc}$		using $\boldsymbol{J}_c$	
Link #	Mass	F_z	$\widehat{F}_z$	Deviation	$\widehat{F}_z$	Deviation
4	1.93	-18.93	-18.75	0.95%	-4.46	76.43%
7	1.93	-18.93	-18.91	0.1%	-18.82	0.58%

  - a mass hung on link 7, and then a second on link 4 so as to emulate a **double** contact

Link #	Mass	F_z	$\widehat{F}_z$	Deviation
4	2.03	-19.91	-19.43	2.41%
7	1.93	-18.93	-19.04	0.58%

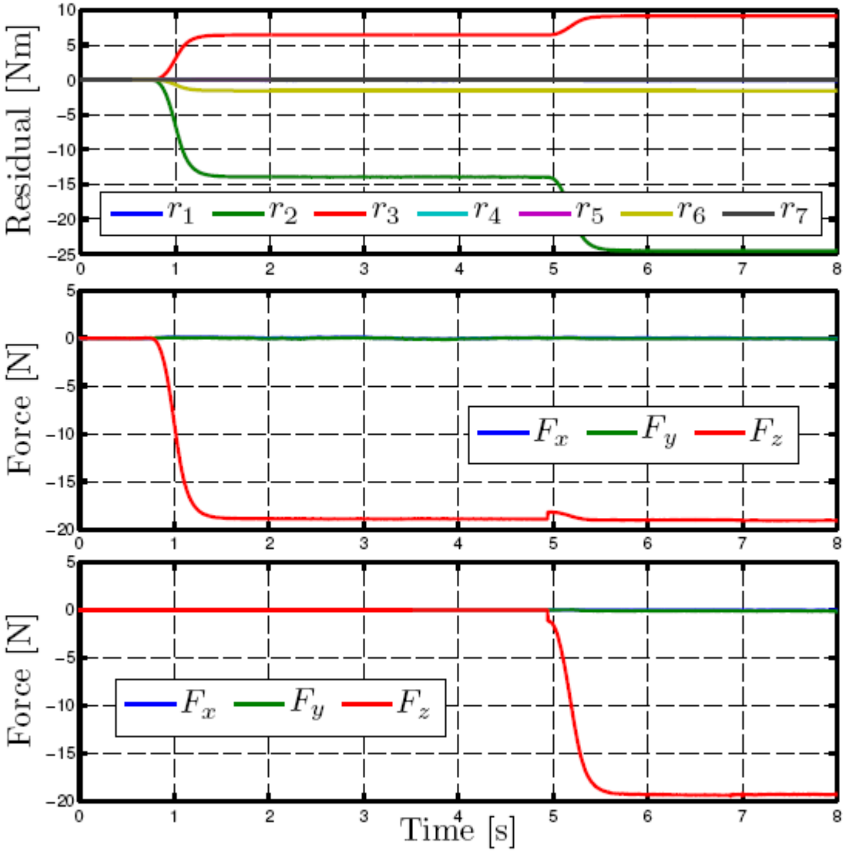

case of two masses

On-line estimation of contact force

Used within an admittance control scheme (IROS 2014)

https://youtu.be/Yc5FoRGJsrc

video

On-line estimation of contact force

Evolution of residuals, estimated forces, and compliant displacements

- control gains are chosen so as to assign a **stiff** behavior at a reference configuration
- at some time, human pushes on robot link 3
- due to the stiff robot behavior, a large force needs to be applied to move the robot
- when the hand is removed, the contact point returns smoothly to its initial position (zero error)

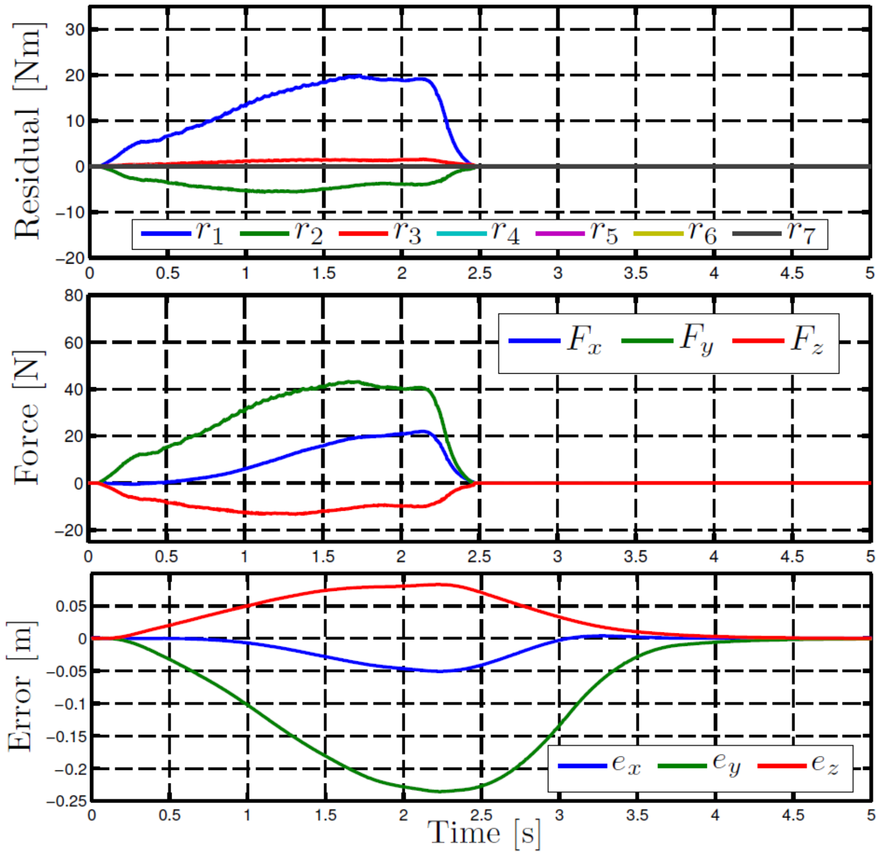

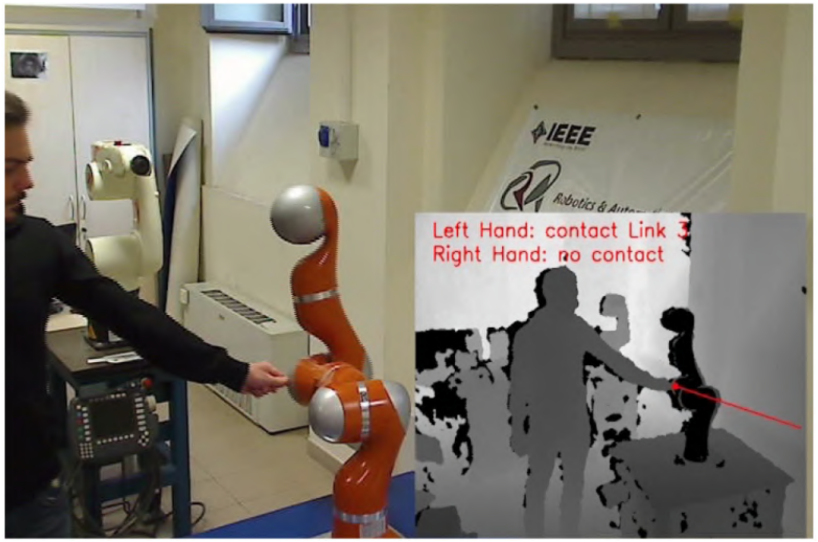

see slide #54 for the chosen **admittance control** scheme

Further validation of virtual force sensor

In static and dynamic conditions, using a hand-held F/T sensor (February 2019)

- comparing the F/T ground truth contact force measure with its residual-based estimation
  - with robot at rest (pushing)
  - in robot motion (hitting)

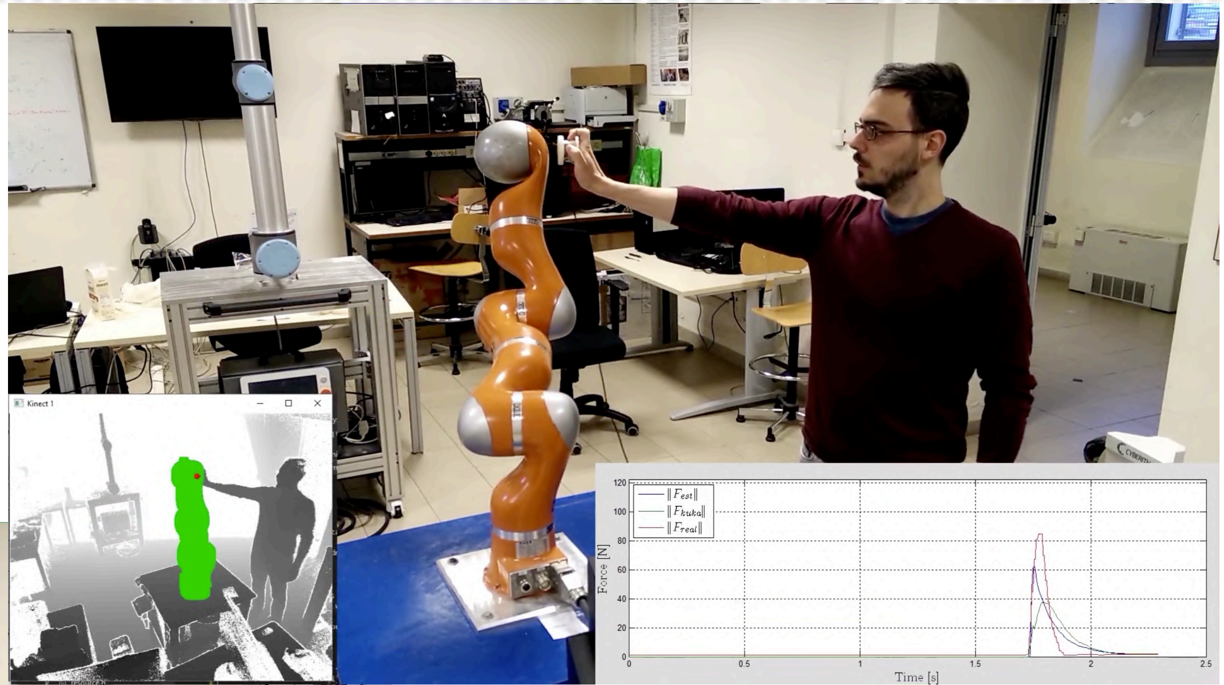

video

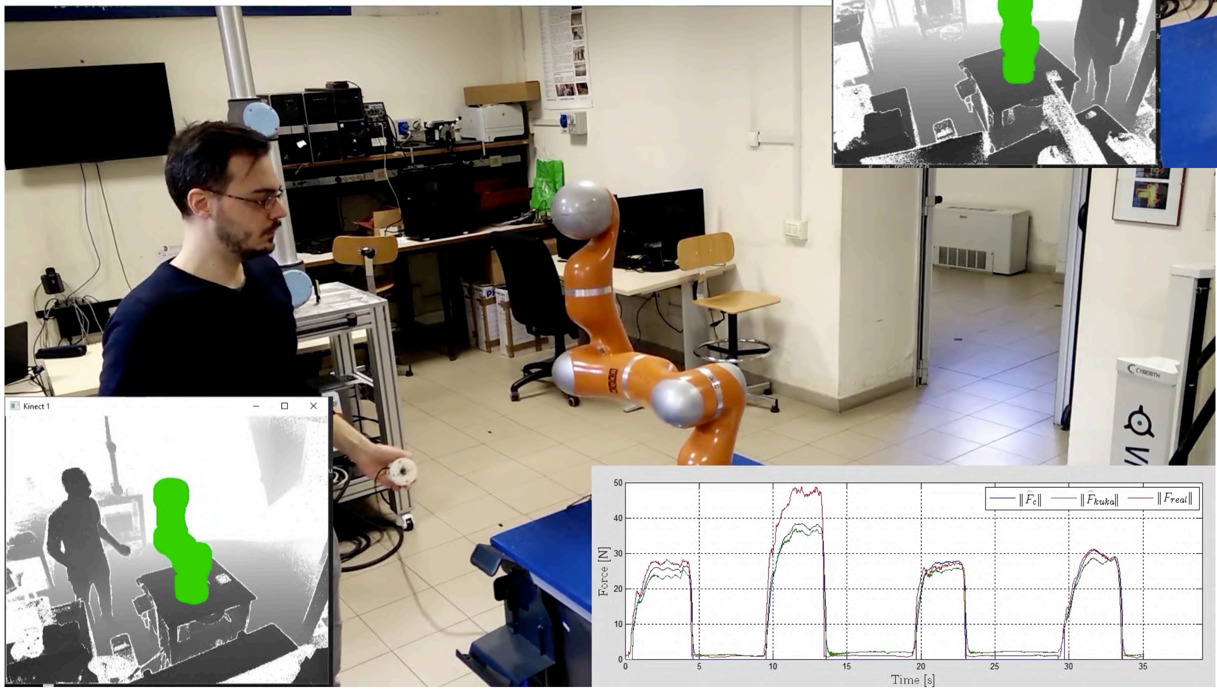

outgrowth of Emanuele Magrini's PhD thesis, May 2016

video

Estimation of contact force

Some limitations of the residual method

- **multiple** simultaneous contacts can be considered (e.g., with **both** human hands)

$$\begin{pmatrix} \widehat{\boldsymbol{F}}_1 \\ \widehat{\boldsymbol{F}}_2 \end{pmatrix} = \begin{pmatrix} \boldsymbol{J}_{L1}^T(\boldsymbol{q}) & \boldsymbol{J}_{L2}^T(\boldsymbol{q}) \end{pmatrix}^{\#} \boldsymbol{r}$$

but with much less confidence in the resulting force estimates (detection is still ok)

- estimates will be limited only to those components of $\boldsymbol{F}_c$ which can be detected by the residual (i.e., that produce work on robot motion)

- all forces $\boldsymbol{F}_c \in \mathcal{N}(\boldsymbol{J}_c^T(\boldsymbol{q}))$ will never be recovered $\Leftrightarrow$ they are 'absorbed' by the robot structure

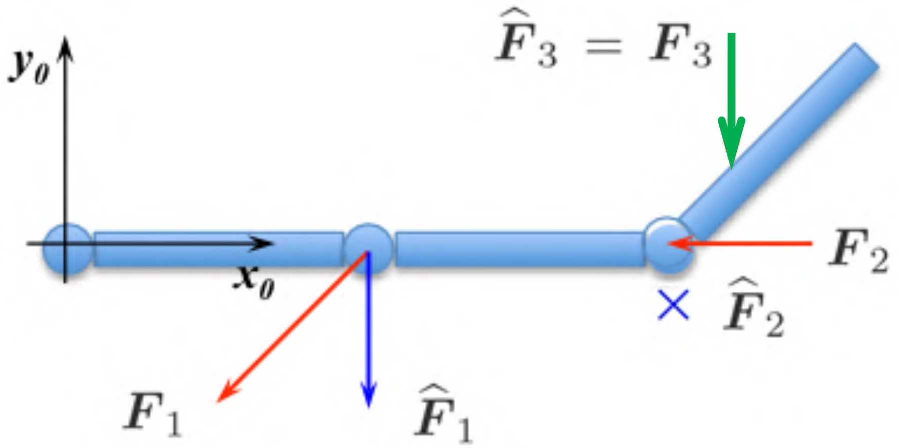

Estimation of contact force

Sometimes, even **without** external sensing

- if contact is sufficiently "down" along the kinematic chain (**≥ 6 residuals** available), the estimation of **pure contact forces** does not need any external information ...

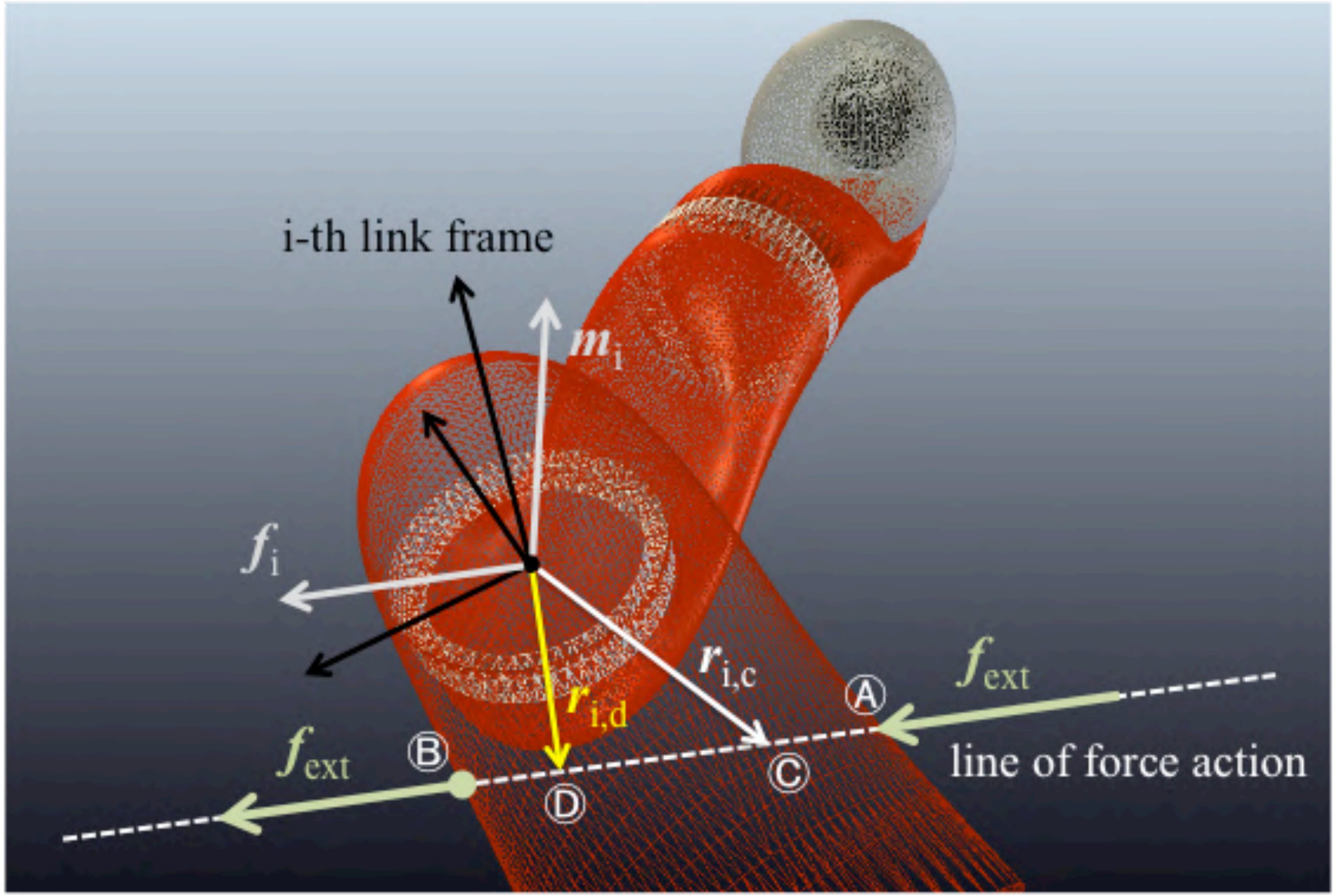

A closer analysis

Which force components are being estimated? Do we really need external sensing?

- a simple 3R planar case, with contact on different links

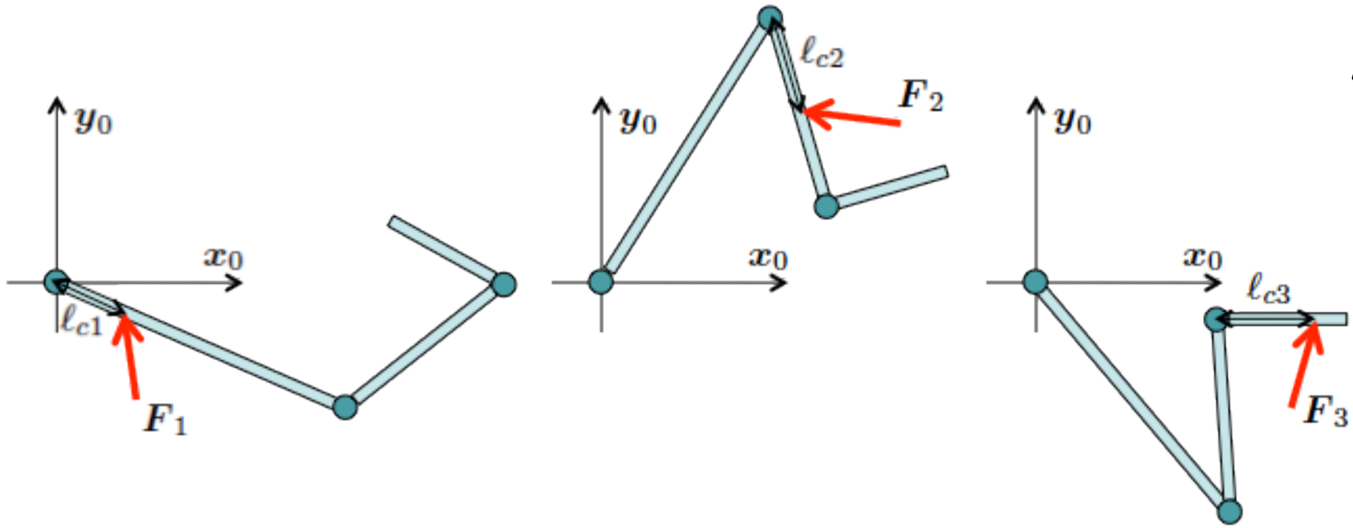

$\boldsymbol{r}$ is a vector of dimension 3

rank $\{ \boldsymbol{J}_{c1} \} = 1$	rank $\{ \boldsymbol{J}_{c2} \} = 2$	rank $\{ \boldsymbol{J}_{c3} \} = 2$
only normal force to link, if contact point is known (1 informative residual signal)	full force on link, if contact point is known (2 informative residuals)	full force on link, **even without** knowing contact (**3** informative residuals)

$\boxed{\hat{\boldsymbol{F}}_i}$

- forces $\boldsymbol{F}_k \in \mathcal{N}(\boldsymbol{J}_k^T(\boldsymbol{q}))$ will never be recovered (even with known contact)

Additional F/T sensor at the base

Combining real & virtual sensors for estimating interaction forces/moments (IROS 2016)

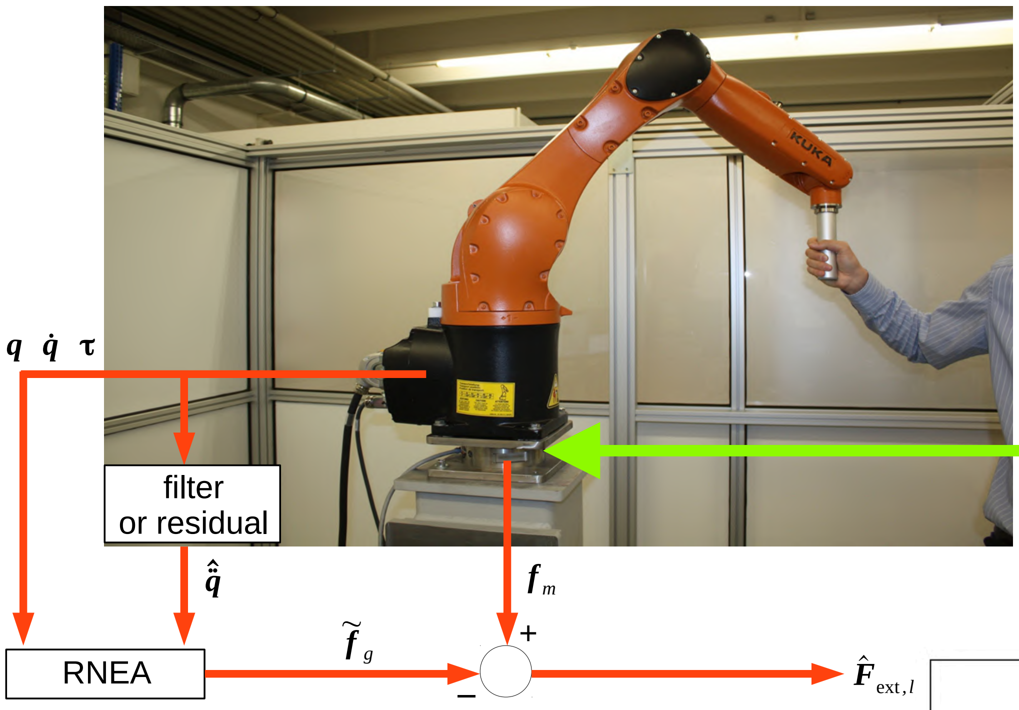

KUKA 6-dof Agilus robot (@Augsburg)

- Recursive Newton-Euler Algorithm (fed by the residuals) for **ground force/moment** prediction
- comparison with **base F/T sensor readings**

(large) F/T sensor mounted at the base

- an external wrench acting on link l will only affect the first l components of $\boldsymbol{\tau}_{ext}$
- effect of $\boldsymbol{F}_{ext}$ on $\boldsymbol{\tau}_{ext}$ depends on point $\boldsymbol{p}_l$ while that of $\boldsymbol{M}_{ext}$ does not, since only the contact link is relevant (isolated by residual)

Table of **possible options/improvements** for a contact wrench $\boldsymbol{W}_{ext,l} = (\boldsymbol{F}_{ext,l}\ ,\ \boldsymbol{M}_{ext,l})$

	l	Known $\boldsymbol{p}_l$	Unknown $\boldsymbol{p}_l$ with pure contact force
$\boldsymbol{F}/\boldsymbol{T}$ sensor at the base	any	Estimate $\boldsymbol{W}_{ext,l}$	Estimate $\boldsymbol{F}_{ext,l}$ and $\boldsymbol{p}_l$
$\boldsymbol{F}$ sensor at the base	any	Estimate $\boldsymbol{F}_{ext,l}$	Estimate $\boldsymbol{F}_{ext,l}$
	≥ 3	Estimate $\boldsymbol{W}_{ext,l}$	Estimate $\boldsymbol{F}_{ext,l}$ and $\boldsymbol{p}_l$
No sensor at the base	≥ 6	Estimate $\boldsymbol{W}_{ext,l}$	Estimate $\boldsymbol{F}_{ext,l}$ and $\boldsymbol{p}_l$

Collision or collaboration?

Distinguishing hard/accidental collisions and soft/intentional contacts

- using suitable low and high bandwidths for the residuals (first-order stable filters)

$$\dot{\boldsymbol{r}} = -\boldsymbol{K}_I \boldsymbol{r} + \boldsymbol{K}_I \boldsymbol{\tau}_K$$

- a threshold is added to prevent false collision detection during robot motion

for generic *j-th* joint

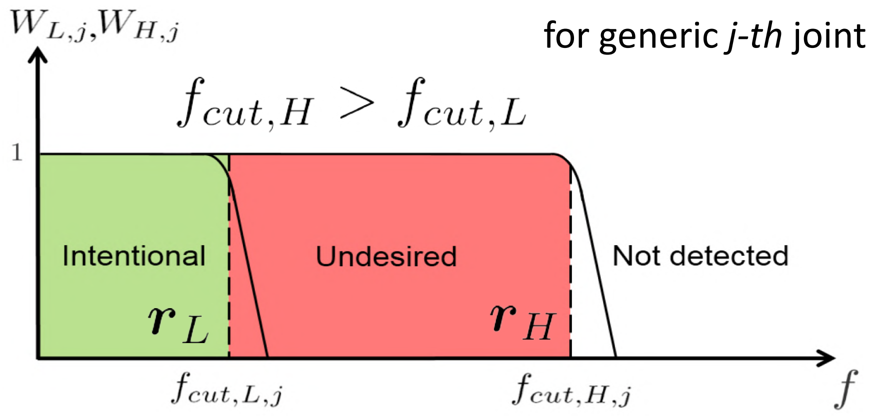

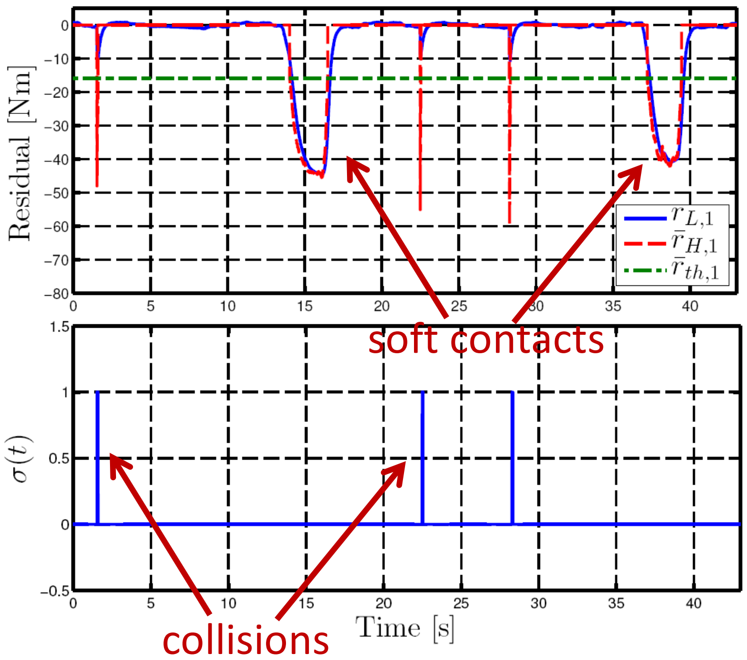

video

Collaboration control

Use of estimate of the external contact force for control (e.g., on a Kuka LWR)

- shaping the robot dynamic behavior in specific **collaborative tasks** with human
  - joint carrying of a load, holding a part in place, whole arm **force** manipulation, ...
  - robot motion controlled by
    - **admittance** control law (in **velocity FRI** mode)
    - **force**, **impedance** or **hybrid force-motion** control laws (needs **torque FRI** mode)

  all implemented **at contact level**
- e.g., admittance control law using estimated contact force (as in video of slide #46)
  - the scheme is realized at the single (or first) contact point
  - desired **velocity** of contact point taken proportional to (**estimated**) contact force

$$\dot{\boldsymbol{p}}_c = \boldsymbol{K}_a \boldsymbol{F}_a, \qquad \boldsymbol{K}_a = k_a \boldsymbol{I} > 0$$

$$\boldsymbol{F}_a = \widehat{\boldsymbol{F}}_c + \boldsymbol{K}_p(\boldsymbol{p}_d - \boldsymbol{p}_c), \qquad \boldsymbol{K}_p = k_p \boldsymbol{I} > 0$$

initial contact point position when interaction begins

Contact force regulation with virtual force sensing

Human-robot collaboration in **torque control mode** (ICRA 2015)

- contact force estimation & control (anywhere/anytime)

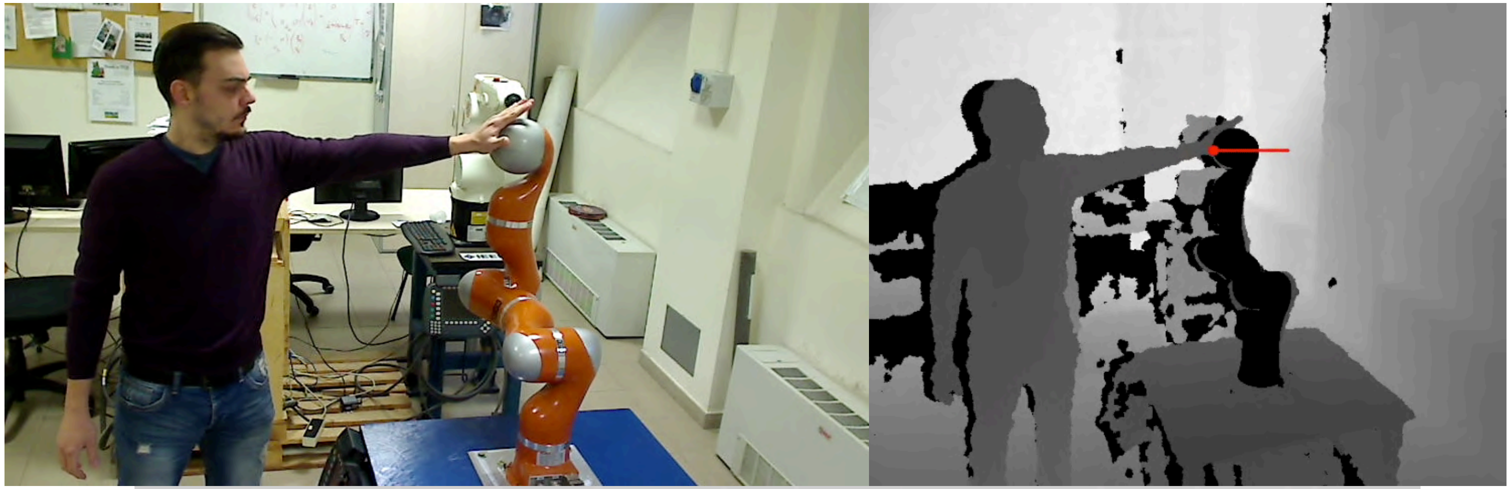

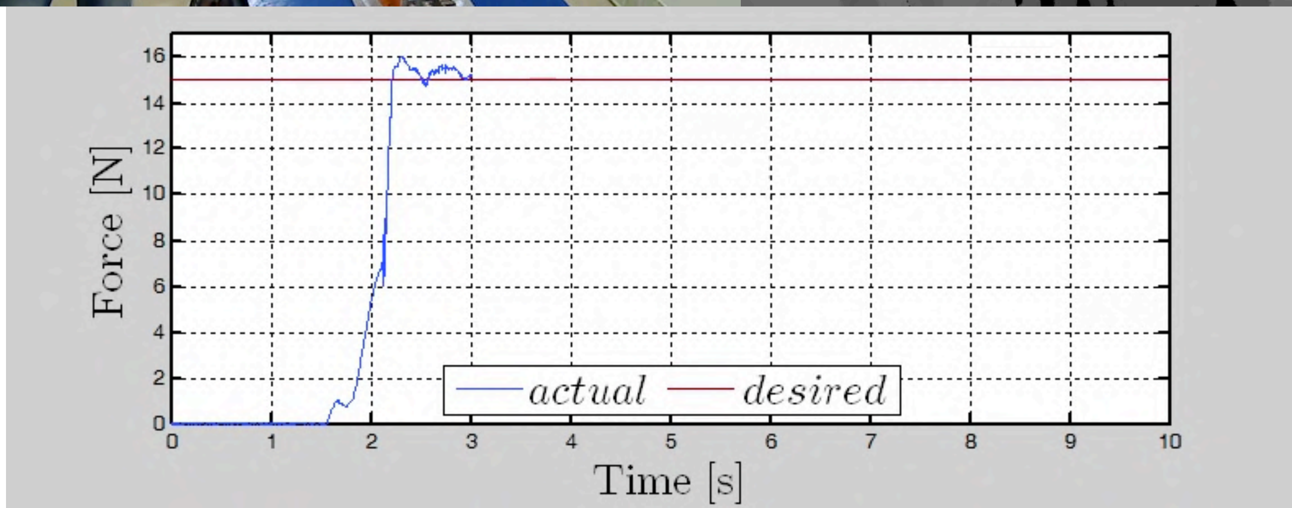

video

see **ICRA 2015 trailer** (at 3’26’’): https://youtu.be/glNHq7MpCG8 (Italian); https://youtu.be/OM_1F33fcWk (English)

Impedance-based control of interaction

Reaction to contact forces by generalized impedance —at **different** levels

consider a fully rigid robot

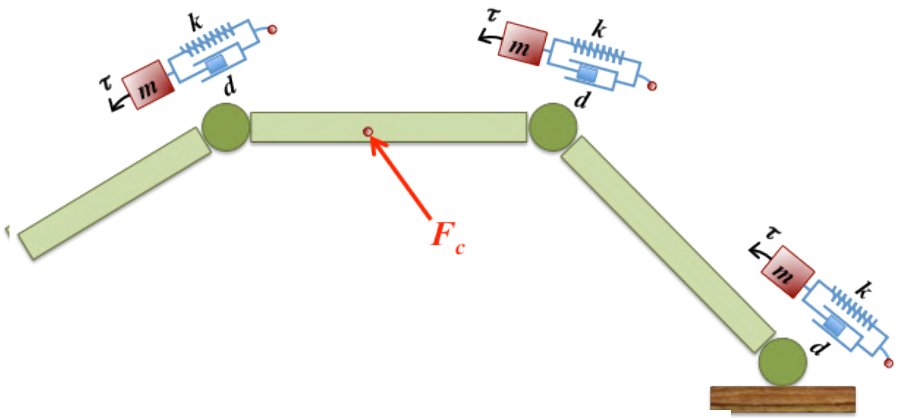

Joint impedance
needs joint torque sensors

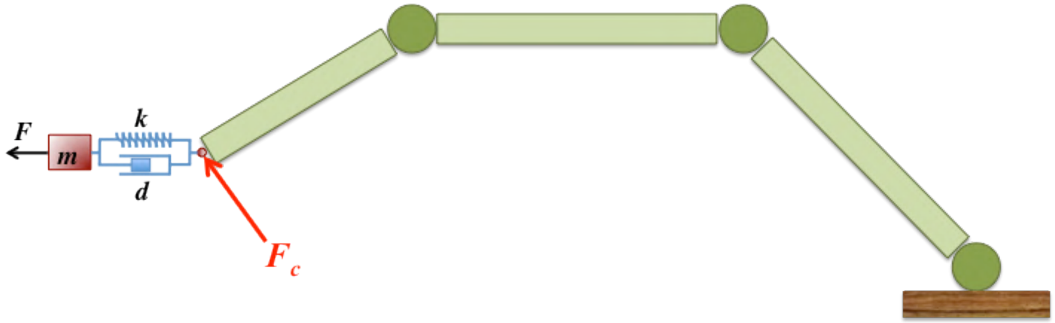

Cartesian impedance
needs F/T sensor

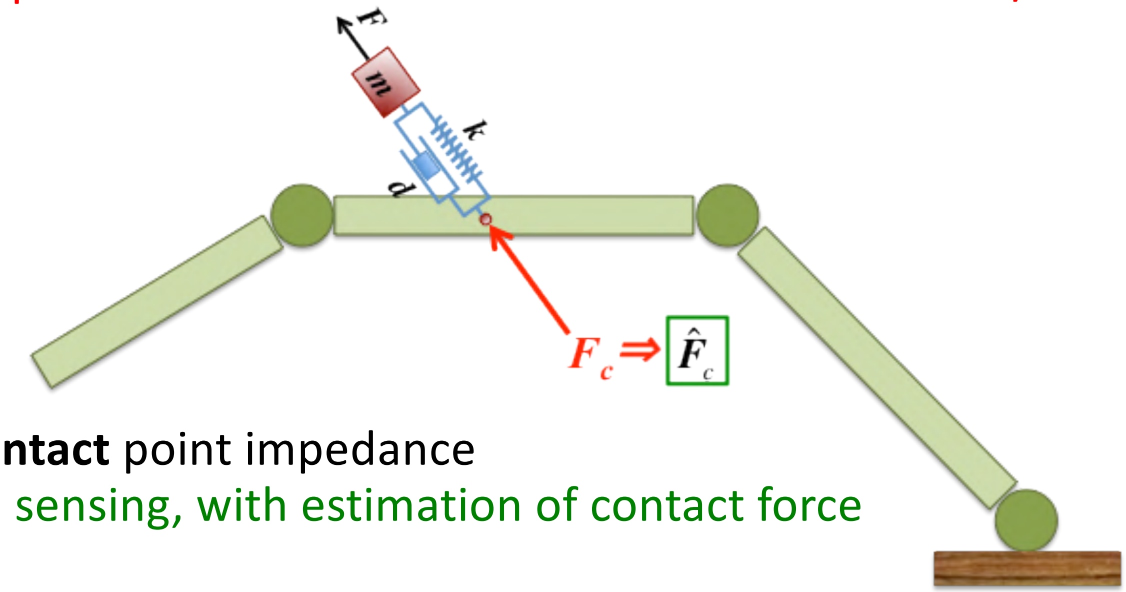

Contact point impedance
without force/torque sensing, with estimation of contact force

Control of generalized impedance

HR collaboration at the contact level (ICRA 2015)

natural (unchanged) robot inertia at the contact

$$M_d = \left(J_c M^{-1} J_c^T\right)^{-1}$$

assigned robot inertia at the contact
with different apparent masses along X, Y, Z

video

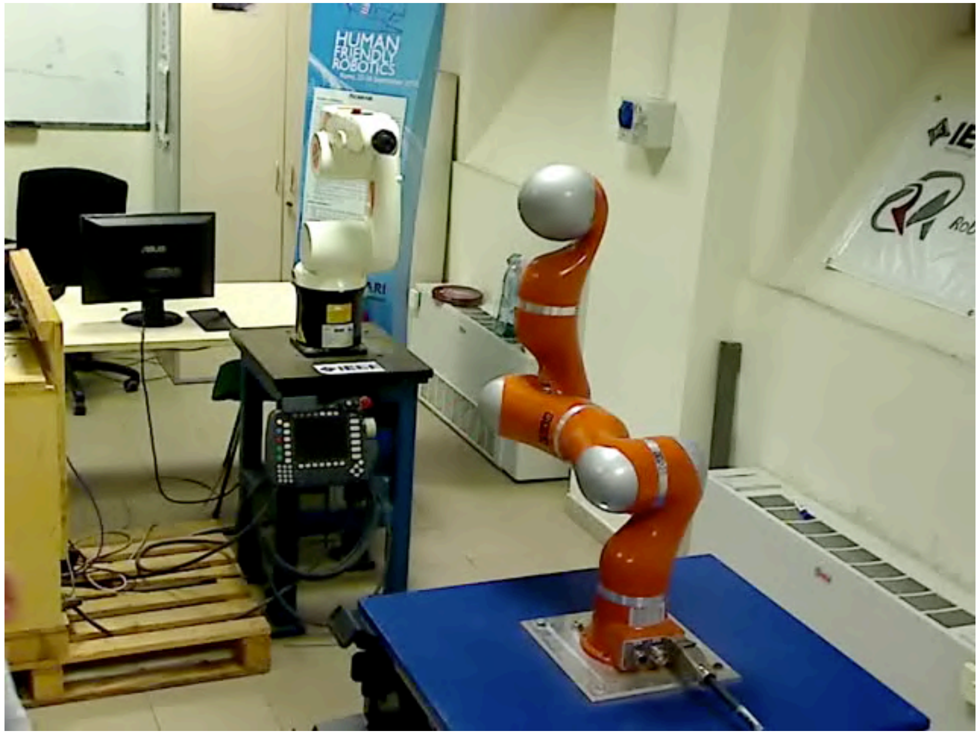

video

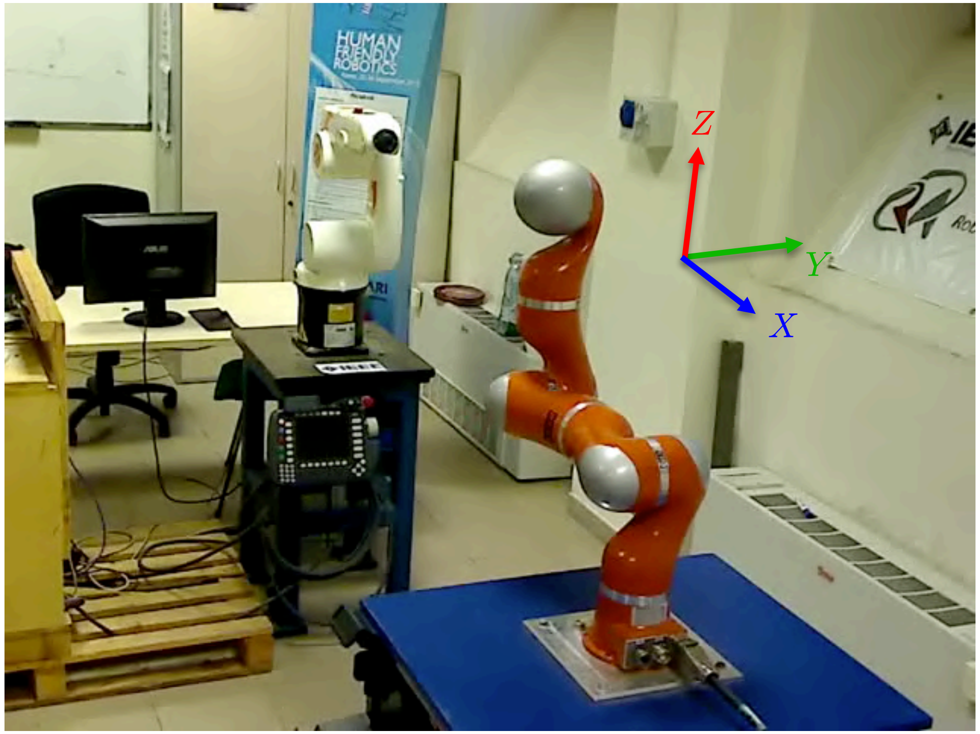

contact force **estimates** are used here **only** to detect and localize contact in order to start a collaboration phase

contact force **estimates** used **explicitly** in control law to modify robot inertia at the contact ($M_{d,X} = 20$, $M_{d,Y} = 3$, $M_{\mathrm{d},Z} = 10$ [kg])

https://youtu.be/NHn2cwSyCCo

Control of generalized contact force

Direct force scheme

- explicit **regulation** of the **contact force** to a desired value, by imposing

$$\boldsymbol{M}_d \ddot{\boldsymbol{x}}_c + \boldsymbol{K}_d \dot{\boldsymbol{x}}_c = \boldsymbol{K}_f (\boldsymbol{F}_d - \widehat{\boldsymbol{F}}_c) = \boldsymbol{K}_f \boldsymbol{e}_f$$

- a force control law needs always a measure (here, an **estimate**) of contact force
- **task-compatibility**: human-robot contact direction vs. desired contact force vector

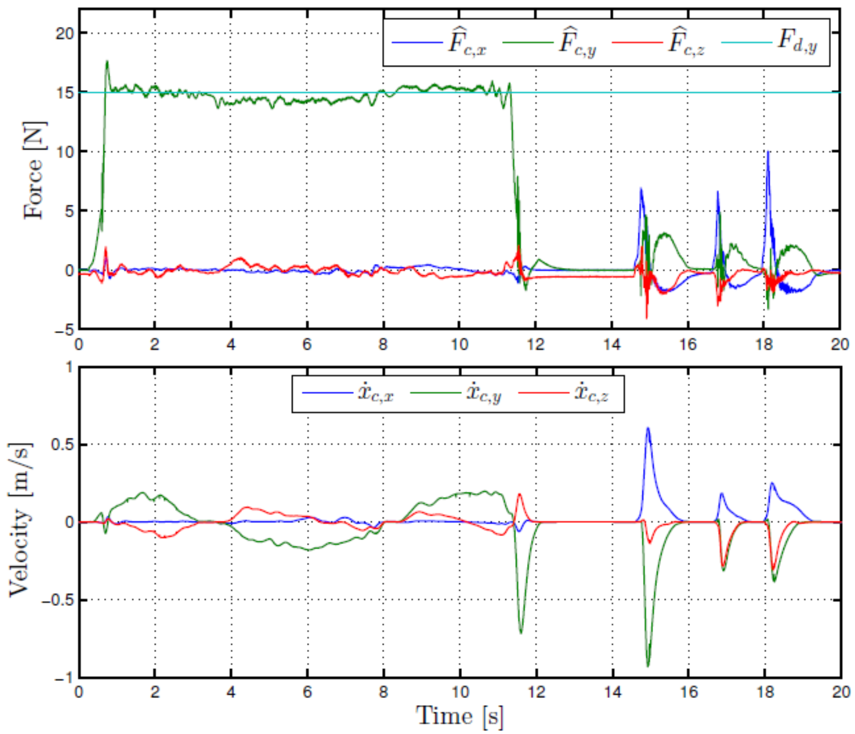

$F_{d,x} = 0, \quad F_{d,y} = 15N, \quad F_{d,z} = 0$

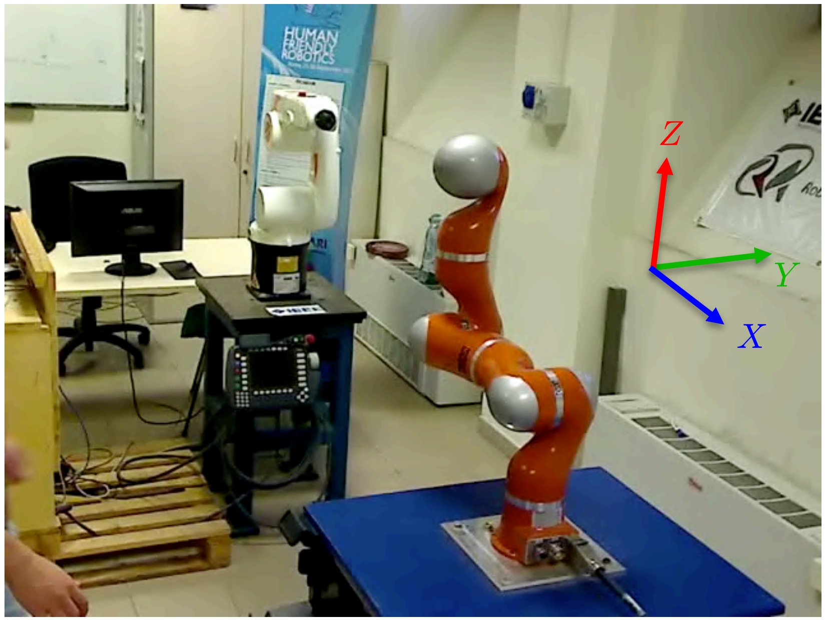

video

however, *drift effects* due to poor control design

Control of generalized contact force

Task-compatible force control scheme (ICRA 2015)

- only the **norm** of the desired contact force is controlled along the instantaneous **direction** of the estimated contact force

$$F_{d,x} = 15\frac{\widehat{F}_{c,x}}{\|\widehat{\boldsymbol{F}}_c\|}, \quad F_{d,y} = 15\frac{\widehat{F}_{c,y}}{\|\widehat{\boldsymbol{F}}_c\|}, \quad F_{d,z} = 15\frac{\widehat{F}_{c,z}}{\|\widehat{\boldsymbol{F}}_c\|} \quad \Leftrightarrow \quad \|F_d\| = 15\ [\mathrm{N}]$$

- in static conditions, the force control law is able to regulate contact forces **exactly**

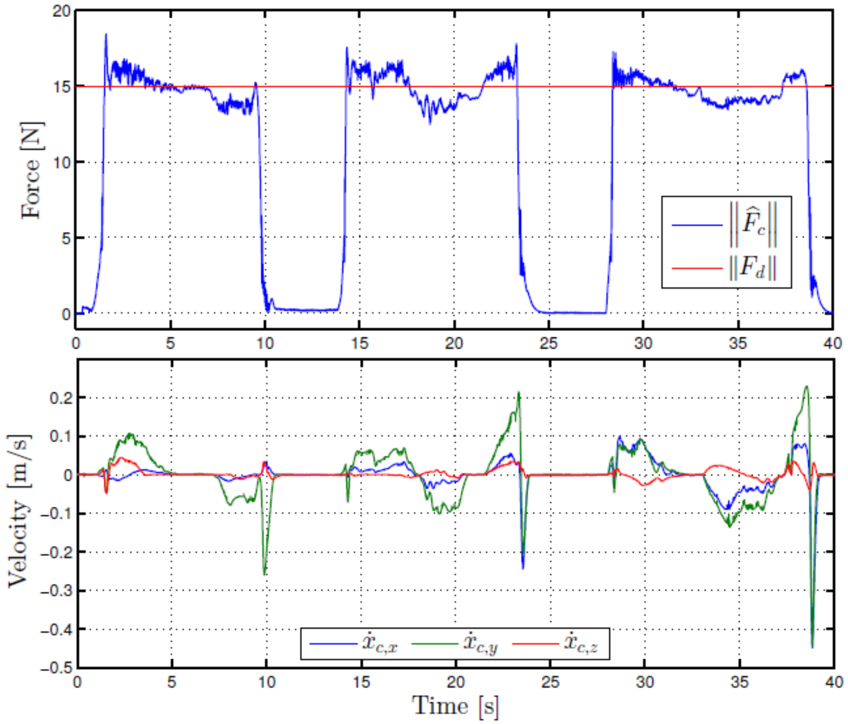

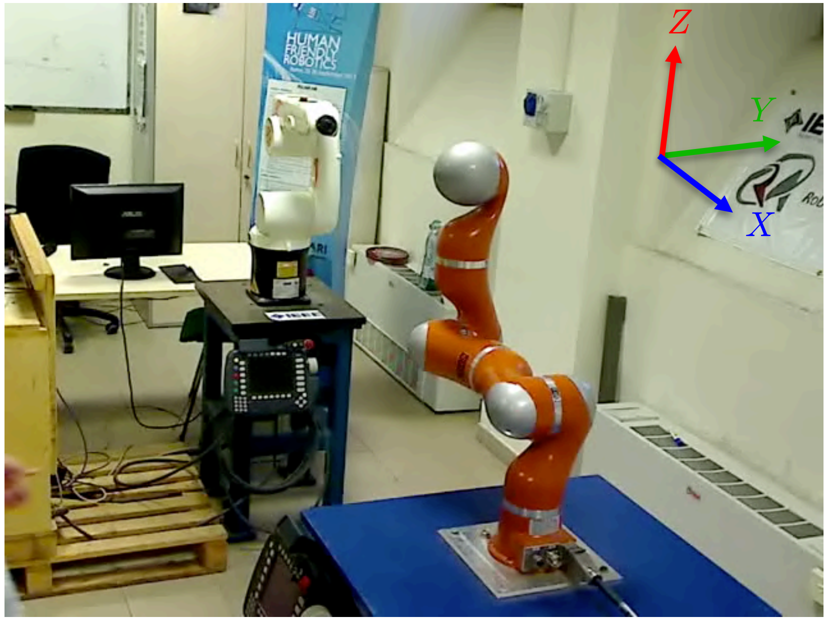

video

task-compatible control of contact force

Collaboration control

Hybrid force/velocity control scheme (ICRA 2016)

- it allows to control **both** contact force and motion in **two** mutually independent sub-spaces
- extends at the contact level a hybrid force/velocity control law, with the orientation of **contact task frame** being determined instantaneously
- task frame obtained by a rotation matrix $\boldsymbol{R}_t$ such that $\boldsymbol{z}_t$ is aligned with the **estimated** contact force

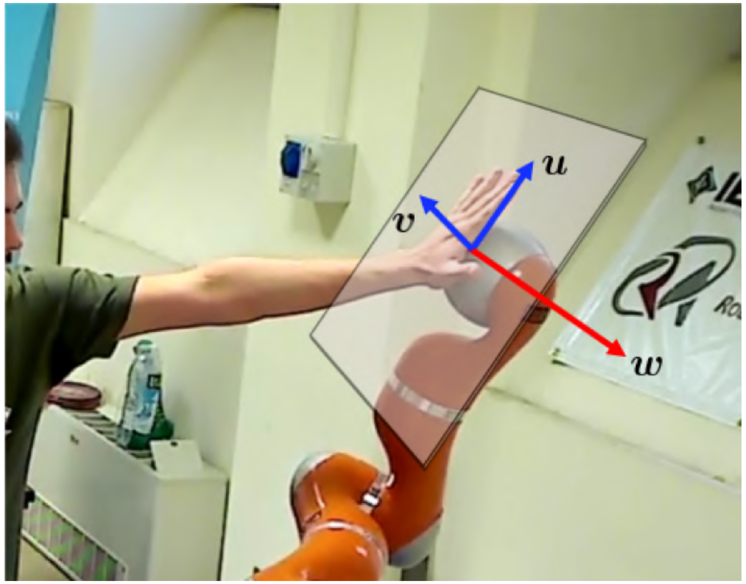

$$\boldsymbol{R}_t = \begin{bmatrix} \boldsymbol{u} & \boldsymbol{v} & \boldsymbol{w} \end{bmatrix} = \left[\begin{array}{ccc} \boldsymbol{u} & \boldsymbol{v} & \dfrac{\widehat{\boldsymbol{F}}_c}{\|\widehat{\boldsymbol{F}}_c\|}, \end{array} \right]$$

- after feedback linearization with $\boldsymbol{\tau} = \boldsymbol{M}\boldsymbol{a} + \boldsymbol{n} - \boldsymbol{J}_c^T \widehat{\boldsymbol{F}}_c$, the acceleration command is

$$\boldsymbol{a} = \boldsymbol{J}_c^{\#} \boldsymbol{M}_d^{-1} (\boldsymbol{R}_t \boldsymbol{a}_c + \boldsymbol{M}_d (\dot{\boldsymbol{R}}_t{}^t \dot{\boldsymbol{x}}_c - \dot{\boldsymbol{J}}_c \dot{\boldsymbol{q}})) + \boldsymbol{P}_c \ddot{\boldsymbol{q}}_0$$

- **complete decoupling** between force control and velocity control can be achieved by choosing the new auxiliary control $\boldsymbol{a}_c$ input as

$$\boldsymbol{a}_c = \boldsymbol{S}_f^c \, \ddot{y}_f + \boldsymbol{S}_\nu^c \, \dot{\boldsymbol{\nu}}$$

Collaboration control

Hybrid force/velocity control scheme

- the force regulation task should be along the instantaneous direction of the applied external force while the motion control task lives in the orthogonal plane
- the selection matrices are chosen as

$$\boldsymbol{S}_f^c = \begin{bmatrix} 0 \\ 0 \\ 1 \end{bmatrix} \qquad \boldsymbol{S}_\nu^c = \begin{bmatrix} 1 & 0 \\ 0 & 1 \\ 0 & 0 \end{bmatrix}$$

- regulation of the contact force to desired constant value $F_d > 0$ is obtained choosing

$$\ddot{y}_f = k_f \left(F_d - \|\widehat{\boldsymbol{F}}_c\| \right) - k_{df} \dot{y}_f$$

- control of the desired velocity can be achieved using

$$\dot{\boldsymbol{\nu}} = \dot{\boldsymbol{\nu}}_d + \boldsymbol{K}_d \left(\boldsymbol{\nu}_d - \boldsymbol{\nu} \right) + \boldsymbol{K}_i \int_0^t \left(\boldsymbol{\nu}_d - \boldsymbol{\nu} \right) \boldsymbol{d}s,$$

- the final control acceleration input becomes

$$\boldsymbol{a} = \boldsymbol{J}_c^{\#} \boldsymbol{M}_d^{-1} \Big[\boldsymbol{R}_t \boldsymbol{S}_f^c \left(k_f e_f - k_{df} \dot{y}_f \right) + \boldsymbol{R}_t \boldsymbol{S}_\nu^c \left(\dot{\boldsymbol{\nu}}_d + \boldsymbol{K}_d \dot{\boldsymbol{e}}_{\boldsymbol{\nu}} + \boldsymbol{K}_i \boldsymbol{e}_{\boldsymbol{\nu}} \right)$$
$$+ \boldsymbol{M}_d \dot{\boldsymbol{R}}_t {}^c\dot{\boldsymbol{x}} - \boldsymbol{M}_d \dot{\boldsymbol{J}}_c \dot{\boldsymbol{q}} \Big] + \boldsymbol{P}_c \ddot{\boldsymbol{q}}_0,$$

Collaboration control

Hybrid force/velocity control at contact level (IROS 2016)

- desired contact force along Y direction regulated to $\boldsymbol{F}_d = 15[N]$
- constant desired velocity to perform a **line** in the vertical XZ plane

$$\boldsymbol{\nu}_d = \begin{bmatrix} 0.015 \\ 0.03 \end{bmatrix} \qquad \dot{\boldsymbol{\nu}}_d = \begin{bmatrix} 0 \\ 0 \end{bmatrix}$$

https://youtu.be/tIhEK5f00QU

video

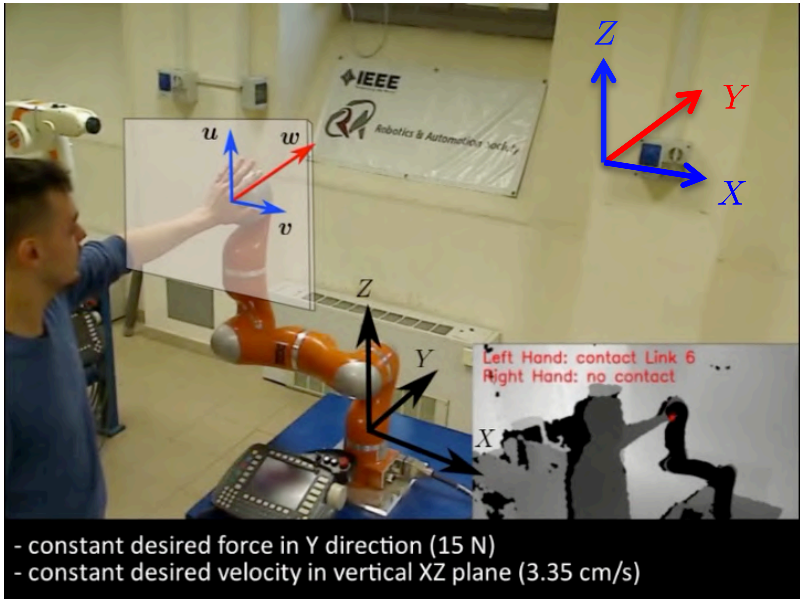

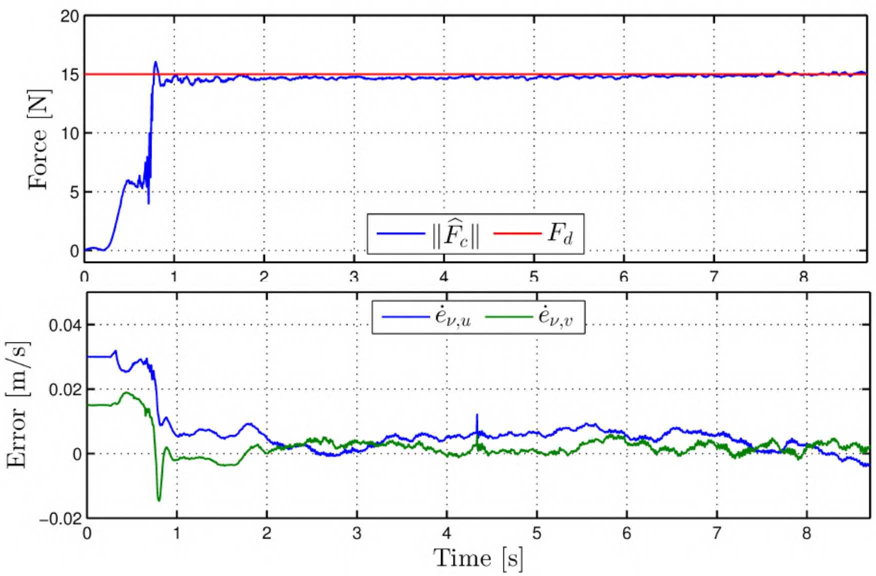

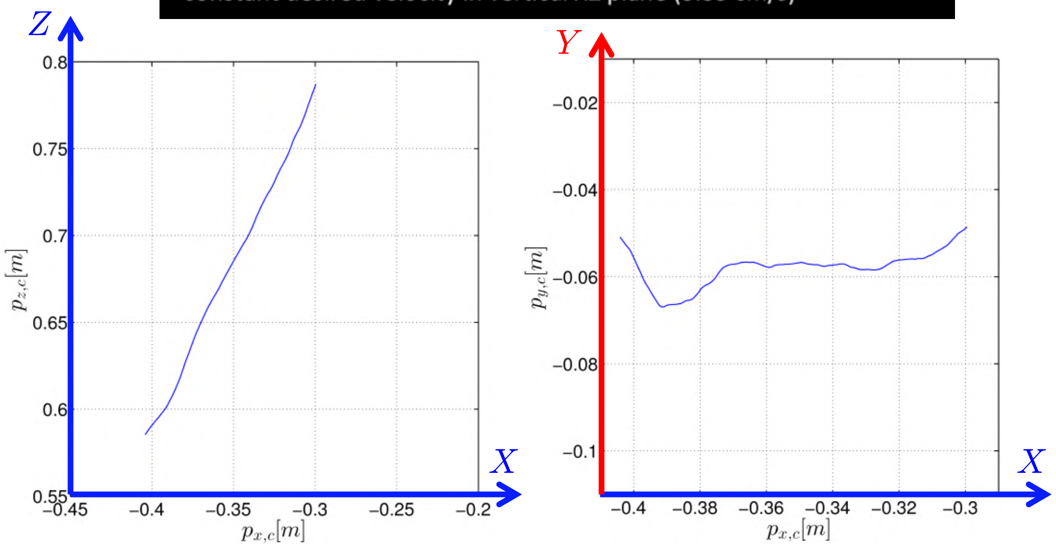

Collaboration control

Hybrid force/velocity control at contact level (IROS 2016)

- desired contact force along the X direction regulated to $\boldsymbol{F}_d = 15[N]$
- desired velocity/acceleration to perform a **circle** in the vertical YZ plane

$$\boldsymbol{\nu}_d = \begin{bmatrix} \omega\rho \sin \omega t \\ \omega\rho \cos \omega t \end{bmatrix} \qquad \dot{\boldsymbol{\nu}}_d = \begin{bmatrix} \omega^2\rho \cos \omega t \\ -\omega^2\rho \sin \omega t \end{bmatrix}$$

video

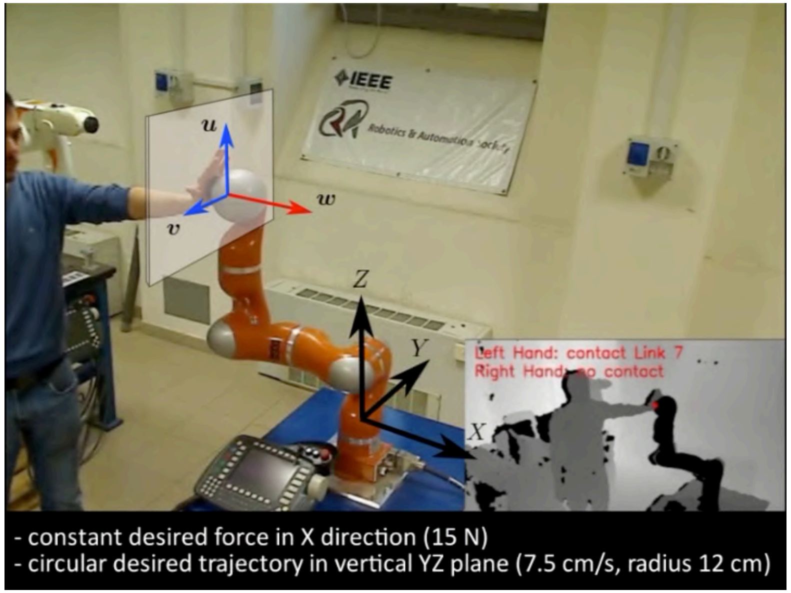

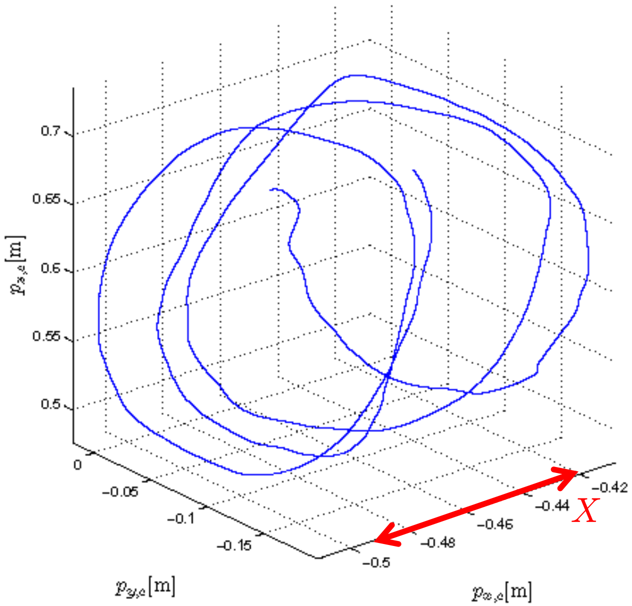

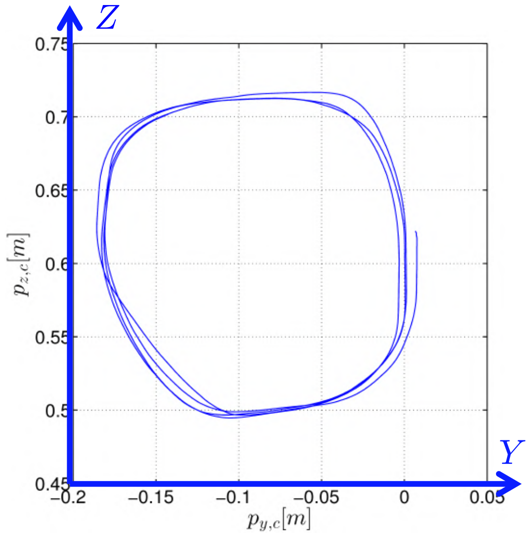

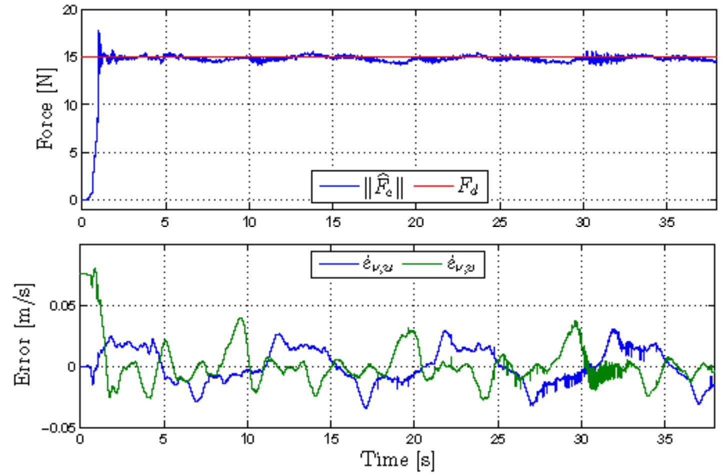

≈ 7 cm of motion in the force-controlled direction

Validation of collaboration control with a F/T sensor

Force and hybrid force/velocity control schemes at contact level (February 2019)

- desired contact force along the estimated contact direction regulated at 15 N
- … and trajectory control with constant speed along a circle in the orthogonal plane

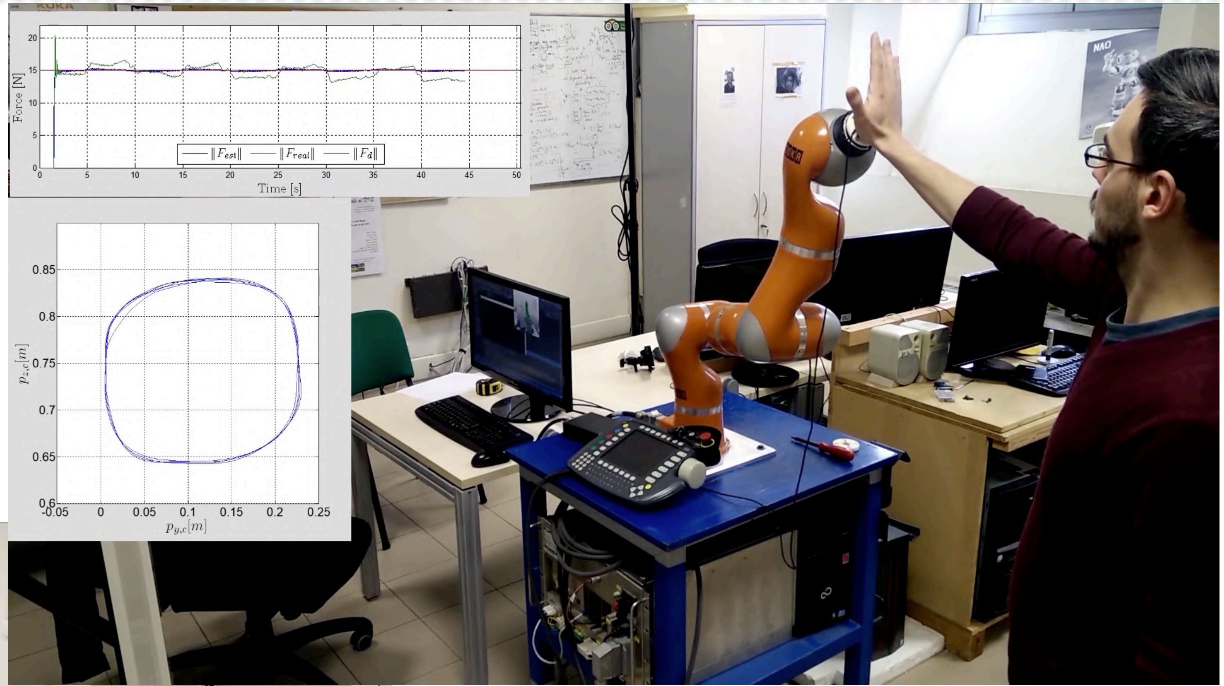

video

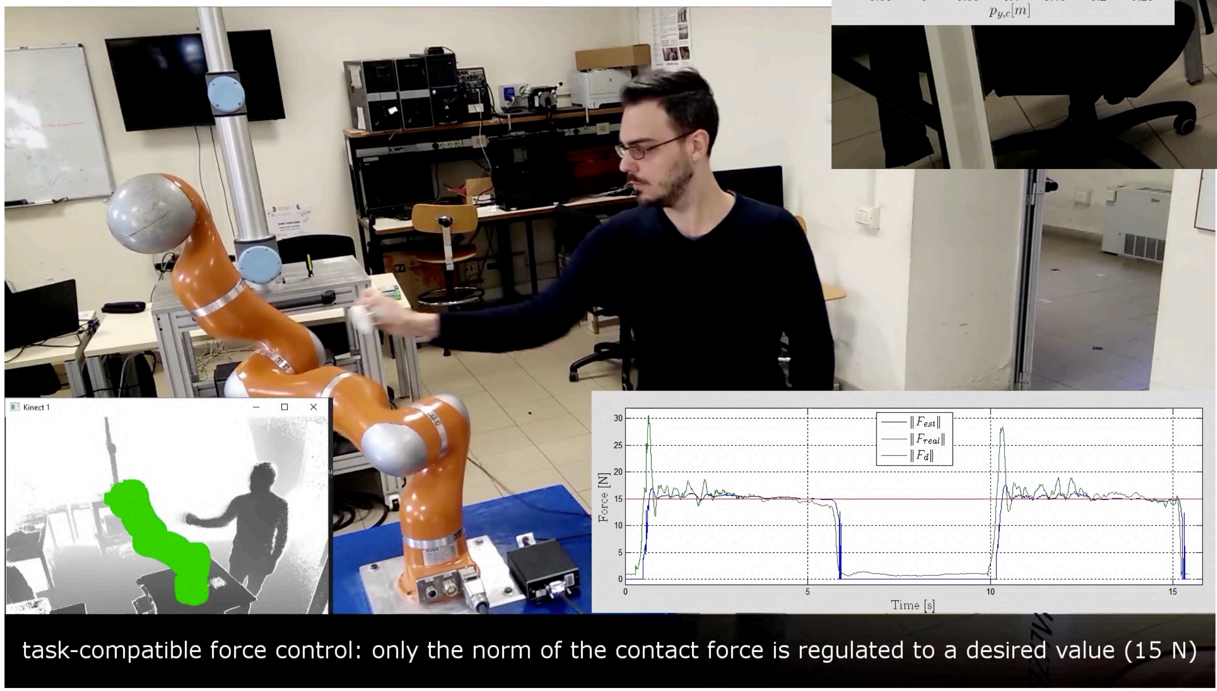

video

SYMPLEXITY cell for laser polishing

Including a manual polishing station with **human-robot physical collaboration**

SYMPLEXITY **H2020 FoF EU project (2015-18)**

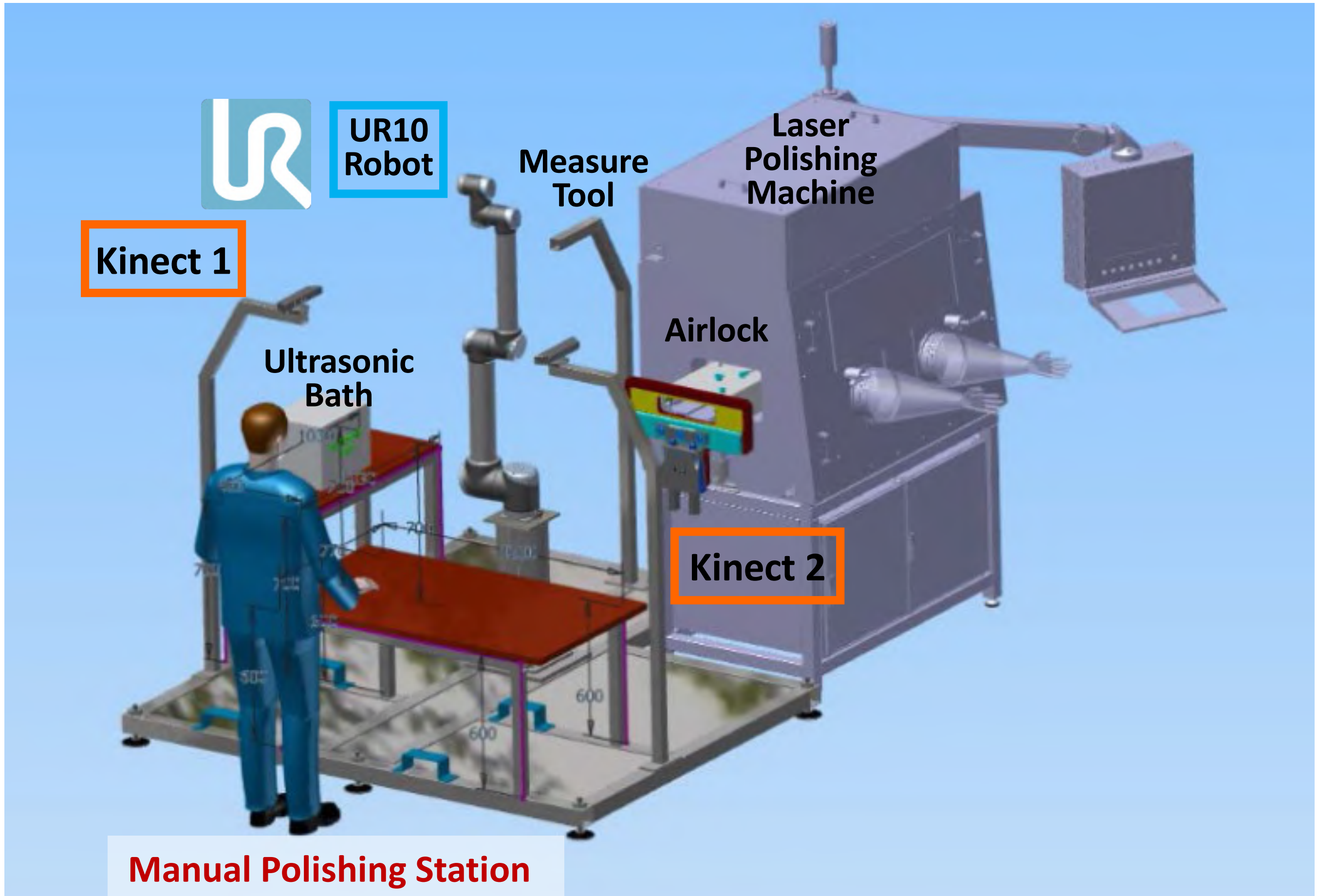

Contact detection (model-based) for **safety**

3D workspace monitoring with 2 Kinects for **HR coexistence**

Use of F/T sensor and of residuals for **HR physical collaboration**

Universal Robots UR10
- lightweight design
- CE safety certified

speed scaling/stop from sensing HR distance (= **0** in physical collaboration) ISO/TS15066:2016

GIZELIS ROBOTICS — Fraunhofer IPT Institut Produktionstechnologie — SAPIENZA Università di Roma

Scenario for HRC in manual polishing

Preparing a metallic part for the final polishing by the laser machine

UR10 robot operation with HR coexistence/collaboration

part to be polished

video

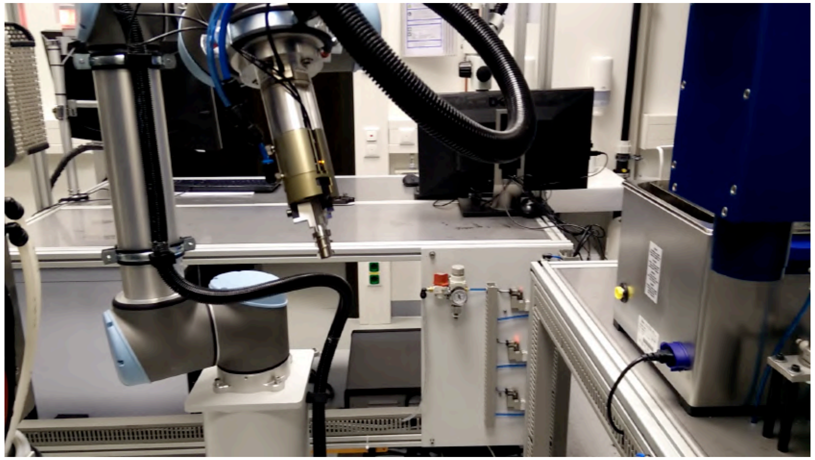

measuring Berlin Heart part with the CWS

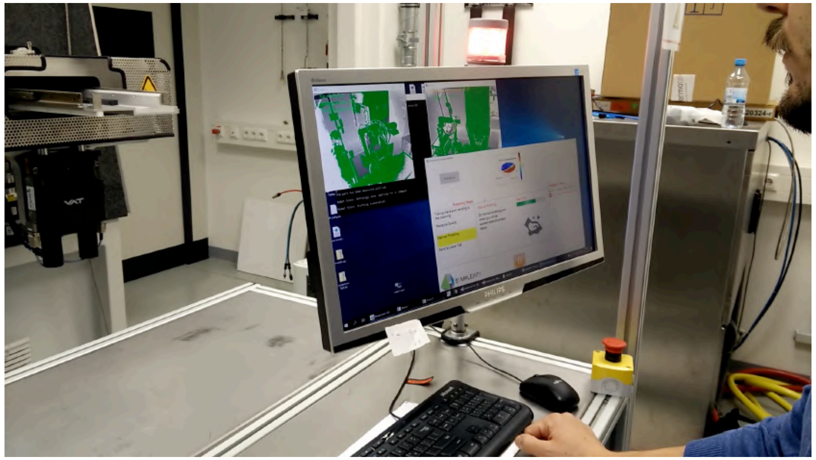

video

physical collaboration in contact

video

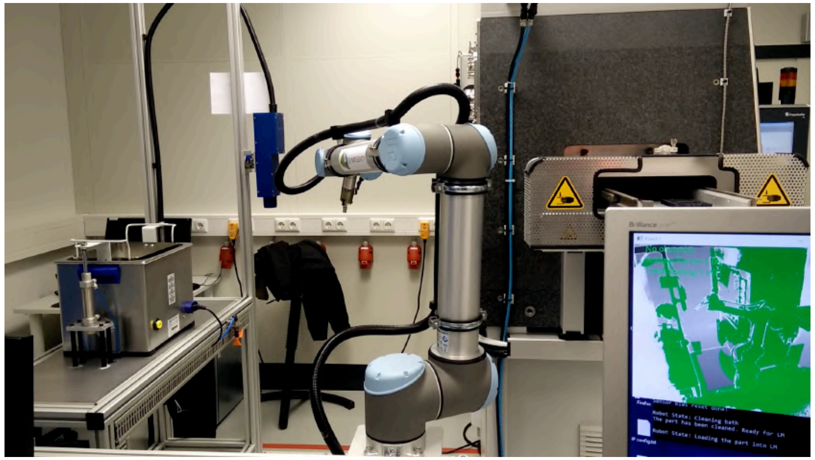

coexistence

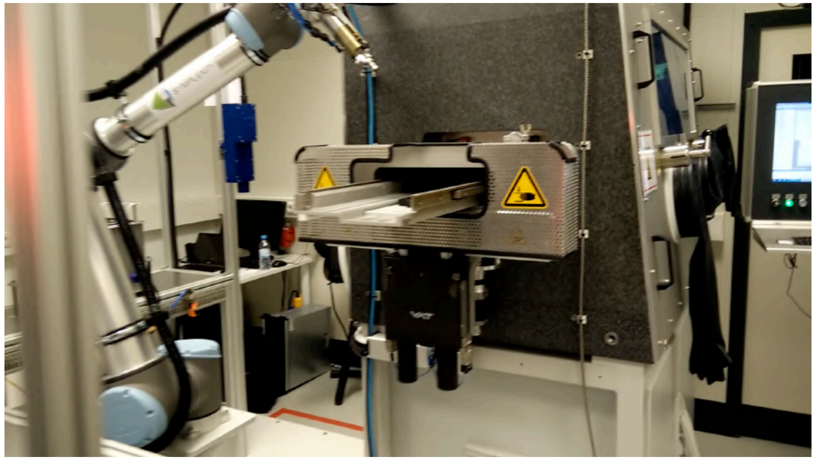

video

coordination with LP machine

CWS = Coherent Wave Scattering (laser measurement of surface quality)

Scenario for HRC in manual polishing

Distinguishing different contact forces

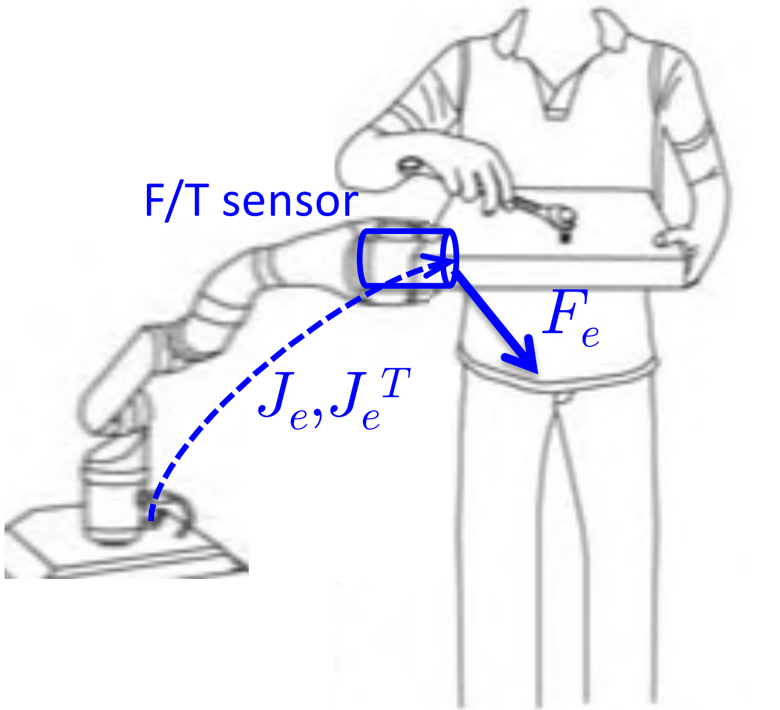

6D Force/Torque (F/T) sensor at wrist
- manual polishing force is **measured**
- end-effector Jacobian J_e is **known**

contact force at unknown location
- **not** measurable by the F/T sensor
- possibly applied by the human **while** manipulating the work piece held by robot
- contact Jacobian J_c is **not** known

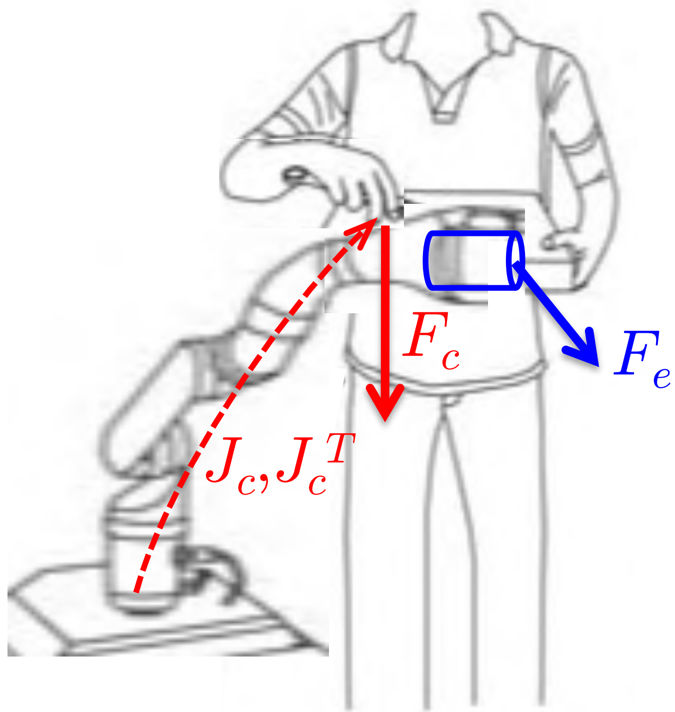

Handling multiple contacts

Dynamic model and residual computation **using also the F/T sensor**

- robot **dynamic model** takes the form

$$M(q)\ddot{q} + \boldsymbol{S}(q,\dot{q})\dot{q} + g(q) = \tau + J_e^T(q)F_e + J_c^T(q)F_c$$

- joint torques resulting from different contacts

(measured) at the end-effector level

$$\tau_e = J_e^T(q)F_e$$

at a generic point along the structure

$$\tau_c = J_c^T(q)F_c$$

- monitor the robot generalized momentum $p = M(q)\dot{q}$

- (model-based) **residual vector** signal to detect and isolate the generic contacts

$$r(t) = K_i\left(p - \int_0^t \left(\boldsymbol{S}^T(q,\dot{q})\dot{q} - g(q) + \tau + J_e^T(q)F_e - r\right)ds\right)$$

$$\boxed{K_i \to \infty \ \text{(sufficiently large)} \quad \Rightarrow \quad r \simeq \tau_c}$$

Admittance control strategy during manual polishing

Human and robot are physically collaborating

- when there is no extra contact along the structure, **position and orientation** of the end-effector are both held **fixed** by a **stiff kinematic control law**

$$\dot{q} = J_e^{\#} \underset{\text{as large as possible}}{K_e} \begin{pmatrix} v_r \\ \omega_r \end{pmatrix} = J_e^{\#} K_e \begin{pmatrix} I & 0 \\ 0 & T(\phi) \end{pmatrix} \begin{pmatrix} p_d - p \\ \phi_d - \phi \end{pmatrix}$$

as large as possible

constant values

- in this way, the control law counterbalances all forces/torques applied by the operator **during manual polishing**
- when the human intentionally pushes on the robot body, control of the end-effector **orientation** is **relaxed**

3×6 for UR10

$$J_e(q) = \begin{pmatrix} J_p(q) \\ J_o(q) \end{pmatrix}$$

$$\boxed{\dot{q} = J_p^{\#} K_p (p_d - p) + \overbrace{\left(I - J_p^{\#} J_p\right) K_r r}^{\text{residual-based admittance reaction to extra contacts}}}$$

- human can reconfigure the arm, thus **reorient the work piece** held by the robot

HRC phase with UR10 robot

Experimental verification in the lab (Mechatronics 2018)

https://youtu.be/slwUiRT_lJQ video

no F/T sensor, switch to **UR FreeDrive** mode

video https://youtu.be/bjZbmlAclYk

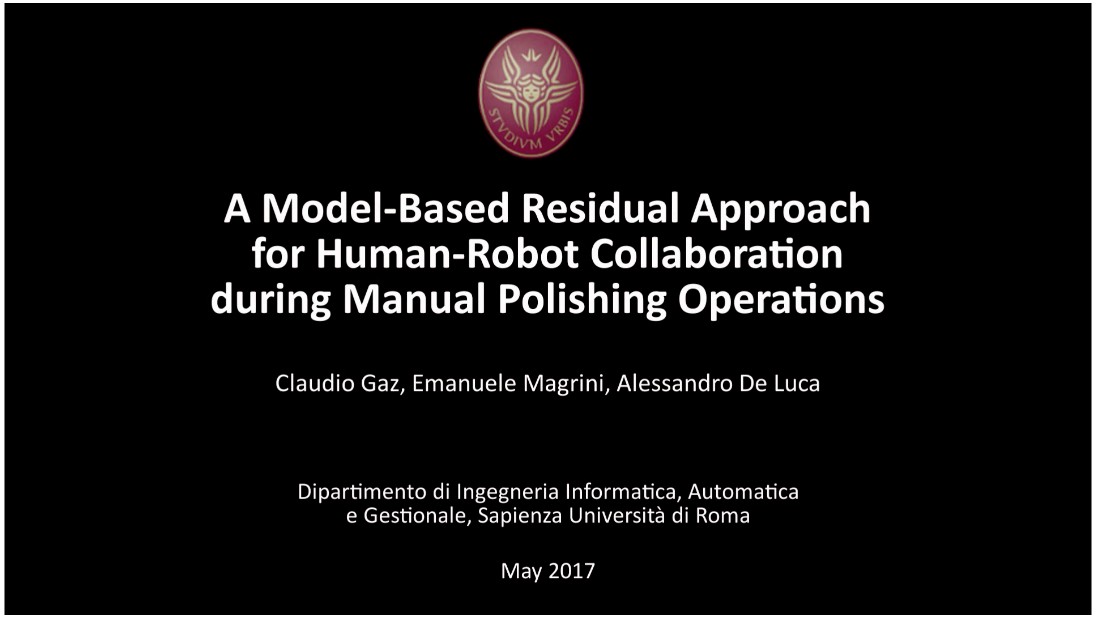

with F/T sensor, using our **residual** method

for a similar behavior with the KUKA LWR
see https://youtu.be/TZ6nPqLPDxI

HRC phase with UR10 robot

Experimental results (separating F/T measures from residuals)

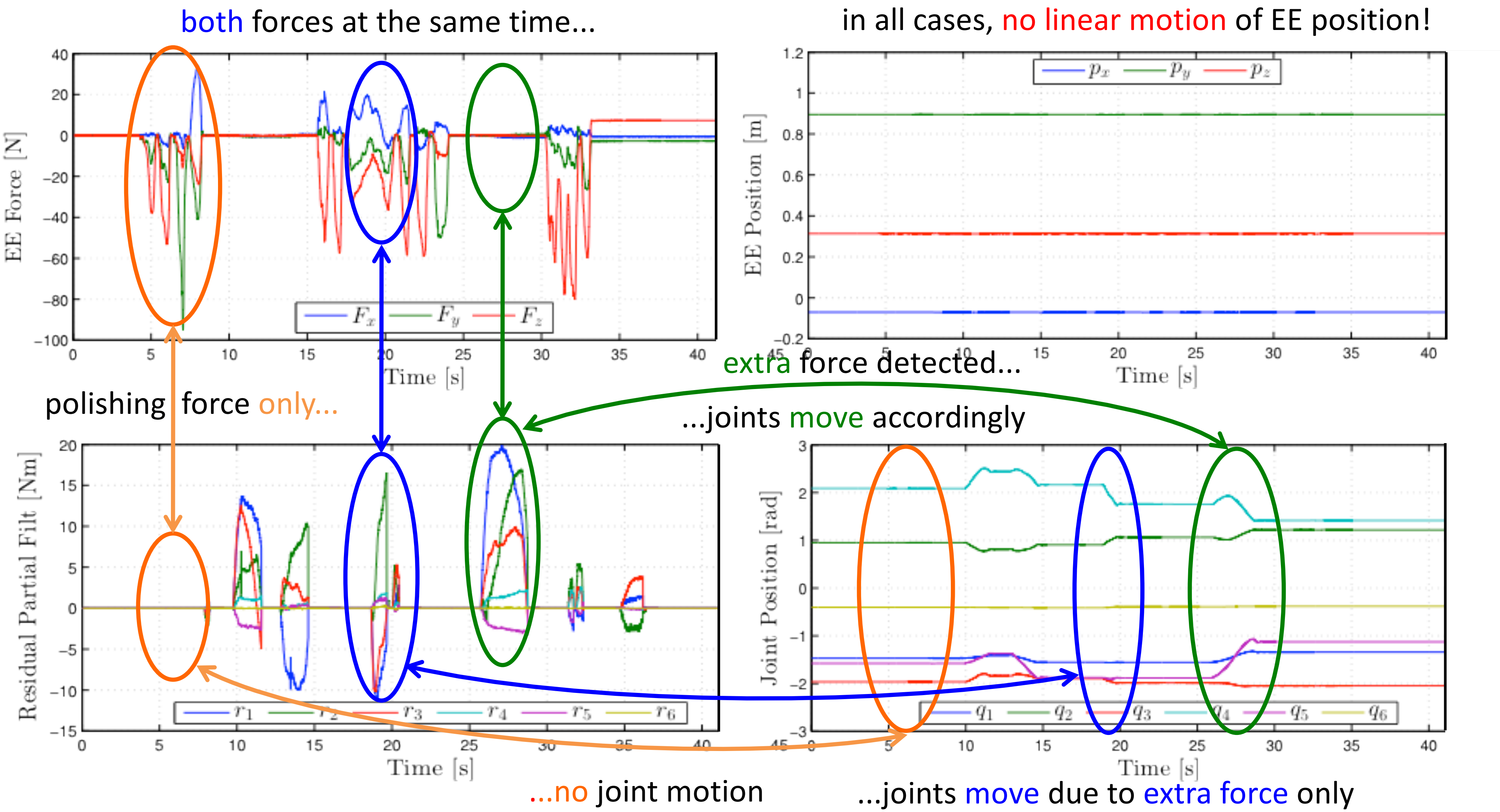

Combining motor currents and F/T sensor data

Enhanced flexible interaction by filtering, thresholding, merging signals (ICRA 2019)

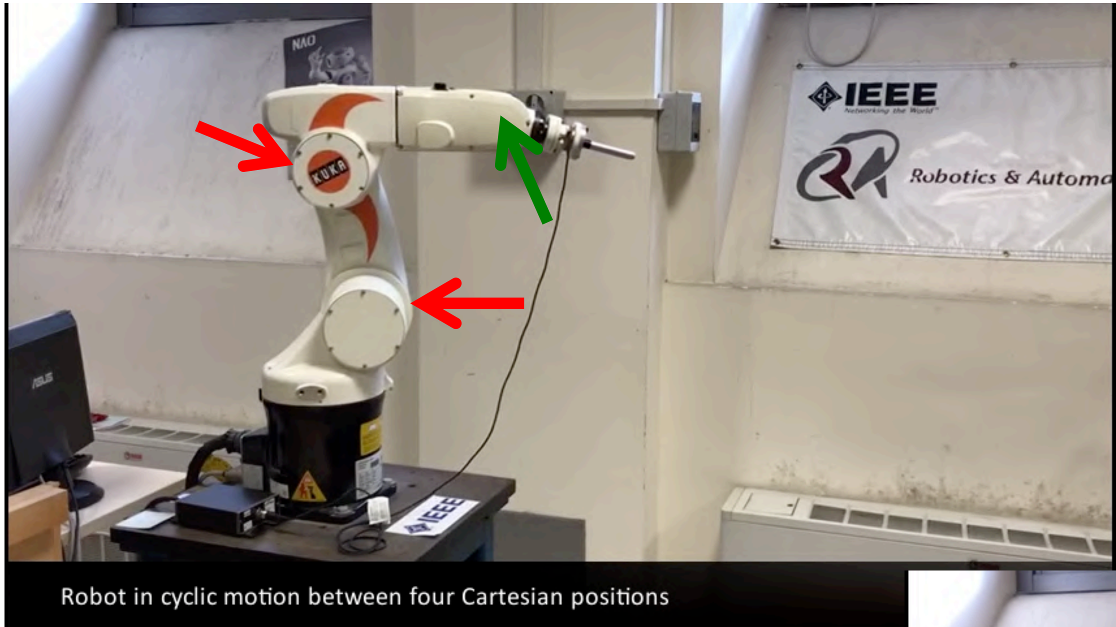

video

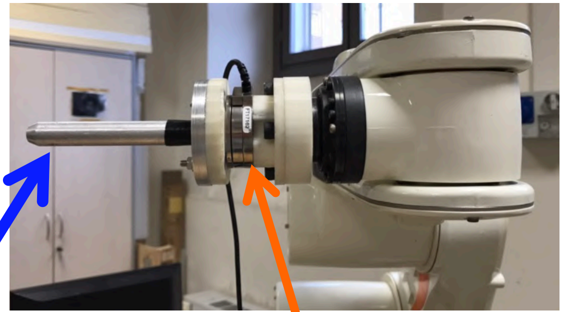

collaborative forces at E-E

ATI Mini45
F/T sensor

video

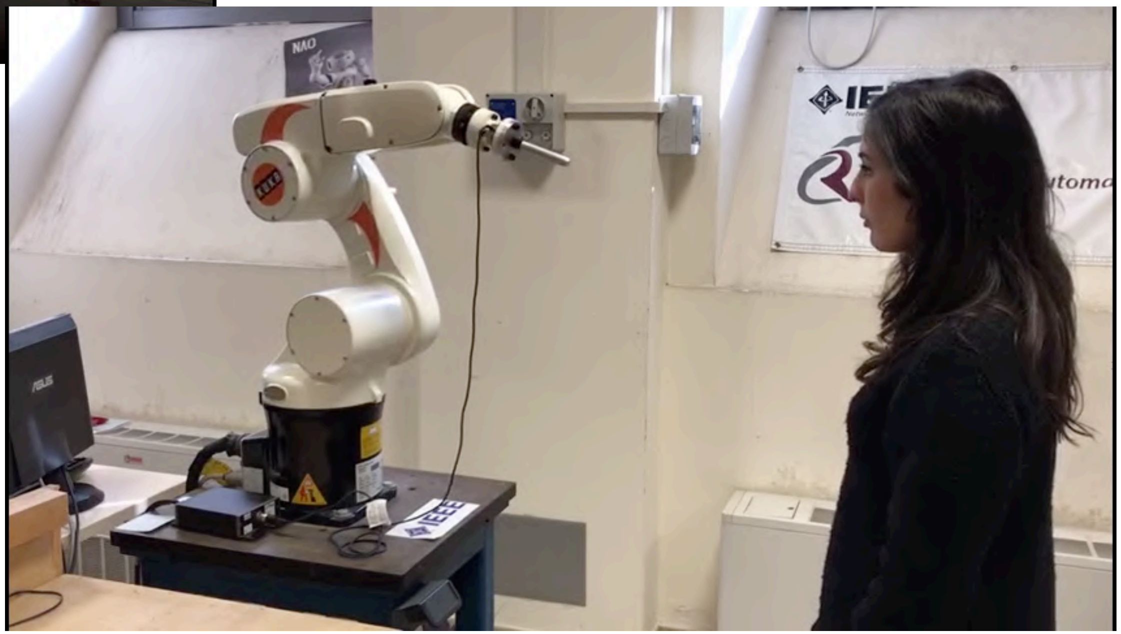

intentional contacts
and/or collisions
may occur **anywhere**

6-dof **KUKA KR5 Sixx** with
closed control architecture
and RSI interface at $T_c = 12$ ms

Our team at DIAG

Robotics Lab of the Sapienza University of Rome (back in 2014)

Acknowledgements

@Sapienza – DIAG - Gabriele Buondonno, Lorenzo Ferrajoli, **Fabrizio Flacco**†,
Claudio Gaz, Milad Geravand, Emanuele Magrini, Eleonora Mariotti, Raffaella Mattone

@DLR – Institute of Robotics and Mechatronics - Alin Albu-Schäffer, Sami Haddadin

@Stanford – Artificial Intelligence Lab - Oussama Khatib, Torsten Kröger

References - 1

Download pdf for personal use at www.diag.uniroma1.it/deluca/Publications

- A. De Luca and R. Mattone, "Sensorless robot collision detection and hybrid force/motion control," IEEE Int. Conf. on Robotics and Automation, pp. 999-1004, 2005.
- A. De Luca, A. Albu-Schäffer, S. Haddadin, and G. Hirzinger, "Collision detection and safe reaction with the DLR-III lightweight manipulator arm," IEEE/RSJ Int. Conf. on Intelligent Robots and Systems, pp. 1623-1630, 2006.
- S. Haddadin, A. Albu-Schäffer, A. De Luca, and G. Hirzinger, "Collision detection and reaction: A contribution to safe physical human-robot interaction," IEEE/RSJ Int. Conf. on Intelligent Robots and Systems, pp. 3356-3363, 2008 (IROS 2008 Best Application Paper Award).
- A. De Luca and L. Ferrajoli, "Exploiting robot redundancy in collision detection and reaction," IEEE/RSJ Int. Conf. on Intelligent Robots and Systems, pp. 3299-3305, 2008.
- A. De Santis, B. Siciliano, A. De Luca, A. Bicchi, "An atlas of physical human-robot interaction," Mechanism and Machine Theory, vol. 43, no. 3, pp. 253–270, 2008 (2017 MMT Award for Excellence).
- A. De Luca and L. Ferrajoli, "A modified Newton-Euler method for dynamic computations in robot fault detection and control," IEEE Int. Conf. on Robotics and Automation, pp. 3359-3364, 2009.
- F. Flacco, A. De Luca, "Multiple depth/presence sensors: Integration and optimal placement for human/robot coexistence," IEEE Int. Conf. on Robotics and Automation, pp. 3916-3923, 2010.
- F. Flacco, T. Kröger, A. De Luca, and O. Khatib, "A depth space approach to human-robot collision avoidance," IEEE Int. Conf. on Robotics and Automation, pp. 338-345, 2012.
- A. De Luca and F. Flacco, "Integrated control for pHRI: Collision avoidance, detection, reaction and collaboration," 4th IEEE RAS Int. Conf. on Biomedical Robotics and Biomechatronics, pp. 288-295, 2012 (BioRob 2012 Best Paper Award).
- M. Geravand, F. Flacco, and A. De Luca, "Human-robot physical interaction and collaboration using an industrial robot with a closed control architecture," IEEE Int. Conf. on Robotics and Automation, pp. 3985-3992, 2013.
- E. Magrini, F. Flacco, and A. De Luca, "Estimation of contact force using a virtual force sensor," IEEE/RSJ Int. Conf. on Intelligent Robots and System, pp. 2126-2133, 2014.
- F. Flacco, T. Kröger, A. De Luca, and O. Khatib, "A depth space approach for evaluating distance to objects —with application to human-robot collision avoidance," J. of Intelligent & Robotic Systems, vol. 80 S.1, pp. 7-22, 2015.

References - 2

Download pdf for personal use at [www.diag.uniroma1.it/deluca/Publications]

- E. Magrini, F. Flacco, and A. De Luca, “Control of generalized contact motion and force in physical human-robot interaction,” IEEE Int. Conf. on Robotics and Automation, pp. 2298-2304, 2015 (ICRA 2015 Best Conference Paper Award Finalist).
- G. Buondonno and A. De Luca, “Combining real and virtual sensors for measuring interaction forces and moments acting on a robot," IEEE/RSJ Int. Conf. on Intelligent Robots and Systems, pp. 794-800, 2016.
- E. Magrini and A. De Luca, “Hybrid force/velocity control for physical human-robot collaboration tasks,” IEEE/RSJ Int. Conf. on Intelligent Robots and Systems. pp. 857-863, 2016.
- F. Flacco and A. De Luca, “Real-time computation of distance to dynamic obstacles with multiple depth sensors,” IEEE Robotics and Automation Lett., vol. 2, no. 1, pp. 56-63, 2017.
- M. Khatib, K. Al Khudir, A. De Luca, "Visual coordination task for human-robot collaboration," IEEE/RSJ Int. Conf. on Intelligent Robots and Systems, pp. 3762-3768, 2017.
- E. Magrini, A. De Luca, “Human-robot coexistence and contact handling with redundant robots,” IEEE/RSJ Int. Conf. on Intelligent Robots and Systems, pp. 4611-4617, 2017.
- S. Haddadin, A. De Luca, and A. Albu-Schäffer, “Robot collisions: A survey on detection, isolation, and identification,” IEEE Trans. on Robotics, vol. 33, no. 6, pp. 1292-1312, 2017.
- C. Gaz, A. De Luca, “Payload estimation based on identified coefficients of robot dynamics --with an application to collision detection, ” IEEE/RSJ Int. Conf. on Intelligent Robots and Systems, pp. 3033-3040, 2017.
- C. Gaz, E. Magrini, A. De Luca “ A model-based residual approach for human-robot collaboration during manual polishing operations,” Mechatronics, vol. 55, pp. 234-247, 2018.
- E. Mariotti, E. Magrini, A. De Luca, “Admittance control for human-robot interaction using an industrial robot equipped with a F/T sensor,” IEEE Int. Conf. on Robotics and Automation, pp. 6130-6136, 2019.
- E. Magrini, F. Ferraguti, A.J. Ronga, F. Pini, A. De Luca, F. Leali, "Human-robot coexistence and interaction in open industrial cells," Robotics and Computer-Integrated Manufacturing, vol. 61, 101846, 2020.

- **Videos**: YouTube channel RoboticsLabSapienza. Playlist: Physical human-robot interaction